CHUN FANG
Finite Element Modeling of Physicochemical Changes during Steaming of Cowpea Seeds
(Under the direction of MANJEET S. CHINNAN)

One of the major constraints to use of cowpea seeds is storage loss due to cowpea weevil infestation. Appropriate steaming and subsequent drying treatments have been known to alter the physicochemical characteristics of cowpea seeds, and thereby reducing losses during storage. Starch is the major component of dry seeds and its gelatinization is involved in the physicochemical changes that occur during the treatment. This research is focused on the gelatinization of starch within the cowpea seeds during steaming. Starch gelatinization is based on simultaneous heat and mass transfer reactions. A finite element model was successfully developed to describe the behavior of simultaneous heat and mass transfer. The predicted temperature and moisture profiles in the seeds agreed well with the experimental results. A kinetics of starch gelatinization was constructed and incorporated in the finite element model to investigate the mechanism of starch gelatinization during steaming. The integrated model was able to quantitatively simulate the gelatinization phenomenon.

INDEX WORDS: Cowpea, Steaming, Finite element method, Heat and mass transfer, Starch gelatinization, Weevil

FINITE ELEMENT MODELING OF PHYSICOCHEMICAL CHANGES DURING STEAMING OF COWPEA SEEDS

by

CHUN FANG

B.Eng., China Agricultural University, 1991

M.Eng., China Agricultural University, 1997

A Thesis Submitted to the Graduate Faculty of The University of Georgia in Partial Fulfillment of the Requirements for the Degree

MASTER OF SCIENCE

ATHENS, GEORGIA

2000

FINITE ELEMENT MODELING OF PHYSICOCHEMICAL CHANGES DURING STEAMING OF COWPEA SEEDS

by

CHUN FANG

Approved:

Major Professor: Manjeet S. Chinnan

Committee: Chi N.Thai
Robert D. Phillips

Electronic Version Approved:

Gordhan L. Patel
Dean of the Graduate School
The University of Georgia
December 2000

ACKNOWLEDGEMENTS

I would like to express my sincere gratitude to my advisor and major professor, Dr. Manjeet S. Chinnan for his guidance, patience, support and encouragement during my studies at UGA. I am very grateful to the members of my committee, Dr. Chi N.Thai and Dr. Robert D. Phillips for their valuable advice during my research. I am very thankful to Dr. Boo-Yong Lee for his advice and assistance.

I would like to extend my thanks to Mr. Glenn D. Farrell for his excellent technical assistance in experiments; Ms. Vijaya Mantripragada for her proofreading and corrections of manuscripts.

I am grateful for all the financial support I received during my graduate studies from the Office of Assistant Dean of Griffin Campus, Department of Biological and Agricultural Engineering, and the USAID Bean/Cowpea CRSP (Collaborative Research Support Program) Project.

Finally, I am thankful to all those people who helped me at the Center for Food Safety and Quality Enhancement and the Department of Biological and Agricultural Engineering.

TABLE OF CONTENTS

CHAPTER 1

INTRODUCTION

Cowpeas (*Vigna unguiculata*) are widely grown in warm to hot regions of the world since they are an important source of vegetable protein, particularly in low-income countries. However, cowpea weevil (*Callosobruchus maculates*) infestation during cowpea storage, together with the inherent anti-nutritional and indigestible substances in cowpea seeds has discouraged their use. The cowpea weevil is a very serious post-harvest pest. Weevil infestation during cowpea storage leads to very high post-harvest losses every year. On the other hand, cowpea contains certain anti-nutritional factors like trypsin inhibitors, phytic acid, oxalic acid, tannin; and indigestible oligosaccharides-verbascose, stachyose and raffinose. These factors reduce the bioavailability of proteins and minerals in cowpeas. Hence, acceptability and availability of cowpeas as human food is below their potential.

Steaming of cowpea seeds has not only reduced the inherent anti-nutritional factors but also successfully prevented weevil infestation. Starch is a major component of cowpea seeds. The starch gelatinization and retrogradation during steaming and subsequent drying treatment leads to complex physicochemical, structural and functional changes in cowpeas, which may lead to its resistance to cowpea weevil penetration and digestion.

The focus of this study is gelatinization of cowpea starch during the steam treatment. Starch gelatinization in intact seeds during steaming is based on simultaneous heat and mass transfer as well as the interaction rate between water and seed starch. Localized temperature and moisture contents vary inside the seeds during steaming. Hence, the rate of gelatinization is a function of spatial temperatures and moisture

contents, which vary with position and time within seeds. The heat and mass transfer within the seeds occur very rapidly during the steaming process. It is very difficult to determine the transient behavior merely from experimental methods. Hence, computer modeling, together with the experimental methods helped to quantitatively investigate transient heat and mass transfer behaviors and physicochemical changes encountered in steaming of cowpea seeds. A clear knowledge of the mechanism of heat and mass transfer and starch gelatinization behavior will further enable us to design effective methods to combat weevil infestation.

A finite element model was developed to describe the behavior of heat and mass transfer successfully (Chapter 3). The prediction from the model agreed well with the experimental data even though the model slightly underestimated temperature during the initial steaming phase. The modeling was able to describe well the different transport mechanisms, which varied and interacted with each other during the steaming process. The assumptions for the model were supported reasonably well by the experimental and predicted data.

Construction of kinetics of starch gelatinization was carried out using cowpea flour under heat-moisture treatment, in which various combinations of moisture content and heating time were designed to obtain gelatinization rate constants, k, at a constant temperature of 100°C (Chapter 4). The heat-moisture treated cowpea starch gelatinized over a range of moisture content during steaming of cowpea seeds. This starch gelatinization kinetics, together with the model already constructed for heat and moisture transfer (Chapter 3), was applied to investigate the process of starch gelatinization in cowpea seeds during steaming (Chapter 5).

The predicted degree of gelatinization in outermost layer of seeds was found to be in good agreement with experimental data. The combined model was able to describe the process of gelatinization in steaming of cowpea seeds (Chapter 5).

Through interpretation of NMR imaging, combined with finite element modeling, the prediction accuracy of the combined model would be further improved. The cowpea digestibility and physicochemical changes after steaming and solar drying treatment needs to be further investigated. To find satisfactory answers to questions about the treatment and its effect on weevil infestation, further investigation is needed.

CHAPTER 2

LITERATURE REVIEW

Cowpeas (*Vigna unguiculata*) are widely grown in many countries throughout the world since they are an important source of vegetable protein, particularly in low-income countries. Worldwide cowpea production was 3.28 million tonnes from 8.6 million hectares in warm to hot regions of the world in 1999 (FAO, 2000). However, cowpea weevil infestation during seed storage together with the inherent anti-nutritional and indigestible substances in seeds has discouraged their utilization.

Weevil infestation of cowpea seeds during storage leads to significant post-harvest losses. The cowpea weevil is a very serious post-harvest pest. In just three months, the weevil can destroy 50% of the stored cowpea seeds. In West Africa alone, cowpea weevil losses were estimated to exceed $50 million annually (Bean/Cowpea CRSP, 2000). On the other hand, overshadowing the nutritional components of cowpeas are certain anti-nutritional factors like trypsin inhibitors, phytic acid, oxalic acid, tannin; and indigestible oligosaccharides- verbascose, stachyose and raffinose. These factors reduce the bioavailability of proteins and minerals in cowpeas. Thus, acceptability and availability of cowpeas for human consumption is well below their immense potential.

STEAM TREATMENT OF COWPEA SEEDS

Steaming of cowpea seeds resulted in significant decrease in tannic acid (Annih-Bonsu et al., 1996) and greatly reduced trypsin inhibitor and indigestible oligosaccharides (Wang et al., 1997). However, steaming treatment had less effect on loss of nutrients than soaking and water blanching treatment (Wang et al., 1997).

Recently steaming has been proposed as a simple treatment to control storage stability of cowpea seeds. The treatment has been successful in preventing weevil infestation. Fifteen minutes of steaming and subsequent solar drying can provide complete protection from cowpea weevil (Sefa-Dedeh et al., 1995a). Cowpea seeds were steamed at atmospheric pressure for 5, 10 and 15 min, followed by solar drying (35-45°C) for 14 hours. After the treated seeds had been inoculated with five-paired weevil adults per 40 g of seeds; the weevil eggs on treated seeds were not significantly different from those on untreated seeds; there was no adult weevil emergence observed on the steam and solar heat treated cowpea seeds during six months of storage; on the contrary the untreated seeds and seeds treated by solar heat alone were completely destroyed by the cowpea weevil (Sefa-Dedeh et al., 1995b).

The process of steaming followed by solar drying leads to complex physicochemical, structural and functional changes in cowpeas that may contribute to resistance to weevil penetration and digestion.

COWPEA RESISTANCE TO WEEVIL DIGESTION

Etokakpan et al. (1982) investigated the effect of weevil infestation on the nutritive value of cowpeas. The results showed slight increase in ash, crude protein and crude fiber content of both infested cowpeas with and without insects when compared with un-infested cowpeas. On the other hand, there was a slight decrease in carbohydrate (excluding fiber) and crude fat content in both the infested samples. The changes in the values of seed nutrients were statistically significant ($P<0.05$). The difference in carbohydrate content (excluding fiber) of infested seeds showed that the insects consumed the carbohydrates and converted it into calories.

Starch is a major component of dry cowpea seeds. Total carbohydrate content in cowpeas varies from 55-58%, of which starch alone accounts for 34 to 52% (Okechukwu et al., 1992; Kerr et al., 2000). Weevils digest cowpea starch by generating α-amylase

(Silva et al., 1999). It was reported that the cowpea weevil problems could be reduced through the development of insect resistant cowpeas, by transforming α-amylase inhibitor (α-AI) gene (Schroeder et al., 1995). Shade et al. (1994) transformed peas (*Pisum sativum*) with the α-AI-Pv gene driven by a strong seed-specific promoter. The levels of α-AI protein in the pea seeds were as high as in bean seeds and the transgenic peas were resistant to cowpea and azuki bean weevils. Morton et al. (2000) transferred the cDNA encoding the α-AI found in seeds of the common bean into pea. The α-AI in the transgenic pea seeds accumulated up to 3% of the soluble protein. The α-AI-1 in pea seeds can provide complete protection against the pea weevil and protected peas from the weevil under field conditions. The α-AI-1 resulted in larval mortality at the first or second instar; the primary effect of α-AI-2 appeared to be a delay in the maturation of the larvae.

Steam treatment of cowpea seeds is a typical heat-moisture treatment. Heat-moisture treatment refers to the exposure of starch to higher temperatures, commonly above the gelatinization temperature, at very restricted moisture content (18-27% w.b.) (Lilia & Harold, 1999). The heat-moisture treatment of starches has been known to produce remarkable changes in the crystallinity of starch molecules in the granules due to rearrangement or higher degree of association of the starch chains. The treated starch increases the gelatinization temperature and decreases the gelatinization enthalpy, the viscosity peak in its Brabender diagram and the endothermic peak in its DSC curve (Maruta et al., 1998). Maruta et al. (1998) found that enzyme-resistant starch was drastically increased 2-3 fold by reduced-pressurized heat-moisture (steam) treatment in high amylose starch more than that in non-treated high amylose starches.

Gelatinized starch, upon cooling, undergoes a relatively slow re-association process commonly termed retrogradation. During retrogradation, starch molecules re-associate and form tightly packed structures stabilized by hydrogen bonding. The association process could be driven further by dehydration (Haralampu, 2000). The

retrograded starch, usually called type III resistant starch, is an indigestible starch and provides no energy.

Similar to the effect of α-amylase inhibitor on cowpea weevil's digestion, the gelatinization and retrogradation of cowpea starch during steaming and subsequent drying treatment may generate enzyme resistant starch that resists digestion in cowpea weevil.

COWPEA RESISTANCE TO PENETRATION OF COWPEA WEEVIL

Some natural physical factors of cowpeas, such as pod wall strength and seed coat thickness prove to be practical means of insect control. Kitch et al. (1991) studied the pod and seed coat resistance to the cowpea weevil. The results suggested that the interactions between pod wall and seed coat characteristics played an important role in the resistance of cowpea to the weevil.

It was suggested that cowpea seeds may be subjected to steaming and subsequent drying treatments to result in the hardening of outer layer, which might have implications of controlling insect infestation damage to seeds during storage (Romey et al., 1998).

Many researchers have studied the effect of heat-moisture treatment on the physicochemical properties of starchy crops. Ong and Blanshard (1995a) proposed that amylose content and the structure of amylopectin were responsible for those architectural features in the granules, which governed these interactions and hence determined the ultimate texture of the cooked, parboiled rice. Hard parboiled rice tended to have a higher amylose content and more of the longer-chain amylopectin than soft cooking rice, a feature which was thought to encourage more extensive intra and/or inter molecular interactions with other components in rice grain, such as protein, lipid and non-starch polysaccharides resulting in a firmer texture. Parboiled rice samples which had all three states of starch (i.e. ungelatinized and recrystallized amylopectin plus the amylose-lipid complex) possessed the hardest eating property but the lowest solubility (Ong &

Blanshard, 1995b). Structure and physicochemical properties of heat-moisture treated legume starches were influenced by the interactions of the amylose content, arrangement of amylose chains, amylose and amylopectin chain lengths, the orientation of starch crystallites and the changes to the granular surface (Hoover & Manuel, 1996).

Gelatinization and retrogradation of cowpea starch during steaming and subsequent drying treatment affect the physicochemical properties of cowpea seed, which may lead to resistance to penetration of cowpea weevil.

OBJECTIVES OF THIS STUDY

This research focused on the gelatinization of cowpea starch during the steaming of cowpea seeds. Starch gelatinization is based on simultaneous heat and mass transfer phenomena, which cause a series of physical, chemical and structural transformations. First, this requires a clear understanding of the heat and mass transfer to investigate the simultaneous physicochemical changes within cowpeas during steaming. The objectives of this study are:

1. To develop a finite element model (FEM) describing heat and mass transfer during steaming of cowpea seeds and to validate the model experimentally
2. To determine kinetics of cowpea starch gelatinization by an isothermal method
3. To predict the degree of cowpea starch gelatinization during steaming by combing FEM model and kinetics model
4. To validate the predicted starch gelatinization values.

REFERENCES

Annih-Bonsu, F. A. M., Sefa-Dedeh, S. & Sakyi-Dawson, E. O. (1996). Effect of processing on anti-nutritional factors in cowpea and cowpea-fortified cereals. UGL-CRSP working paper 96-6.

Bean/Cowpea CRSP. (2000, October 1). Contributions to agriculture in developing countries. Retrieved October 16, 2000 from CRSP on the World Wide Wed: http://www.isp.msu.edu/crsp/crsphc.htm

Etokakpan, O. U., Eka, O. U. & Ifon, E. T. (1982). Chemical evaluation of the effect of pest infestation on the nutritive value of cowpeas (V*igna unguiculata*). Food Chemistry. 12: 149-157

FAOSTAT, (2000, October 27). FAO Statistical Databases. Agriculture Data. Retrieved October 30, 2000 from FAO on the World Wide Web: http://apps.fao.org/page/collections?subset=agriculture

Haralampu, G. G. (2000) Resistant starch - a review of the physical properties and biological impact of RS_3. Carbohydrate Polymers. 41: 285-292.

Hoover, R. & Manuel, H. (1996). Effect of heat-moisture treatment on the structure and physicochemical properties of legume starches. Food Research International. 29 (8): 731-750.

Kerr, W. L., Ward, C. D. W., McWatters, K. H. & Resurrection, A. V. A. (2000). Effect of milling and particle size on functionality and physicochemical properties of cowpea flour. Cereal Chemistry. 77 (2). 213-219.

Kitch, L. W., Shade, R. E., & Murdock, L. L. (1991). Resistance to the cowpea weevil (C*allosobruchus maculatus*) larva in pods of cowpea (V*igna unguiculata*). Entomologia Experimentalis Et Applicata. 60 (2): 183-192.

Lilia, S.C., & Harold, C. (1999). Heat-moisture treatment effects on sweet potato starches differing in amylose content. Food Chemistry. 65: 339-346.

Maruta, I., Kurahashi, Y., Takano, R., Hayashi, K., Kudo, K. & Hara, S. (1998). Enzymatic digestibility of reduced-pressurized, heat-moisture treated starch. Food Chemistry. 61 (1/2): 163-166.

Morton, R. L., Schroeder, H. E., Bateman, K. S., Chrispeels, M. J., Armstrong, E. & Higgins, T. J. V. (2000). Bean alpha-amylase inhibitor 1 in transgenic peas (*Pisum sativum*) provides complete protection from pea weevil (*Bruchus pisorum*) under field conditions. Proceedings of the National Academy of Sciences of the United States of America. 97 (8): 3820-3825.

Romey, N. S., Chinnan, M. S., Phillips, R. D. & Sefa-Dedeh, S. (1998). Physical and functional changes resulting from hydrothermal treatment of whole cowpea seeds. Bean/Cowpea CFSQE Project Report. Center for Food Safety and Quality Enhancement. University of Georgia. Griffin. GA.

Okechukwu, P. E., Rao, M. A., Ngoddy, P. O. & McWatters, K. H. (1992). Firmness of cowpea gels as a function of moisture and content, oil content, and storage. Journal of Food Science. 57: 91-95

Ong, M. H. & Blanshard, M. V. (1995a). Texture determinants in cooked, parboiled rice. I: Rice starch amylose and the fine structure of amylopectin. Journal of Cereal Science. 21: 251-260.

Ong, M. H. & Blanshard, M. V. (1995b). The significance of starch polymorphism in commercially produced parboiled rice. Starch/Starke. 45 (1): 7-13.

Shade, R. E., Schroeder H. E., Pueyo, J. J, Tabe, L. M., Murdock, L. L., Higgins, T. J. V. & Chrispeels, M. J. (1994). Transgenic pea-seeds expressing the alpha-amylase inhibitor of the common bean are resistant to bruchid beetles. Bio-Technology. 12 (8): 793-796.

Sefa-Dedeh, S. & Saalia, F. K. (1995a). Studies on weevil (*callosubruchus maculatus*) infestation of steamed cowpeas during storage. (Unpublished report). Department of Nutrition and Food Science. University of Ghana. Legon.

Sefa-Dedeh, S., Allotey, J., Osei, A. K. & Collison, E. K. (1995b). Effect of steam and solar heat-treated cowpea seeds on some aspects of the developmental biology and control of *callosubruchus maculatus*. (Unpublished report) Department of Nutrition and Food Science. University of Ghana. Legon.

Schroeder, H. E., Gollasch, S., Moore, A., Tabe, L. M., Craig, G., Hardie, D. C., Chrispeels, M. J., Apencer, D & Higgins, T. J. V. (1995). Bean alpha-amylase inhibitor confers resistance to the pea weevil (*Bruchus-pisorum*) in transgenic peas (*Pisum-sativuml*). Plant Physiology. 107 (4): 1233-1239.

Silva, C. P., Terra, W. R., Xavier-Filho J, M. F. G., Lope, A. R. & Pontes. E. G. (1999). Digestion in larvae of *Callosobruchus maculates* and *Zabrotes subfasciatus* (*Coleoptera: Bruchidae*) with emphasis on alpha-amylases and oligosaccharidases. Insect Biochemistry and Molecular Biology. 29 (4): 355-366.

Wang, N., Lewis, M. J., Brennan, J. G. & Westby, A. (1997). Effect of processing methods on nutrients and anti-nutritional factors in cowpea. Food Chemistry. 58 (1/2): 59-68.

CHAPTER 3

FINITE ELEMENT MODELING OF HEAT AND MASS TRANSFER DURING STEAMING OF COWPEA SEEDS[1]

[1]Fang, C. and Chinnan, M. S. 2000. To be submitted to Journal of Food Engineering

The process of steaming cowpea seeds, which results in increased temperature and moisture content in the seeds, is not a simple process of conduction and diffusion. It is quite complex in that the ambient steam condensation (absorption) at the surface of the seeds leads to a rapid heat conduction and a slow diffusion of liquid water across the seeds; on the other hand, different transport mechanisms vary and interact with each other and result in starch gelatinization and other physicochemical changes in the seeds.

ASSUMPTIONS FOR HEAT AND MASS TRANSFER MODEL

1. Heat transfer
   - Latent heat is released from condensation of ambient steam on seed surface. Partial heat flow occurs between the seed surface and the surrounding by convection whenever temperature difference exists.
   - Heat conduction occurs within the seed whenever temperature gradient exists.
2. Mass transfer
   - Ambient steam vapor is permanently absorbed at the surface of the seed.
   - Moisture slowly diffuses from the surface of seed into the interior in liquid form.
3. Driving force for mass transfer
   - Vapor pressure differences at the seed surface
   - Moisture gradient in the seed interior
4. Seed is homogeneous and isotropic.
5. Moisture absorption leads to negligible swelling.
6. Cowpea seed is simplified as an axisymmetrical model.
7. Initial temperature and moisture content are uniformly distributed.

1. Heat transfer

Stapley et al. (1999) studied the steaming of whole wheat grains and reported that in the initial heating phase, condensation of steam on the surface of samples raised the sample temperature from its initial temperature to steam temperature. Most of this heating resulted from the latent heat released upon condensation of steam on the cold sample. After a short initial heating phase, that took just a few seconds, the process entered main steaming period, during which water was slowly but permanently taken up by the seeds and the temperature of the sample varied only slightly above steam temperature. Stapley et al. (1997a) found that the grain temperature was typically 2-4°C higher than that of steam itself, and that the actual temperature difference might have been higher. This phenomenon was caused by the release of latent heat of condensation (more correctly, absorption) to the grain, whereby moisture was taken up and converted from steam phase to liquid water at the surface. The release of latent heat from condensation raised the seed temperature higher than that of the surrounding steam and was ultimately conducted away by convection.

Hence, it can be assumed that the heat transfer during steaming includes the latent heat released from condensation on the seed surface, the heat flow by convection between the surface and the ambient steam as well as the heat conduction within the seeds; and there is no condensation film on the surface since the temperature of the seed remains above that of steaming during the main steaming period.

2. Mass transfer

Stapley et al. (1997b) reported that there was a large initial uptake of moisture by condensation (adsorption) of water on the surface of the grain in the initial stages of steaming. NMR imaging results for steamed wheat grains showed a much more uniform moisture profile across the grain, and the levels rose slowly with steaming time. DSC (Differential Scanning Calorimetry) of steamed whole grains further supported the uniform moisture profiles in the grain; Steamed grains showed a much narrower

gelatinization temperature range than boiled grains. A more uniform moisture gradient distribution can easily account for this observation (Stapley et al., 1997a).

It is reasonable to assume that steam vapor is taken up only on the surface of the seeds where it converts from the steam phase to liquid water. Moisture slowly diffuses from the seed surface to the interior in liquid form.

3. Driving force for mass transfer

On the surface of seeds, the driving force can be assumed to be the vapor pressure difference between the seed surface vapor pressure and that of ambient steam (Stapley et al., 1999). During the steaming process, the surface vapor pressure throughout the seeds remained below the saturation vapor pressure of ambient steam. Before the surface temperature of seeds rose above that of steam, the vapor pressure difference was produced mostly by temperature difference between the cold seed surface and the hot ambient steam. After the surface temperature rose above that of steam, the vapor pressure at the seed surface was lowered by chemical affinity between seed starch (and/or other seed components) and water. Stapley et al. (1999) reported that the chemical affinity between starch and water allowed absorption to occur despite the grain being at a higher temperature than the surrounding steam.

The driving force can be expressed in terms of partial pressure differences. The sample vapor pressure, P_s is related to the surface water content, M_s, and the surface temperature, T_s, through a water activity function, $P_s = P(T_s) * \alpha(T_s, M_s)$. Where, $P(T_s)$ is the saturated vapor pressure of water at the sample surface temperature, T_s. $\alpha(T_s, M_s)$ is water activity at surface temperature and moisture content (Stapley et al., 1999).

Driving force for mass transfer in the seed interior is due to the moisture gradient existing within the seed.

4. Seed is homogeneous and isotropic

Several microstructures of raw cowpeas can be seen distinctly: starch granules, protein bodies, cell wall and the middle lamella by using scanning electron microscopy

(Sefa-Dedeh et al., 1978). The primary cell wall in cowpeas consists of cellulose microfibrils that are loosely woven together in an irregular pattern and embedded in an amorphous matrix (Sterling, 1963). Sefa-Dedeh and Saalia (1995) studied the contribution of cowpea seed coat to water uptake during steaming. The decorticated seeds and intact seeds were steamed for different time intervals and then compared for moisture gain after steaming. The experimental data showed that the seed coat of cowpea did not significantly affect the water uptake during steaming. NMR imaging results for steamed wheat grains showed essentially uniform moisture profile across the wheat grain and the levels rose slowly with steaming time (Stapley et al., 1997b).

Hence, whole cowpea is assumed to consist of homogeneous and isotropic material.

5. Moisture absorption leads to negligible swelling

Sefa-Dedeh and Saalia (1995) reported that a 5 min steaming process raised the moisture content of cowpea seeds from 13.00 in the unsteamed seeds to 16.01% (w.b.). The samples that were steamed for 10 minutes had 17.25% moisture content (w.b.).

This suggested that the length of time of steaming did not have a strong influence on moisture gain. Based on the preliminary experiments, the overall moisture uptake during steaming was much slower than that of boiling, starch granule swelling in the outer layer resulted in an increased resistance to water diffusion into the interior of seed and restricted the overall swelling of the whole seed. The volume swelling was considered negligible in this study.

6. Cowpea seed is simplified as an axisymmetrical model.

To simplify the model to an axisymmetrical problem, the seed is assumed to have a circular cross section vertically.

7. Initial temperature and moisture content are uniformly distributed

The cowpea seeds were stored under room temperature for 2 weeks to equilibrate moisture and temperature and then used for experiments.

HEAT AND MASS TRANSFER MODEL

Transient heat and mass transfer in a cylindrical coordinate system is governed by Fourier's equation for heat transfer:

$$\nabla^T(rK\nabla T) + rq_v = r\rho c_p \frac{\partial T}{\partial t} \tag{1}$$

and, Fick's equation for mass transfer:

$$\nabla^T(rD\nabla M) = r\frac{\partial M}{\partial t} \tag{2}$$

Initial condition:

$$T(r,z,0) = T_0 \tag{3}$$

$$M(r,z,0) = M_0 \tag{4}$$

Boundary conditions along the surfaces:

a) Heat transfer due to convection and condensation (or absorption):

$$-rK\frac{\partial T}{\partial n}\Big|_\Gamma = rh_t(T_s - T_{st}) - r[\lambda - c_{st}(T_s - T_{st})]\frac{\partial[\int_{(v)} M(r,z,t)\rho dv]}{\partial t \cdot \int_{(S)} dS} \tag{5}$$

The heat flow is positive if heat is moving out of the sample and is in the direction opposing temperature increase. The Eqs. (1) and (2) are coupled due to introduction through the time derivative term of Eq. (5), which includes the effect of mass transfer on heat transfer. The expression is approximate due to using the total average moisture variation per surface area unit. (n is the outward normal unit vector to the boundary, which is assumed positive in the outward direction).

b) Moisture transfer due to condensation (or absorption):

$$-rD\rho\frac{\partial M}{\partial n}\Big|_\Gamma = rh_m(P_s - P_{st}) \tag{6}$$

In Eq. (6), P_s is the function of temperature and moisture content at the sample surface, which introduces the effect of heat transfer on mass transfer. Eqs. (1) and (2) are two-

way coupled by the boundary conditions Eqs. (5) and (6) that may better describe the simultaneous heat and mass transfer phenomena.

One half of longitudinal section of a cowpea seed was first divided into 3 layers, and each layer was further divided into 3-node linear triangular elements (Fig. 3.1). Within each element, the temperature and moisture were expressed in terms of the temperature or moisture at its three nodes:

$$T^{(e)}(r,x,t) = [N^{(e)}(r,z)]\{T\} \tag{7}$$

$$M^{(e)}(r,x,t) = [N^{(e)}(r,z)]\{M\} \tag{8}$$

Taking the weights (W_l, l=i, j, m) same as the interpolation functions (N_l). Employing the Galerkin weighted residual method to the Eqs. (1) and (2) and setting the residual of the weighted errors to zero

$$\iint_{\Omega} W_l[\nabla^T(rK\nabla T) + rq_v - r\rho c_p\frac{\partial T}{\partial t}]drdz = 0 \tag{9}$$

$$\iint_{\Omega} W_l[\nabla^T(rD\nabla M) - rD\frac{\partial M}{\partial t}]drdz = 0 \tag{10}$$

Using the Green's formula (integration by parts), Eqs. (9) and (10) can be stated as:

$$\iint_{\Omega}(K\nabla^T W_l\nabla T - q_v W_l + \rho c_p W_l\frac{\partial T}{\partial t})rdrdz - \int_{\Gamma} KW_l\frac{\partial T}{\partial n}rd\Gamma = 0 \tag{11}$$

$$\iint_{\Omega} D\nabla^T W_l\nabla M + W_l\frac{\partial M}{\partial t})rdrdz - \int_{\Gamma} DW_l\frac{\partial M}{\partial n}rd\Gamma = 0 \tag{12}$$

The equations can be written in matrix form:

For non-boundary elements as:

$$\begin{bmatrix} C_T & 0 \\ 0 & C_M \end{bmatrix}\begin{Bmatrix} \dot{T} \\ \dot{M} \end{Bmatrix} + \begin{bmatrix} K_T & 0 \\ 0 & K_M \end{bmatrix}\begin{Bmatrix} T \\ M \end{Bmatrix} = \begin{Bmatrix} F_T \\ F_M \end{Bmatrix} \tag{13}$$

where, C_T, C_M, K_T and K_M are global matrices and F_T, F_M(=0), T and M are global vectors of total nodes. These matrices and vectors were assembled from the following element matrices (matrix size of 3×3) and element vectors (size 3×1):

$$[C_T^{(e)}] = \rho^{(e)} c_p^{(e)} \iint_{(e)} [N]^T [N] r dr dz \tag{14}$$

$$[K_T^{(e)}] = \iint_{(e)} [B]^T [K][B] dr dz \tag{15}$$

$$\{F_T^{(e)}\} = q_v^{(e)} \iint_{(e)} [N]^T r dr dz \tag{16}$$

$$[C_M^{(e)}] = \rho^{(e)} \iint_{(e)} [N]^T [N] r dr dz \tag{17}$$

$$[K_M^{(e)}] = \rho^{(e)} \iint_{(e)} [B]^T [D][B] dr dz \tag{18}$$

For boundary elements:

$$\begin{bmatrix} C_T & 0 \\ 0 & C_M \end{bmatrix} \begin{Bmatrix} \dot{T} \\ \dot{M} \end{Bmatrix} + \begin{bmatrix} K_T & 0 \\ 0 & K_M \end{bmatrix} \begin{Bmatrix} T \\ M \end{Bmatrix} = \begin{Bmatrix} F_T \\ F_M \end{Bmatrix} \tag{19}$$

$$[K_T^{(e)}] = \iint_{(e)} [B]^T [K][B] dr dz + h_t \int_{\Gamma} [N_s]^T [N_s] r d\Gamma + \frac{\partial [\int_{(v)} \rho M(r,z) dv]}{\partial t \cdot \int_{(S)} dS} c_{st} \int_{\Gamma} [N_s]^T [N_s] r d\Gamma \tag{20}$$

$$\{F_T^{(e)}\} = q_v^{(e)} \iint_{(e)} [N]^T r dr dz + h_t T_{st} \int_{\Gamma} [N_s]^T r d\Gamma + \frac{\partial [\int_{(v)} \rho M(r,z) dv]}{\partial t \cdot \int_{(S)} dS} \{C_v T_{st} \int_{\Gamma} [N_s]^T r d\Gamma - \lambda^{(e)} \int_{\Gamma} [N_s]^T r d\Gamma\} \tag{21}$$

$$\{F_M^{(e)}\} = h_m \int_{\Gamma} P_s^{(e)} [N_s]^T r d\Gamma - h_m P_{st} \int_{\Gamma} [N_s]^T r d\Gamma \tag{22}$$

where, $[C_T]$, $[C_M]$ $[K_M]$ are the same as those of non-boundary elements. The detailed numerical formulation of Eqs. (13) and (19) is shown in Appendix.

Surface vapor pressure, P_s is a nonlinear function of sample surface temperature and moisture content. Gaussian-Legendre quadrate (three base points) was used for the numerical integration.

Eqs. (13) and (19) when combined can be written in a more general form as:

$$[C]\{\dot{U}\}+[K]\{U\}=\{F\} \tag{23}$$

where, $\{U\}^T=[T\ M]$ is the vector of unknown nodal temperature and moisture. Solution of Eq. (23) will result in the set of nodal temperature and moisture content values for every time step.

SOLUTION METHODOLOGY

Using backward difference method, Eq. (23) can be rewritten at time $t+\Delta t$:

$$[C]\{\dot{U}\}^{t+\Delta t}+[K]\{U\}^{t+\Delta t}=\{F\}^{t+\Delta t} \tag{24}$$

The time derivative in the backward difference is:

$$\{\dot{U}\}^{t+\Delta t}=\frac{\{U\}^{t+\Delta t}-\{U\}^{t}}{\Delta t} \tag{25}$$

Combining Eqs. (24) and (25) results in:

$$(\frac{[C]}{\Delta t}+[K])\{U\}^{t+\Delta t}=\frac{[C]}{\Delta t}\cdot\{U\}^{t}+\{F\}^{t+\Delta t} \tag{26}$$

The solution of U at time $(t+\Delta t)$ can be obtained from the solution at time t. the backward difference technique is unconditionally stable. The finite element equation is non-linear because the governing equation is nonlinear. The system capacitance matrices, [C] and conductance matrices, [K] are temperature and moisture dependent due to the temperature and moisture dependent physical and thermal properties.

Newton-GMRES method

Newton-GMRES method (Kelley, 1995) was used to advance the solution of non-linear finite element equations (Fig. 3.2). The values of density, $\rho^{(e)}$, thermal conductivity, $k^{(e)}$, latent heat, $\lambda^{(e)}$ and water activity, a_w were recomputed for each element and each iteration step during each time step using average temperature and moisture content of the element in this time step. Before each iteration during each time step and after all element matrices' modifications were completed, overall average temperature, $T_{ave}^{(v)}$, and moisture content, $M_{ave}^{(v)}$, were obtained by volume-averaging each

node temperature and moisture content values from the previous iteration. $T_{ave}^{(v)}$ and $M_{ave}^{(v)}$ were stored after convergence for next time step. The above solution method was coded in MATLAB version 5.3 /release 11 (cell_da.m, point_da.m, f.m, feasmbl1.m, feasmbl2.m, feeldof.m, dirder.m, givapp.m, fdgmres.m, tri_cont.m, tri-grid.m, solgmres.m, node.m and gcoord.m and so on, start MATLAB 5.0 or 5.3, type: solgmres).

Gaussian elimination method

Gaussian elimination method (Kwon & Bang, 1997) was used to solve the overall assembled equation (26). The calculation of temperature and moisture content was divided into 4 steps as follows (Fig. 3.3):

1) Calculation of amount of water uptake

The moisture content was calculated from the mass transfer Eq. (2). When the moisture content was known, the overall water uptake was determined by volume-averaging the moisture content difference at each node.

2) Computation of temperature at each node

The overall water uptake was added to the boundary Eq. (5) of heat transfer and the temperature at each node was computed from heat transfer Eq. (1).

3) Update of the amount of water uptake

Vapor pressure differences at the boundary Eq. (6) of mass transfer were calculated by using the new temperature at the boundary nodes according to the equation of saturated water vapor. The vapor pressure differences were added to the mass transfer equation to calculate new overall water uptake.

4) Recalculation of the temperature and moisture content at all nodes.

All thermophysical properties were upgraded by using the average values of the new temperature and moisture content and those at last time step. The temperature and moisture content at each node was recalculated by using the new values of water uptake and temperature. These steps were repeated within each time step until the total steaming time was achieved.

The solution method was coded in MATLAB version 5.3 /release 11 (cell_da.m, point_da.m, f.m, feasmbl1.m, feasmbl2.m, feeldof.m, tri_cont.m, tri-grid.m, solgauss.m, node.m and gcoord.m and so on, start MATLAB 5.0 or 5.3, type: solgauss). This solution method is simple and fast. The coupling effect of heat transfer and mass transfer is computed just once when the temperature and moisture content were recalculated again. Unlike the method of Newton-GMRES, the temperature and moisture content at each node were recalculated every time at each iteration.

GEOMETRIC MODELING AND MESH GENERATION

The geometric modeling and mesh generation were calculated by Algor® Superdraw III 12. Twenty points were measured using a caliper with 0.01mm resolution (Ultra-Cal Mark III, Fred. V. Fowler Co., Inc., Newton, MA) in short and long diameters along the longitudinal axis of symmetry (Z=0) and then the values were averaged. The Z and R coordinates of 20 points were matched by interpolating spline (Fig. 3.4).

THERMAL AND PHYSICAL PROPERTIES FOR THE MODEL

1. Specific heat, c_p (J kg/K)

Stapley et al. (1997a) concluded that grain moisture content was the most dominant factor influencing specific heat, and any effect of cooking (such as the glass transition of starch) on specific heat capacities was minor. The specific heat calculated by Siebel's equation neglects the effect of bound water and temperature. Siebel's equation has been found to agree closely with experimental values when M (w.b.) > 0.7 and when no fat was present (Toledo, 1991). Choi and Okos' correlation (1987) is more accurate at lower moisture contents and for a wider range of product composition.

The value of specific heat in the model was calculated based on Choi and Okos' equation. Table 3.1 shows the composition of cowpea seed (Deshpande & Damodaran, 1990).

Specific heat as a function of temperature, T, (°C) for various components of foods is as follows:

Water $c_w = 4176.2 - 9.0862e\text{-}5\times T + 5473.1e\text{-}6\times T^2$

Protein $c_{pr} = 2008.2 + 1208.9e\text{-}3\times T - 1312.9e\text{-}6\times T^2$

Fat $c_f = 1984.2 + 1473.3e\text{-}3\times T - 4800.8e\text{-}6\times T^2$

Carbohydrate $c_c = 1548.8 + 1962.5e\text{-}3\times T - 5939.9e\text{-}6\times T^2$

Fiber $c_{fi} = 1845.9 + 1930.6e\text{-}3\times T - 4650.9e\text{-}6\times T^2$

Ash $c_a = 1092.6 + 1889.6e\text{-}3\times T - 3681.7e\text{-}6\times T^2$

The specific heat of cowpea seed is a function of moisture content during steaming:

$$c_{tm} = M\times c_w + (1\text{-}M)\times x_{pr}\times c_{pr} + (1\text{-}M)\times x_f\times c_f + (1\text{-}M)\times x_c\times c_c + (1\text{-}M)\times x_{fi}\times c_{fi} + (1\text{-}M)\times x_a\times c_a$$

2. Thermal conductivity, k (W/mK)

The effect of variations in the composition of material on thermal conductivity has been reported by Choi and Okos (1987). Calculation of k from the thermal conductivity of pure component, k_i and the volume fraction of each component, x_{vi} follows:

$$k = \sum (k_i\, x_{vi})$$

Thermal conductivity of the pure component;

Water $k_w = 0.57109 + 0.0017625\times T - 6.7306e\text{-}6\times T^2$

Protein $k_{pr} = 0.1788 + 0.0011958\times T - 2.7178e\text{-}6\times T^2$

Fat $k_f = 0.1807 - 0.0027604\times T - 1.7749e\text{-}7\times T^2$

Carbohydrate $k_c = 0.2014 + 0.0013874\times T - 4.3312e\text{-}6\times T^2$

Fiber $k_{fi} = 0.18331 + 0.0012497\times T - 3.1683e\text{-}6\times T^2$

Ash $k_a = 0.3296 + 0.001401\times T - 2.9069e\text{-}6\times T^2$

The volume fraction, x_{vi} of each component is determined from the mass fraction;

Water $x_{wv} = M\times\rho/\rho_w$

Protein $x_{prv} = (1\text{-}M) \times x_p \times \rho/\rho_p$

Fat $x_{fv} = (1\text{-}M) \times x_f \times \rho/\rho_f$

Carbohydrate $x_{cv} = (1\text{-}M) \times x_c \times \rho/\rho_c$

Fiber $x_{fiv} = (1\text{-}M) \times x_{fi} \times \rho/\rho_{fi}$

Ash $x_{av} = (1\text{-}M) \times x_a \times \rho/\rho_a$

Individual densities of the pure component:

Water $\rho_w = 997.18 + 0.0031439 \times T - 0.0037574 \times T^2$

Protein $\rho_{pr} = 1329.9 - 0.5181401 \times T$

Fat $\rho_f = 925.59 - 0.41757 \times T$

Carbohydrate $\rho_c = 1599.1 - 0.32056 \times T$

Fiber $\rho_{fi} = 1311.5 - 0.36589 \times T$

Ash $\rho_a = 2423.8 - 0.28063 \times T$

3. Density, ρ (kg/m^3)

The density of cowpea seed changes with moisture content:

$\rho_{cowpea} = \rho_0 \times (1 - M_0)/(1 - M_{current})$

4. Vapor pressure at the sample surface, P_s (Pa)

The vapor pressure, P_s is related to the surface water content, M_s and the surface temperature, T_s of the sample through a water activity function $P_s = P(T_s)*a(T_s, M_s)$. Where $P(T_s)$ is the saturated vapor pressure of water at the sample surface temperature. Water activity, a_w can be evaluated as a function of the surface water content and temperature of the sample through a water activity model. However, these correlations for starchy food have not been well documented under high temperature.

Oswin's modified model was fitted with the experimental data that was measured at temperatures ranging between 100 and 140°C for potato starch (Bassal et al., 1993):

$$M = (k_1 + k_2 T)\left[\frac{a_w}{1 - a_w}\right]^{(k_3 + k_4 T)} \quad (27)$$

According to the equation, the vapor pressure on sample surface can be calculated as:

$$P_s = P(T_s)^* a_w(T_s, M_s) \quad (28)$$

However, the simulated results were much underestimated by using the correlation in this heat and mass model. Stapley et al. (1999) suggested that the starch sorption isotherms were nonlinear, but for the range of moisture content that is of interest to us, it could be approximated satisfactorily by a straight line:

$$P_s = P(T_s)^* a_w(T, M) = P(T_s)^* \gamma^* M_s \quad (29)$$

Where, $\gamma = 1.82$

According to Teten's equation (Weiss, 1977), saturated water vapor pressure at the evaporating surface, P_s can be calculated at T_s, (°C):

$$P(T_s) = P_{sat} = 610.78 \exp\left(\frac{17.2693882 T_s^{(e)}}{T_s^{(e)} + 237.30}\right) \quad (30)$$

5. Latent heat, λ (J/kg)

According to Weiss (1977), latent heat can be calculated at T_s, (°C) as:

$$\lambda = 2.5008 \times 10^6 - 2366.8T \quad (31)$$

6. Mass transfer coefficient, h_m (s/m or kg_{water}/Pa m^2s)

There is no available data on mass transfer coefficient during the steaming of cowpea seeds. The values of mass transfer coefficient were calculated by direct application of the following equation (Marek, 1997):

$$h_m = -\frac{d\bar{M}/dt}{S(a_w(M)P_s - P_{st})} \quad (32)$$

where, M is moisture content (decimal, d.b.) and $a_w = 1.82M$

7. Heat transfer coefficient, h_t (W/m^2 K)

The overall heat balance during steaming can be calculated by the equation as (Stapley et al., 1999):

$$h_t S(T - T_{st}) = \lambda \frac{dM}{dt} - \frac{d([c_d W_d + c_w(W - W_d)]T)}{dt} \quad (33)$$

8. Moisture diffusivity, D (m^2/s)

The diffusion coefficient decreases with increasing temperature. As starch is gelatinized at the outer layer, the starch granule retains water, which then results into granule swell and restricting the moisture diffusion. Thus, higher temperatures result in greater local moisture capacity, ultimately resulting in a reduced diffusion coefficient across the gelatinized layer (Lund, 1984).

Little information could be found to fully describe water diffusion in starchy food during starch gelatinization. A power law relationship with moisture for effective moisture diffusivity, $D=9.5e\text{-}8*(M_{w.b.})^{3.5}$, which was reported for wheat grains during boiling (Stapley et al., 1998), was used in the numerical simulations.

MODEL TESTING

It is not possible to obtain an exact solution to the problem of the two-way coupled nonlinear parabolic partial differential equations (Miketinac et al., 1992). Prior to applying the model, the heat transfer of the model (solved by Newton GMRES method and Gaussian method) was validated by comparing the solutions to those calculated using commercial software under the same geometry, material properties and boundary conditions.

Since the commercial software, Algor could only analyze heat transfer, only the heat transfer part of the model was tested by assigning a zero value to mass transfer part of the model. Good agreements were found between the values predicted by the two programs.

The relative errors of all nodes are displayed in Fig. 3.5 after 60s respectively. All the relative errors at all nodes after 60 s are within 0.005% to 0.065%. The greatest relative error is at the node 116 due to the non-uniform mesh generation. The error decreased with increase in time. The results showed that Newton-GMRES method is more accurate than the Gaussian method.

MATERIALS AND METHODS

Sample preparation

Samples of cowpea seeds (*Vigna unguiculata*, cv. B5, C&F Food Inc., City of Industry, CA) were selected on the basis of seed weight and conformity to three specific dimensions of the seed: length, breadth, and thickness. Three measurements were taken using a caliper (Ultra-Cal Mark III, Fred. V. Fowler Co., Inc., Newton, MA). Cowpea seeds were previously stored at room temperature for 2 weeks to allow the initial moisture content within and among individual seeds to stabilize uniformly. Individual intact cowpea seeds were then vacuum-dried at 70°C for 9 days to evaluate the initial moisture content (Stapley et al., 1999). The samples were weighed before the steaming tests.

Instantaneous moisture content measurement

Individual sample seed, anchored by a nylon line, was suspended from a balance (Fisher Scientific, model A-250, Atlanta, GA) with a precision of ± 0.1 mg (Fig. 3.6). Deionized water was boiled at atmospheric pressure in a vessel to produce steam.

In order to produce saturated steam vapor free of any air, water droplets or superheat, the glass tube was preheated to 100°C by a heating cord. Three thermocouples were placed inside the tube to control its temperature and to keep the temperature of steam vapor at 100±0.45°C by adjusting the current and voltage of the heating cord. The deviation in steam temperature during the experiments was less than 1°C.

Vacuum pipes were used to absorb the outside vapor to protect the balance (Fig. 3.6). The vapor condensation could not only damage the balance but also affect accuracy. Steam vapor was continuously generated from boiling water in the vessel. When the seed was pulled up and held suspended in the glass tube, the lid of the vessel was quickly closed and steam vapor entered into the tube (in usually less than 1 s). The steaming process was timed from the moment the sample met with steam vapor and held for the required length of time. The weight of the sample was recorded every one second

by a computer which was connected to the balance. The increased mass was attributed to the water absorbed. The experimental tests were performed in triplicate.

Instantaneous temperature measurement

All thermocouples (T type, 0.5mm in diameter) were calibrated before beginning the tests. Two insulated thermocouples were inserted into predrilled holes in the seed (Fig. 3.7). Two holes were drilled from the seed surface along the horizontal centerline to a depth of 1 and 1.5 mm respectively. The holes were drilled using a pen-drill (Huot drill Y-HSD-74, 0.0225", St. Paul, MN) and the depth (1 and 1.5 mm) was carefully controlled with a drill stop fashioned out of stainless steel tubing. Another thermocouple was attached by carefully gluing it to the skin of the seed and exposing the thermocouple junction precisely at the surface.

Two thermocouples were hung near the suspended sample cowpea to read temperature of the heating steam and ensure accuracy between the thermocouples. All seeds were carefully cut after the test to check the actual thermocouple locations. These experimental tests were also performed in triplicates. All thermocouples were connected to a digital recorder (Hewlett Packard, model 34970 A, Atlanta, GA) for data acquisition.

RESULTS AND DISCUSSION

During the steaming process, there were two distinct phases with different behaviors of heat and mass transfer, which were distinguished by whether the temperature of whole seed registered above or below 100°C (Fig. 3.8).

1) The initial steaming phase, seed temperature ≤100°C

In the initial steaming phase (0-55 s), the latent heat liberated from water condensing on the cold seed surface raised the temperature of seed from its initial temperature to steam temperature and led to a rapid rise in moisture content at the surface. The length of the initial phase depended on the thermal response of sample. The amount of water condensation depended on the length of time the seed temperature took

to rise above that of the surrounding. The temperature at the cold surface of seed had the most dominant influence on heat and mass transfer.

2) The main steaming phase, seed temperature >100°C

In this phase (55-900s), the chemical affinity between water and cowpea starch had major effect on heat and mass transfer. The initial water condensation was followed by a steady increase in moisture content due to starch gelatinization in the outer layer of cowpea. During the main steaming phase, the amount of water absorption dependent on the chemical affinity between seed starch (or/and other seed components) and water. The temperature of the seed varied from 1-2°C above that of the surrounding. The difference in temperature slowly decreased in response to a decline in the rate of moisture uptake. The latent heat released was balanced by heat convection. The rate of heat and mass transfer was closely related to the chemical affinity between cowpea starch and water.

When the temperature of whole seed was below that of the surrounding, the direction of overall heat flow was negative and moved into the seed. As the temperature of the part of the seed rose above that of the surrounding, the latent heat was conducted away by conduction or convection. As the temperature of whole seed rose above that of the steam, the heat flow by convection eventually balanced the latent heat flow that was liberated from condensation or absorption. The direction of moisture flow in the seeds was always in the same direction as moisture increase (dM/dt) due to the pressure difference and chemical affinity between water and starch.

After the short initial steaming period that took 55 s, the sample temperature rose above 100°C; and after 30 s of steaming, there was no condensation observed on the surface of the cowpea seed. Table 3.4 shows that the overall moisture content of seeds increased to 22.7% (w.b.) after 60 min of steaming. This indicates that starch granule swelling resulted in an increased resistance to water diffusion into the interior of seed and restricted the overall swelling of the whole seed.

Estimation of average heat and mass transfer coefficients

The heat transfer coefficient of steam condensation is often calculated with empirical correlations of dimensionless numbers and combined with the effects of condensation and convection together, to obtain a high overall heat transfer coefficient. The heat flux of this model was separated into latent heat flow and heat flow by convection, which were related to the values of mass transfer coefficient and heat transfer coefficient respectively. The quantity of heat transfer coefficient is proportional to the amount of heat transfer by convection between the sample surface and the surroundings. The quantity of mass transfer coefficient is closely related to the amount of latent heat liberated from condensation at the sample surface. The transfer coefficients, h_t and h_m can be estimated by fitting the heat and mass balance equations jointly to experimental data (Mareck, 1997) or optimized by minimizing the residual sum of squares between $T_{simulated}$, $M_{simulated}$ and $T_{experimental}$, $M_{experimental}$ together (Miketinac et al., 1992). The latter procedure would require enormous computational time; hence, is not very practical.

In this study, the transfer coefficient, $h_{t,}$ and h_m were estimated experimentally by fitting the Eqs. (32) and (33) to the experimental data (dM/dt) (Fig. 3.9). The instantaneous values of h_t and h_m varied very much at each time step (time interval of 1 second). In order to avoid calculating coefficient values for small step, the h_m and h_t were calculated by averaging the two for the five distinct stages of the steaming process of cowpeas (Fig. 3.8).

The value (8.25e-8 (s/m)) of h_m was much higher in the first 5 seconds, decreased with time, and finally approached a constant value (1.80e-9 (s/m)) after the initial heating phase (Table 3.2). This value, 1.80e-9 (s/m) is close to the reported vlaue, h_m=1.57e-9 (s/m) for steaiming of whole wheat grains (Stapley et al., 1999).

The value of h_t was 252.8 (W/m^2K) in the first 5 s of steaming. The temperature of seed rose from 24.00 to 81.14°C in this phase and both heat flow by convection and latent heat contributed to the increase in seed temperature. During the period ranging

from 5s to 55s of steaming, the latent heat liberated from condensation was conducted away by convection and conduction within seeds and the temperature of the seed increased slowly; the direction of convection was reversed.

As for the main steaming phase, because the temperature of the seed changed slightly (1-2°C over steam temperature), latent heat was balanced by convection between the seed and the surroundings. The value of h_t can be calculated by the heat balance Eq. (34) as:

$$\lambda \frac{dM}{dt} = h_t S(T - T_{st}) \tag{34}$$

where

$$S_a^{(v)} = \sum_{e=1}^{m} \pi(r_j + r_m)\sqrt{(r_j - r_m)^2 + (z_m - z_j)^2} \quad (m^2) \tag{35}$$

The heat transfer coefficient, h_t=94.1 was obtained by assuming the temperature difference, $(T-T_{st})$ = 1.5°C. The value of h_t =-94.1 (W/m^2K) (Table 3.3) is close to the reported value, h_t = 108 (W/m^2K) for steaming of wheat grains (Stapley et al., 1999).

Moisture and temperature profiles with Newton-GMRES method

The moisture profiles (Figs. 3.11-3.12) show the coupled effect of heat and mass transfer. During the initial steaming phase, the simulated moisture profiles showed that moisture content was highest at the surface of mid-section while an opposite trend was observed for the temperature gradients (Fig. 3.11). During the initial stage, much more water condensed on the mid surface of the seed than on other locations. The rapid temperature increase at the top and bottom surface significantly reduced the driving force for mass transfer. The temperature at the top and bottom surface of cowpea seed exceeded 100°C after 55 s of steaming and was higher than that of steam vapor. The temperature at mid-surface increased slower than that of other locations. The lower temperature at the mid-surface enabled it pick up more moisture by condensation from the ambient steam. The highest moisture content at the surface of top and bottom sections indicates that there was no coupled effect after 600 s of steaming, because

temperatures were uniformly distributed within the seed during the main steaming phase (Figs. 3.13-3.14). The highest moisture content at the surface of top and bottom sections was due to the higher surface-area to volume ratio at the top and bottom sections compared with other locations. The major moisture content gradient was built up on the outermost layer of the seed during the whole steaming process. The liquid moisture gradient slowly moved toward the center of the sample due to low water diffusivity. The maximum predicted moisture content at the mid surface of the cowpea exceeded 50% (d.b.) after 50 s of steaming. The moisture content of the innermost layer remained at a low level after 15 min of steaming (Fig. 3.14). During the main steaming process, the temperature of seed was higher than that of the surrounding (Figs. 3.12-3.14). In addition, the temperature gradient was almost negligible.

Moisture profiles during initial stages of steaming were not smooth contour lines, particularly near the edges and innermost layer. Also, the moisture contour of the innermost layer was not very different from the initial moisture content of the seed (12.9% d.b.). At the beginning of steaming, solutions were subject to disturbance due to an abrupt change of the boundary conditions in the initial steaming phase. Rough edges of the contour lines is probably due to few layers and less elements, only three considered in the seed as well as due to size and number of finite elements modeling the seed. More layers, finer mesh, and shorter time intervals can significantly correct this situation. The level of refinement applied in this study was a compromise between the required accuracy and the effectiveness of computations.

The solution of Newton-GMRES resulted from the two-way coupled set of heat and mass transfer equations due to the inclusion of moisture term in the heat transfer boundary and temperature term in the moisture transfer boundary. The temperature term was included in mass transfer boundary by introducing sample vapor pressure, (P_s) which is the exponential correlation of sample surface temperature, (T_s) and water activity, (a_w). A small deviation at the surface temperature could result in great change in the driving

force for mass transfer due to the exponential correlation. The rapid increase in T_s significantly reduced the driving force (P_s-P_{st}) for mass transfer. Similarly, small amount of moisture increase could produce large latent heat liberation resulting in an increase in the rate of heat transfer. In the initial steaming period, the moisture variation term in heat transfer boundary played the important role in heat transfer during steaming due to the latent heat release of steam vapor condensation.

Moisture and temperature profiles with Gaussian method

The moisture content, compared with the Newton GMRES method, on the surface appears to be uniformly distributed (top, mid and bottom sections) (e.g. Figs. 3.16 and 3.18); whereas this was not the case with the Newton-GMRES method computations. This is due to the fact that the coupled effect of heat and mass transfer was not completely performed in the Gaussian method computations and finer mesh was applied.

The change in temperature gradients with increased steaming time was similar in both computation methods (Gaussian and Newton-GMRES).

Comparison of observed and estimated moisture content histories

Plots of comparison of observed and estimated total moisture uptake histories of cowpea seed during 15 min of steaming are presented in Fig. 3.19. In the beginning of the steaming process, the predicted moisture uptake increased very rapidly, followed by a steady increase of moisture gain as steaming progressed. During the main steaming stage, the rate of change in moisture uptake and the temperature difference between the seed and the surrounding declined slightly as steaming time progressed further (Figs. 3.19 - 3.20). On comparing the observed and estimated moisture data, the maximum deviation was 1.63 (relative error 8.30%) and 1.56 mg (relative error 9.69%) from using Newton-GMRES and Gaussian methods, respectively.

Comparison of observed temperature at different locations

Observed surface temperature of cowpea seed rose faster than those of other two locations during the first 25 s of steaming (Fig. 3.20). The locations where temperature

was measured are shown in Fig. 3.7. The temperature at all the locations exceeded 100°C after steaming of 55 s. There was slightly less than 1 °C temperature difference among different points in the seed after 55 s steaming. The observed temperature at 1.5 mm below seed surface was typically 1 - 2 °C higher than the steam temperature after 100 s steaming. The reason might be that the vapor pressure inside the seed exceeded atmospheric pressure, resulting in the temperature of the seed to exceed steam temperature. The higher temperature at the center (1.5 mm below seed surface) over those of other locations was likely caused by heat convection that was switched to the opposite direction after the initial steaming and gradually lowered the temperature at the surface and 1.0 mm below the surface. The heat convection has a lesser effect on the center temperature. Another reason might be due to the drilled hole (1.5mm long), which allowed more ambient steam to release latent heat. This temperature difference between the seed and the surrounding steam gradually lapsed off at all points after 150 s (Fig. 3.20). The drop in the temperature difference indicated a slower rate of moisture uptake.

Comparison of observed and estimated temperature histories

In the previous section, it was discussed that the temperature at the surface was generally lower than at the center during the main steaming phase. This effect was not clearly supported by the profiles obtained from the simulations, because as the steaming progressed the temperature gradients between the surface and the interior diminished. It may be noted that if a different h_t value was used in computing the temperature profiles that it may be possible to get results similar to those observed.

For the Gaussian method, the maximum deviation of temperature at 1.5 mm below surface between observed and predicted values was 37.1°C (relative error: 50.0%) during the first 10s of steaming. The average deviation was 1.1°C (relative error: 1.2%) during 15 min of steaming (Fig. 3.21). The maximum deviation of surface temperature was 10.8°C (relative error: 12.0%) during 15 min of steaming. The average deviation of

surface temperature was 0.8°C (relative error: 0.8%) during 15 min of steaming (Fig. 3.22).

In case of Newton-GMRES method, the maximum deviation of temperature at 1.5 mm below surface was 36.2°C (relative error: 48.8%) during the first 10s of steaming. The average deviation was 0.9°C (relative error: 1.0%) during 15 min of steaming (Fig. 3.21). The maximum deviation of surface temperature was 12.0°C (relative error: 13.2%) in the 15 min of steaming. The average deviation of surface temperature was 0.8°C (relative error: 0.9%) during 15 min of steaming (Fig. 3.22).

Comparison of the Newton-GMRES and Gaussian methods

The model solved by Newton-GMRES took several hundred iteration steps at each time step (5 s) to obtain convergence (tol <1e-8). The reason was due to the highly sensitive coupling as well as temperature and moisture dependent physical and thermal properties. Since the moisture uptake and temperature changed very slightly during the main steaming phase, the convergence tolerance should be less than 1e-8. The Newton-GMRES solver took over 20 hours to simulate the 15-min steaming process. The method of Gaussian is simple and fast, usually taking 2-3 hours to solve the model. However, The predicted profiles obtained by Newton-GMRES method reasonably well described the coupled effect between heat and mass transfer.

The causes of errors

The current model ignored the product swelling, which most likely introduced some errors. Insufficient accuracy of thermophysical properties, which were obtained from the literature, may also have resulted in errors. Given the accuracy of thermophysical properties, we can expect to further improve.

CONCLUSIONS

The prediction from the model agreed well with the experimental data even though the model slightly underestimated temperature during the initial steaming phase.

Modeling was able to describe well the different transport mechanisms, which varied and interacted with each other during the steaming process. The assumptions for the model were supported reasonably well by the experimental and predicted data.

NOTATION

a_w Water activity

A Element area (m^2)

c Heat capacity (J/kg K)

[C] Capacitance matrix

d.b. Dry basis

D Moisture diffusivity (m^2/s)

dM/dt Rate of change of water uptake, (kg/s)

{F} Forcing vector

h_t Heat transfer coefficient (W/m^2K)

h_m Mass transfer coefficient ($kg_{water}/Pa\ m^2\ s$)

K Thermal conductivity (W/m K)

[K] Conductance matrix

M Moisture content

M.C. Moisture content

$$M_{ave}^{(v)} = \frac{\sum_{e=1}^{n} \frac{\pi A^{(e)}}{6}[(R + r_i)M_i^{(e)} + (R + r_j)M_j^{(e)} + (R + r_m)M_m^{(e)}]}{\sum_{e=1}^{n} \frac{2\pi}{3} A^{(e)} R} \qquad \text{(d.b.)}$$

n Outward normal unit vector to boundary

N Interpolation function

P Vapor pressure (Pa)

q_v Rate of inner heat generation (W/m^3)

r, z Cylindrical coordinates (m)

R $R=r_i+r_j+r_m$ (m)

S Surface area of whole cowpea (m^2)

t Time (s)

T Temperature (K)

$$T_{ave}^{(v)} = \frac{\sum_{e=1}^{n} \frac{\pi A^{(e)}}{6}[(R+r_i)T_i^{(e)} + (R+r_j)T_j^{(e)} + (R+r_m)T_m^{(e)}]}{\sum_{e=1}^{n} \frac{2\pi}{3} A^{(e)} R} \quad (K)$$

Δt Time difference (s)

{U} Temperature and moisture content vector

V Volume (m^3)

w.b. Wet basis

W Mass of cowpea seed (kg)

Wl Weight function

x Fraction of components

Greek letters

ρ Density (Kg/m^3)

λ Enthalpy of condensation, (J/kg)

∇^T $\nabla^T = [\frac{\partial}{\partial r} \quad \frac{\partial}{\partial x}]$

Γ Surface boundary (m^2)

Ω Domain of interest (m^3)

Subscripts

0 Initial

a Ash

ave Average

c Carbohydrate

d Dry material of cowpea seed

e Element

f Fat

fi Fiber

M Moisture

pr Protein

s Surface

st Steam

T Temperature

tm Temperature and moisture content

w Water

Superscripts

e Element

v Volume

REFERENCES

Bassal, A., Vasseur, J. & Loncin, M. (1993). Sorption isotherms of food materials above 100°C. Lebensmittel_Wissenschaft und_Technologie. 26 (6): 182-185.

Bressani, R. (1985). Nutritive Value of cowpea. Cowpea-Research, Production and Utilization. 353-361. Singh, S. R. and Rachie, K. O. John Wiley & Sons, New York.

Choi, Y. & Okos, M. R. (1987). Effects of temperature and composition on thermal properties of foods. In: Food Engineering and Process Applications, M. LeMaguer and P. Jelen eds. Vol. 1. 93-102. Elsevier Appl. Science Publishers, New York.

Deshpande, S. S., & Damodaran, S. (1990). Food legumes: Chemistry and technology. Advances in cereal science and technology. Vol. X. Y. Pomeranz, ed. 147:241. Am. Assoc. Cereal Chem. St. Paul, MN.

Kelley, C. T. (1995). Iterative methods for linear and nonlinear equations. 95:110. Siam. Philadelphia, PA.

Kwon, Y. W. & Bang, H. (1991). The finite element method using Matlab. 119:153. CRC Press, Inc. New York.

Lund, D. (1984). Influence of time, temperature, moisture, ingredients, and processing conditions on starch gelatinization. CRC Critical Reviews in Food Science and Nutrition. 20 (4): 249-273.

Marek, M. (1997). Air-drying of vegetables: evaluation of mass transfer coefficient. Journal of Food Engineering. 34: 55-62.

Miketinac, M. J., Sokhansanj, S., & Tutek, Z. (1992). Determination of heat and mass transfer coefficients in thin layer drying of grain. Trans. ASAE. 35 (6): 1853-1858.

Sefa-Dedeh, S. & Saalia, F. K. (1995). Studies on weevil (*callosubruchus maculatus*) infestation of steamed cowpeas during storage. (Unpublished report). Department of Nutrition and Food Science. University of Ghana. Legon.

Sefa-Dedeh, S., Stanley, D. W. & Voisey, P. W. (1978). Effects of soaking time and cooking conditions on texture and microstructure of cowpeas. Journal of Food Science. 43: 1832-1838.

Stapley, AGF. & Fryer, P. J. (1998). Diffusion and reaction in whole wheat grains during boiling. AIChE Journal. 44 (8): 1777-1789.

Stapley, AGF., Gladden, L. F. & Fryer, P. J. (1997a). A differential scanning calorimetry study of wheat grain cooking. International Journal of Food Science and Technology. 32: 473-486.

Stapley, AGF., Hyde, T. M., Gladden, L. F. & Fryer, P. J. (1997b). NMR imaging of the wheat grain cooking process. International Journal of Food Science and Technology. 32: 355-275.

Stapley, AGF., Landman, K. A., Please, C. P. & Fryer, P. J. (1999). Modeling the steaming of whole-wheat grains. Chemical Engineering Science. 54: 965-975.

Sterling, C. (1963). Texture and cell wall polysaccharides in foods. Recent Advances in Food Science. Ed. J. M. Leitch and D. M. Roberts. Butterworth. London.

Toledo, R. (1991). Fundamentals of Food process Engineering. Chapman & Hall. New York.

Weiss, A. (1977). Algorithms for the calculation of moist air properties on a hand calculator. Trans. ASAE. 20: 1133-1136.

Zanoni, B., Peri, C. & Bruno, D. (1995). Modeling of starch gelatinization kinetics of breadcrumb during baking. Lebensmittel_Wissenschaft und_Technologie. 28 (3): 314-318.

LIST OF TABLES

Table 3.1 Chemical composition of cowpea seed (Deshpande & Damodaran, 1990)

	Protein (x_p)	Fat (x_f)	Fiber (x_{fi})	Ash (x_a)	Carbohydrate (x_c)	Moisture Content (M)
Dry basis (%)	0.271	0.015	0.044	0.034	0.637	0.0
Wet basis (%)	0.240	0.013	0.039	0.030	0.564	0.114

Table 3.2 Calculation of average mass transfer coefficient, h_m, (s/m) by using Eq. (32)

Time interval (s)	a_w	dM/dt (kg/s)	S (m^2)	T_{st} (°C)	Average h_m (s/m)
0-5	1.82M	1.56E-06	2.6e-04	100.0	8.25E-08
5-10	1.82M	1.22E-06	2.6e-04	100.0	7.80E-08
10-20	1.82M	4.30E-07	2.6e-04	100.0	3.39E-08
20-55	1.82M	8.00E-08	2.6e-04	100.0	7.10E-09
55-900	1.82M*	1.38E-08	2.6e-04	100.0	1.80E-09

* Mean of moisture content (d.b.) at 55 and 900 s of steaming

Table 3.3 Calculation of heat transfer coefficient, h_t, (w/m^2 °C) by using Eq. (33)

Time interval (s)	dM/dt (kg/s)	T_{st}-T_s* (°C)	T_{st}-T_{seed}** (°C)	Average h_t (w/m^2 °C)
0-5	1.56E-06	76.00	57.14 (T_{seed} = 81.14)	252.8
5-10	1.22E-06	10.93	8.98 (T_{seed} = 90.12)	-526.8
10-20	4.30E-07	4.91	6.89 (T_{seed} = 97.01)	-381.2
20-55	8.00E-08	1.62	3.44 (T_{seed} =100.5)	-266.9
55-900	1.38E-08	-1.5	0 (T_{seed} = 101.5)	-94.1

*T_s = average temperature at surface of cowpea seeds

**T_{seed} = average temperature at three points of cowpea seeds (Fig. 7)

Table 3.4 The moisture content of cowpea seeds after various steaming intervals

Time (min)	0	1	5	10	15	20	30	60
M.C. (w.b.) %	11.4	16.4	17.4	18.4	19.2	19.7	20.6	22.7

LIST OF FIGURES

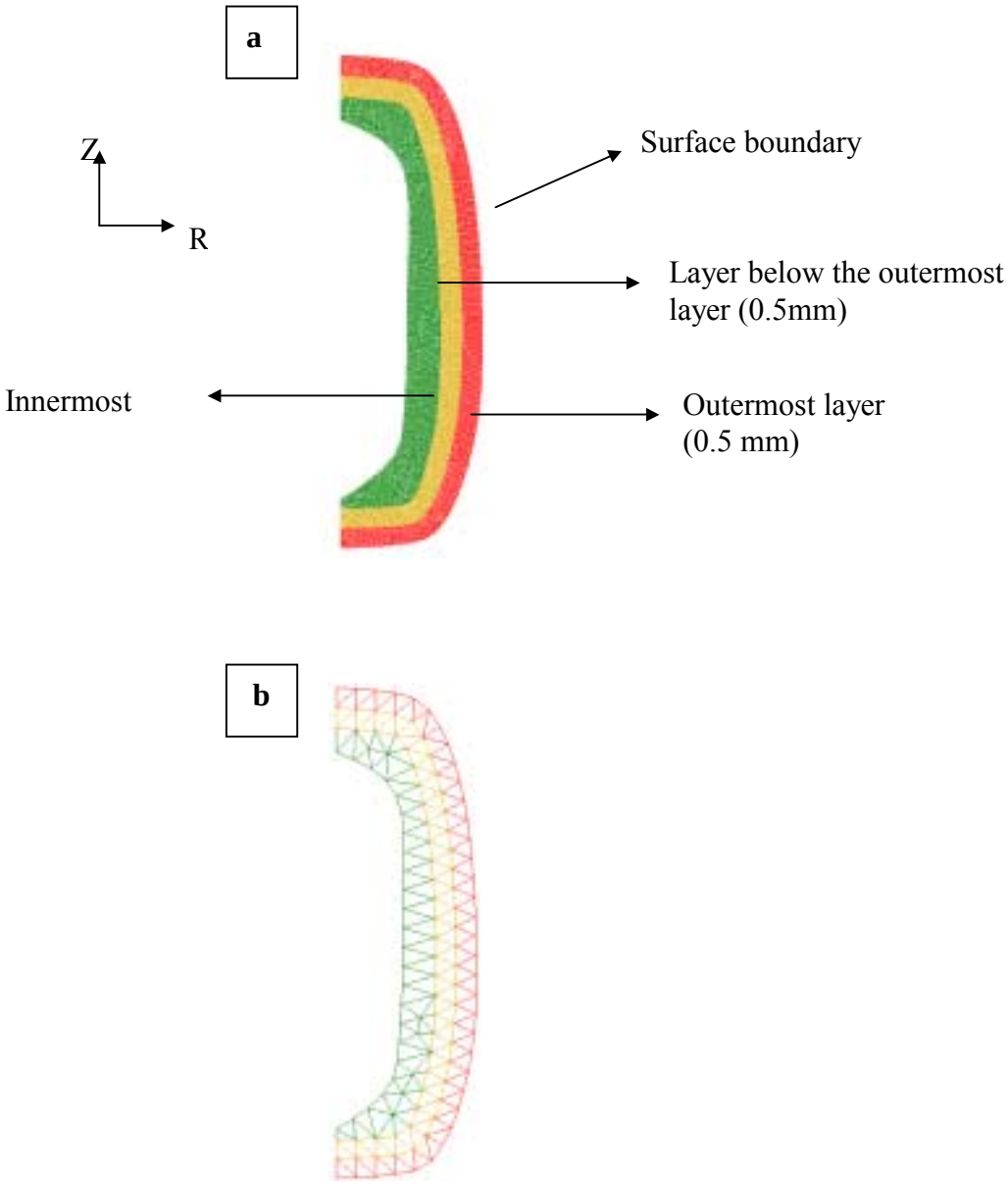

Fig. 3.1. Longitudinal section of a cowpea seed

a. Section divided into three layers

b. Triangular finite elements superimposed on the three layers

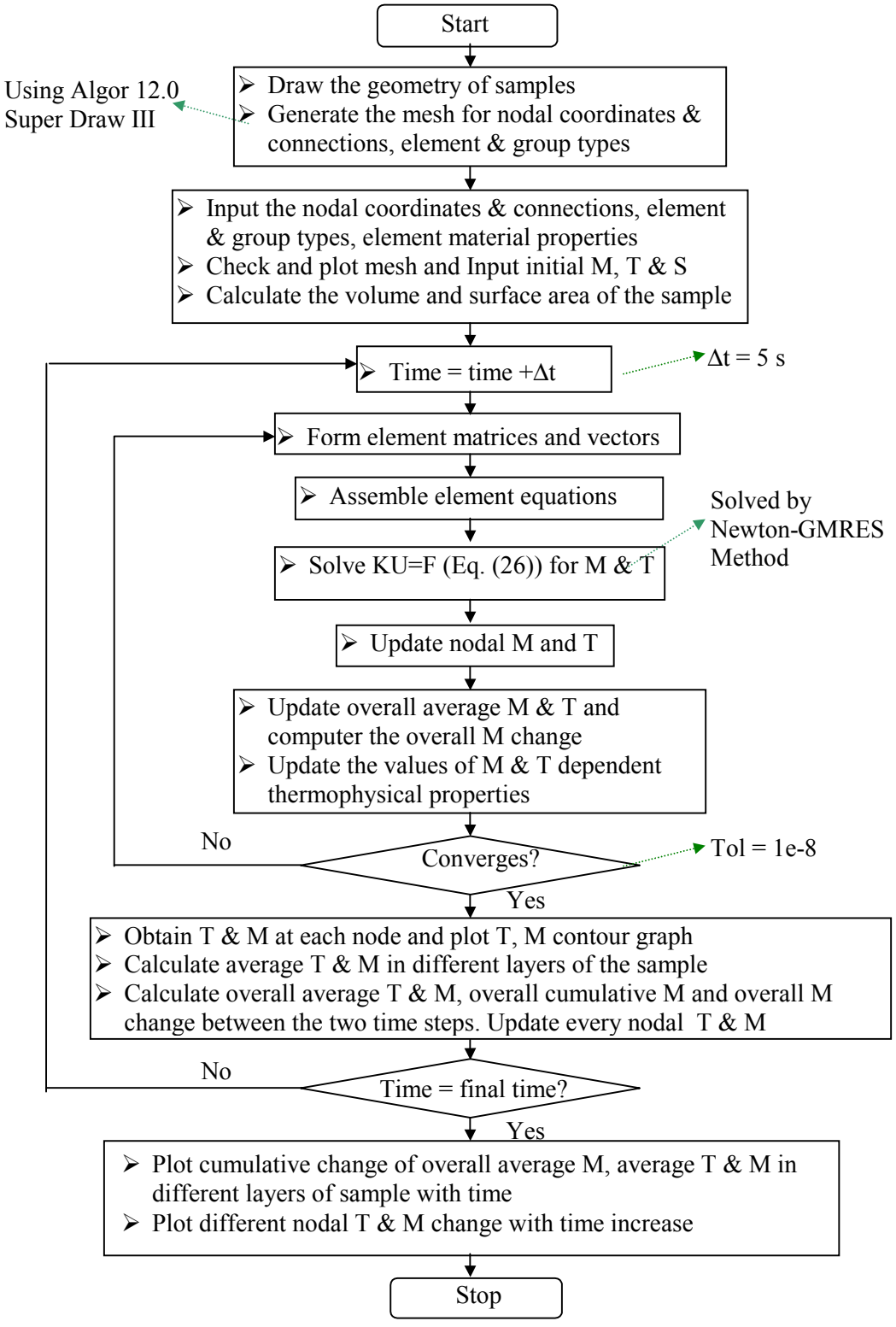

Fig. 3.2 Flow chart showing algorithm with Newton-GMRES method

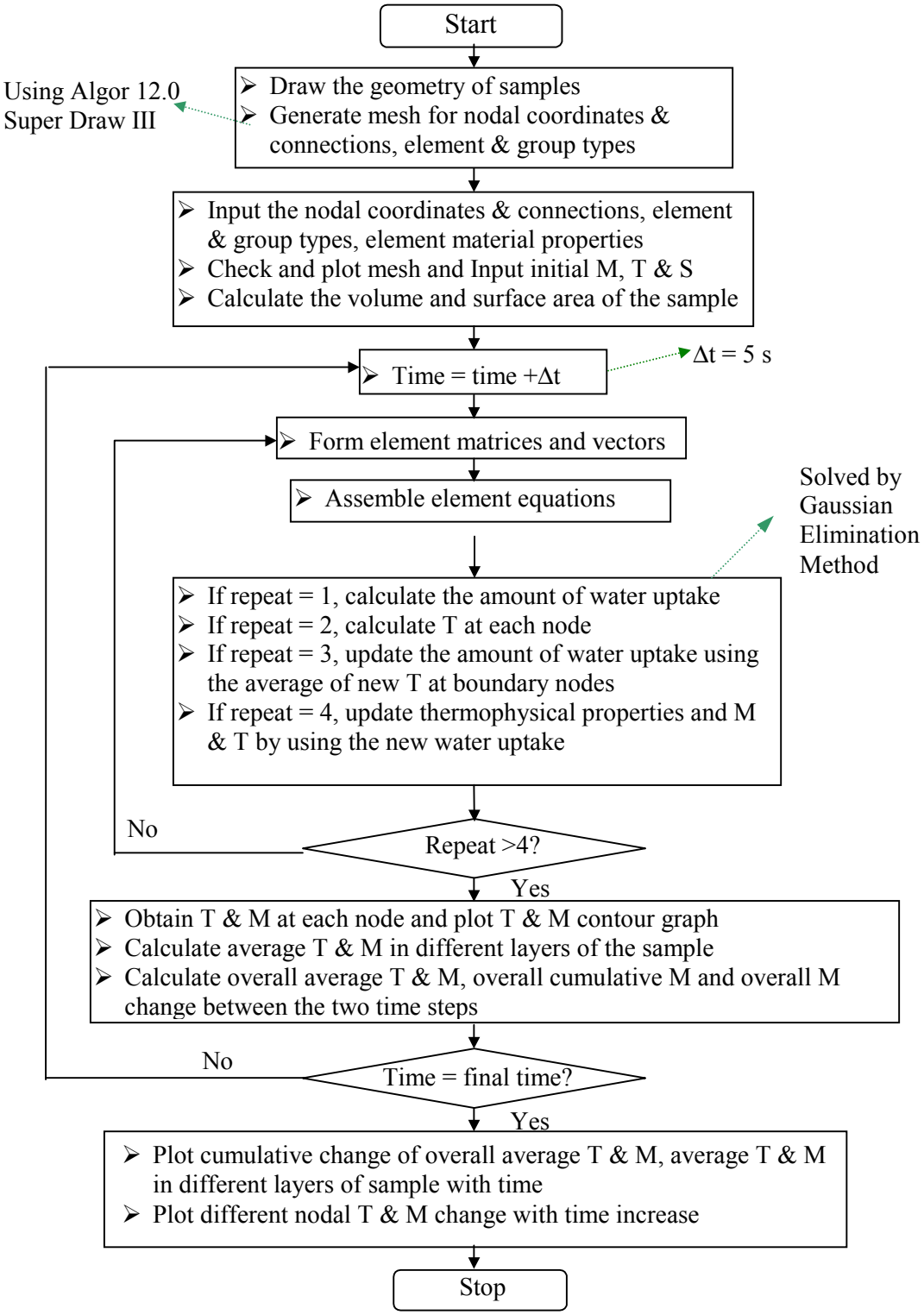

Fig. 3.3. Flow chart showing algorithm with Gaussian Elimination method

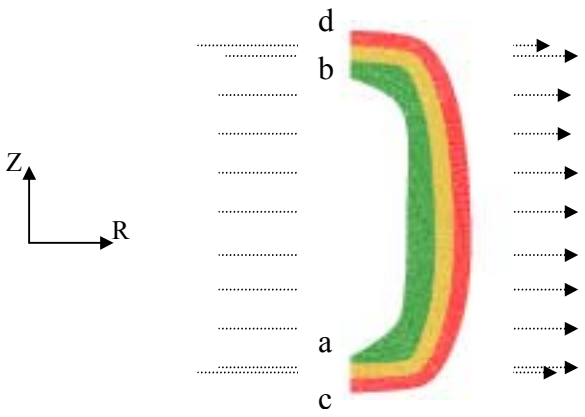

Using Spline to match the 20 measured geometrical data to draw the geometry of sample. Dividing the domain into three groups: the outmost layer (0.5-mm, red color); the layer below outmost layer (0.5-mm, yellow color); the innermost layer (green color)

Draw spline line from point, a <0,0.01053> to point, b <0,0.00121>

Point	r (m)	z (m)
1	0	0.00121
2	0.001420	0.00206
3	0.001518	0.00306
4	0.001623	0.00456
5	0.001598	0.00606
6	0.001658	0.00756
7	0.001683	0.00906
8	0.001305	0.01006
9	0	0.01053

Draw spline line from point, c <0,0> to point, d <0,0.01212>

Point	r (m)	z (m)
1	0	0
2	0.001817	6.E-5
3	0.002970	0.00156
4	0.003328	0.00306
5	0.003432	0.00456
6	0.003418	0.00606
7	0.003347	0.00756
8	0.003182	0.00906
9	0.002855	0.01056
10	0.001680	0.01206
11	0	0.01212

Fig. 3.4. Geometric modeling of the half longitudinal section of the cowpea seed

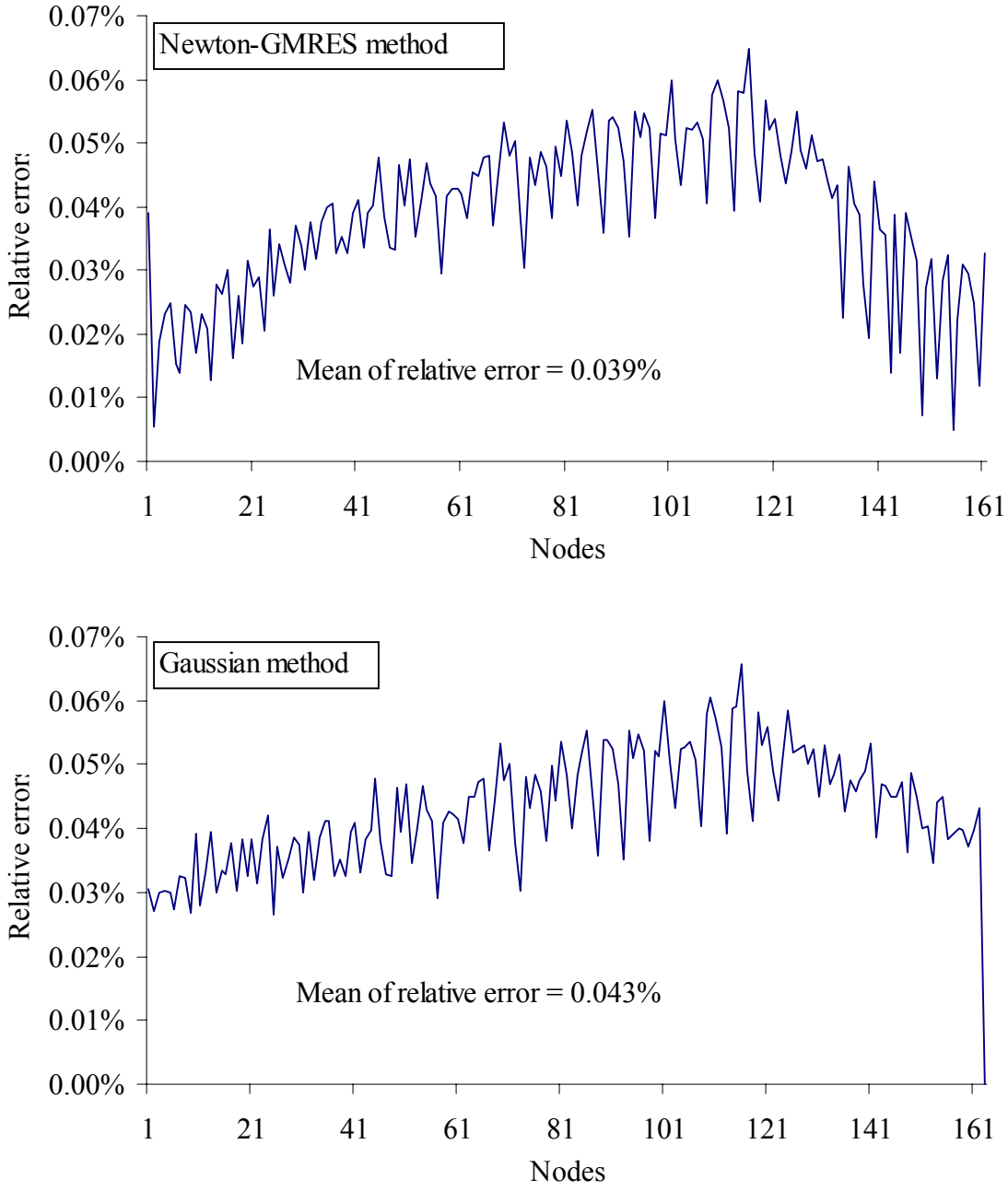

Fig. 3.5. Comparison of relative errors of the solution of FEM model using Newton GMRES method and Gaussian method with that of Algor after 60 s, at all 161 nodes in temperature range of 90-100°C

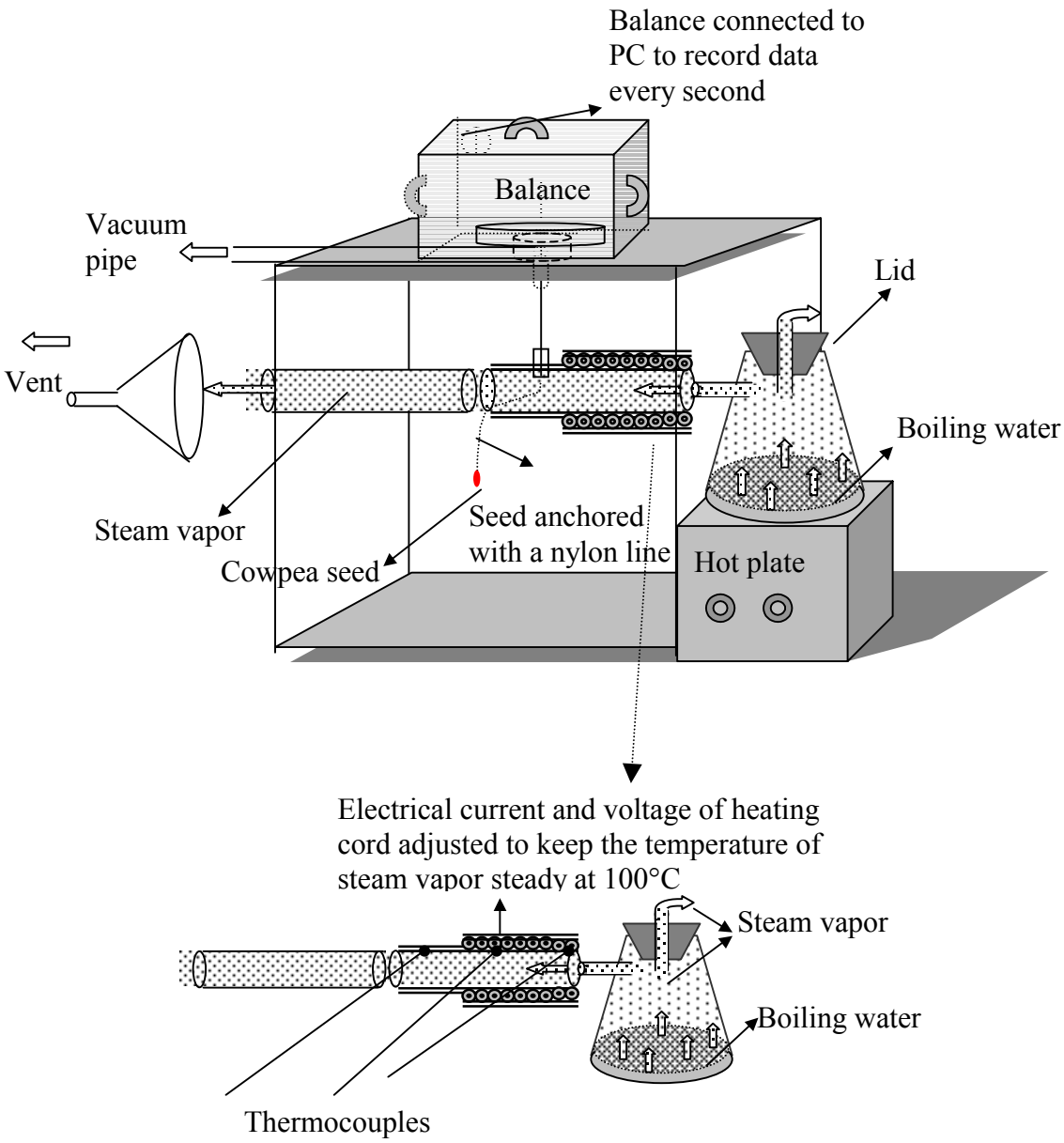

Fig. 3.6. Instantaneous moisture content measurement

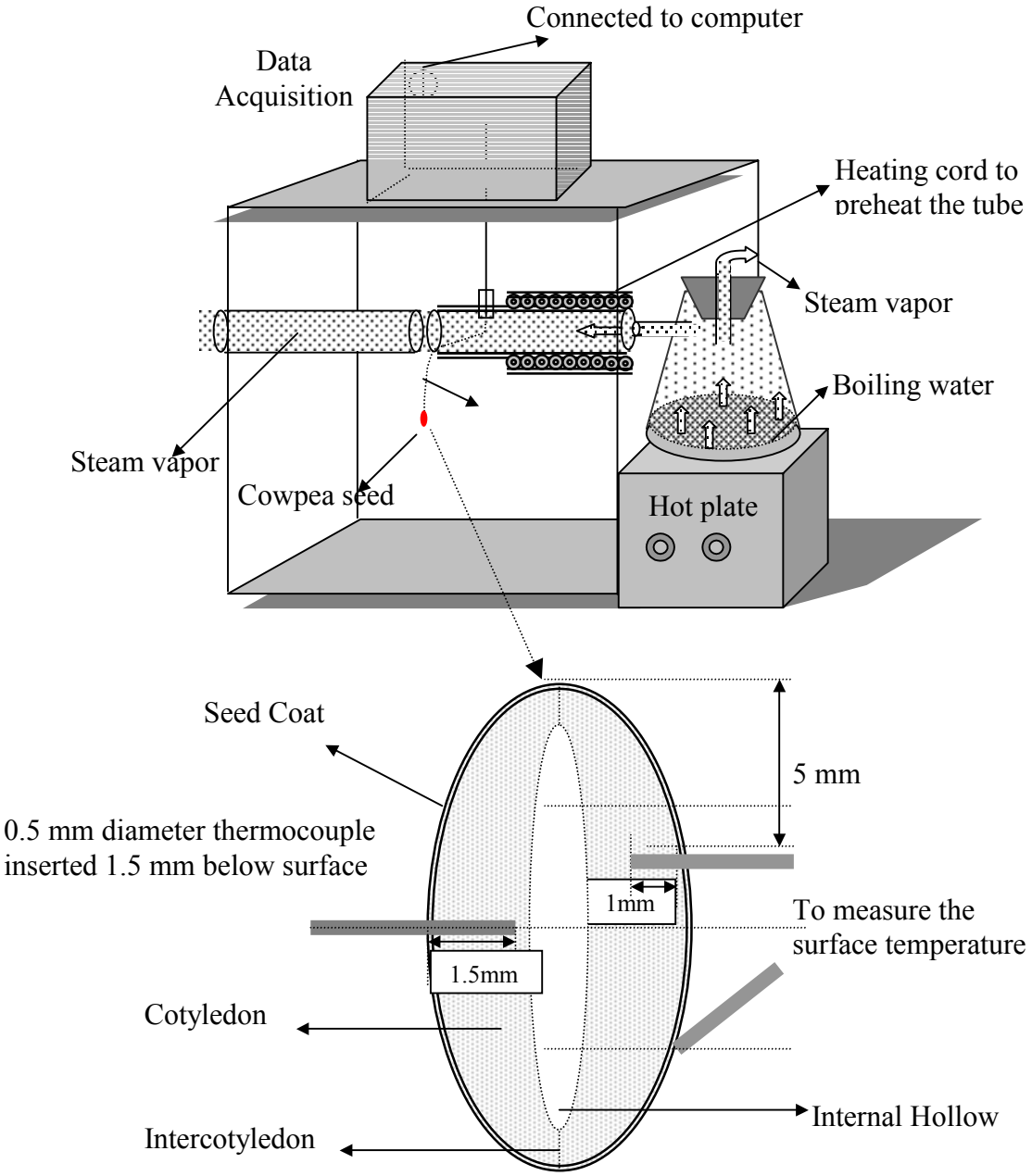

Fig. 3.7. Instantaneous temperature measurement and locations of thermocouples

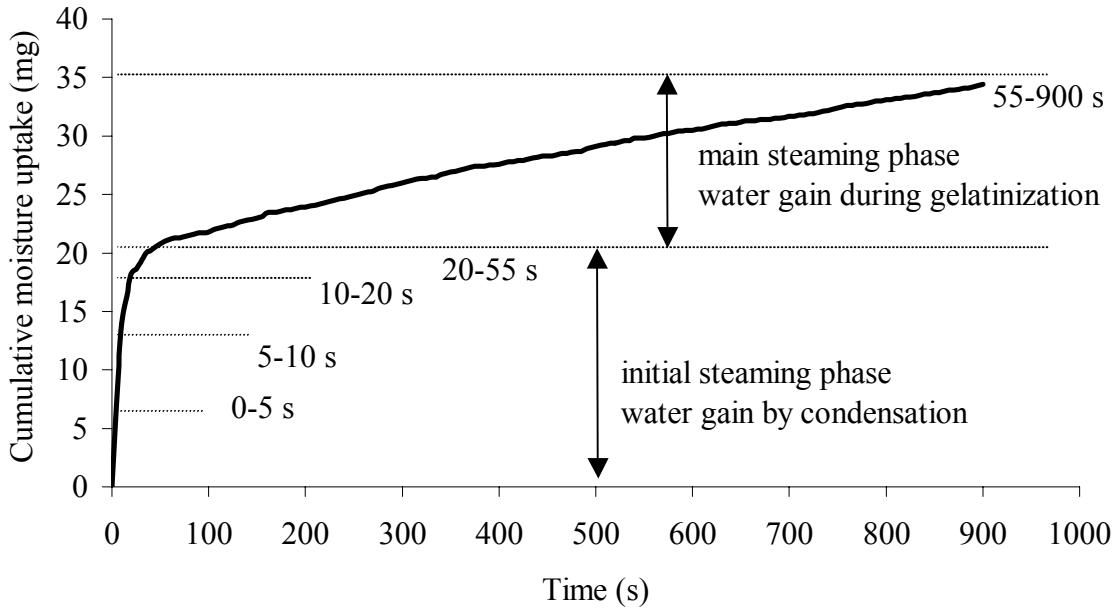

Fig. 3.8. Observed cumulative moisture uptake versus time in cowpea during steaming

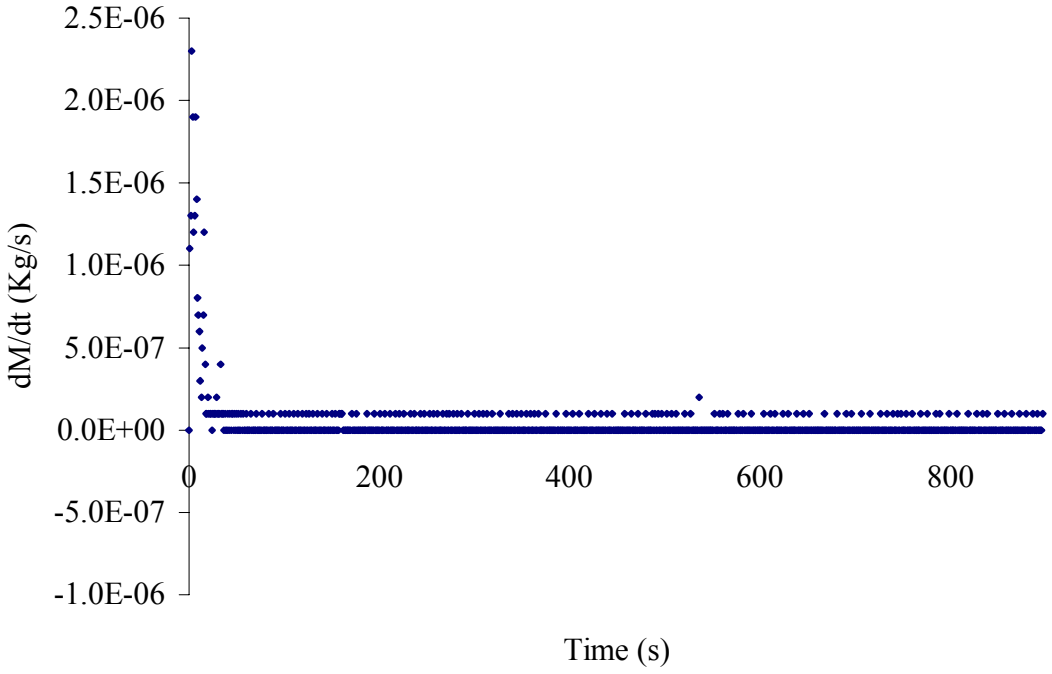

Fig. 3.9. Observed water uptake rate versus time in cowpea during steaming

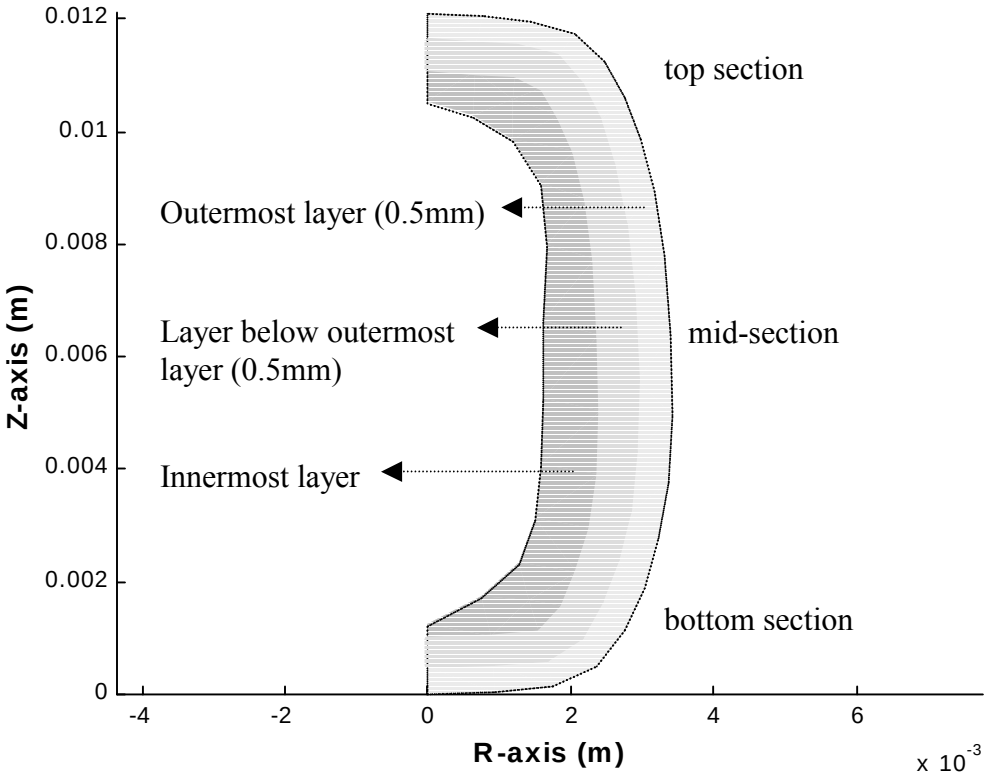

Fig. 3.10. Three layers in a half of cross-section of the cowpea seed

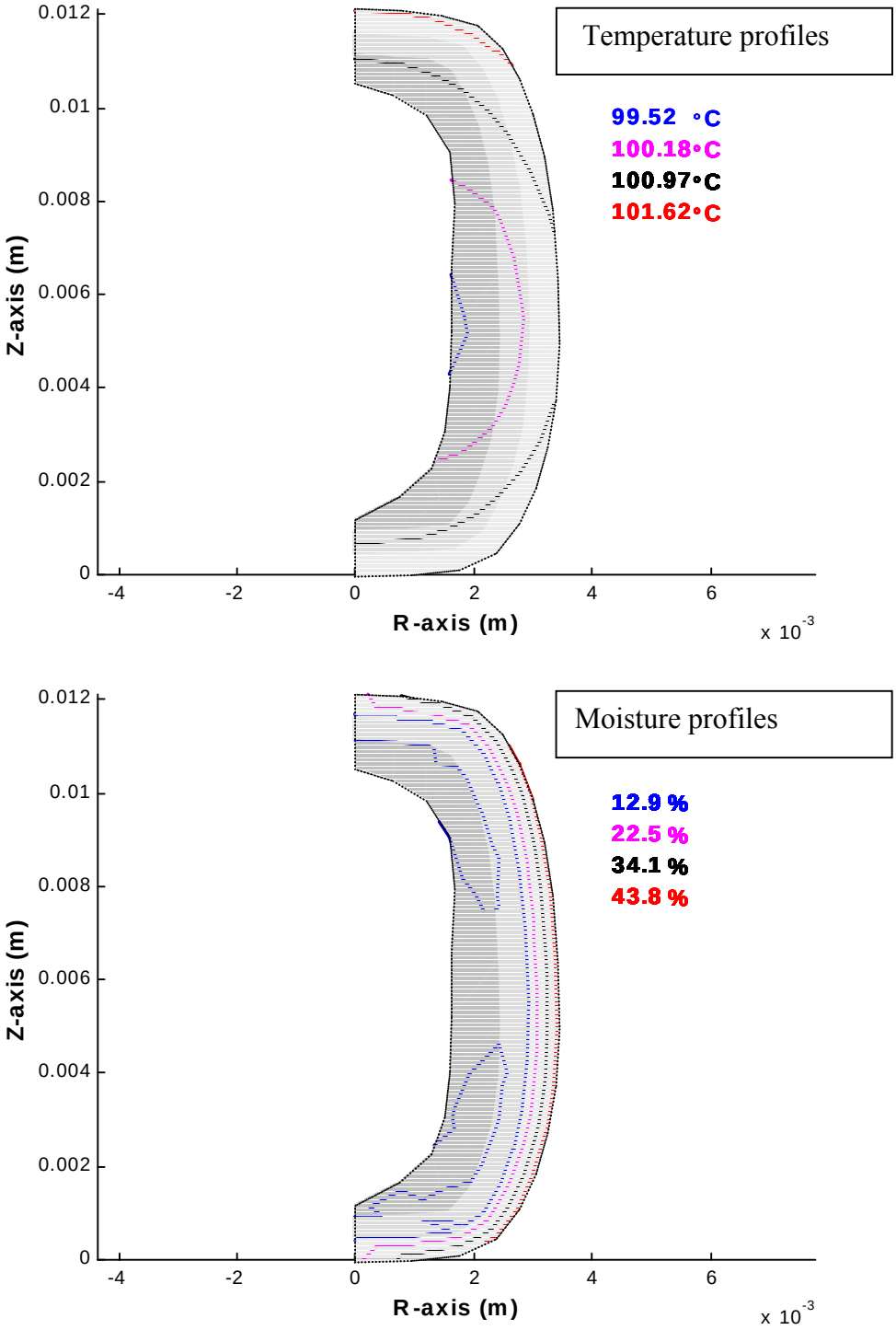

Fig. 3.11. Simulated temperature and moisture profiles (d.b.), by Newton-GMRES method, in a cowpea seed after 50s of steaming.

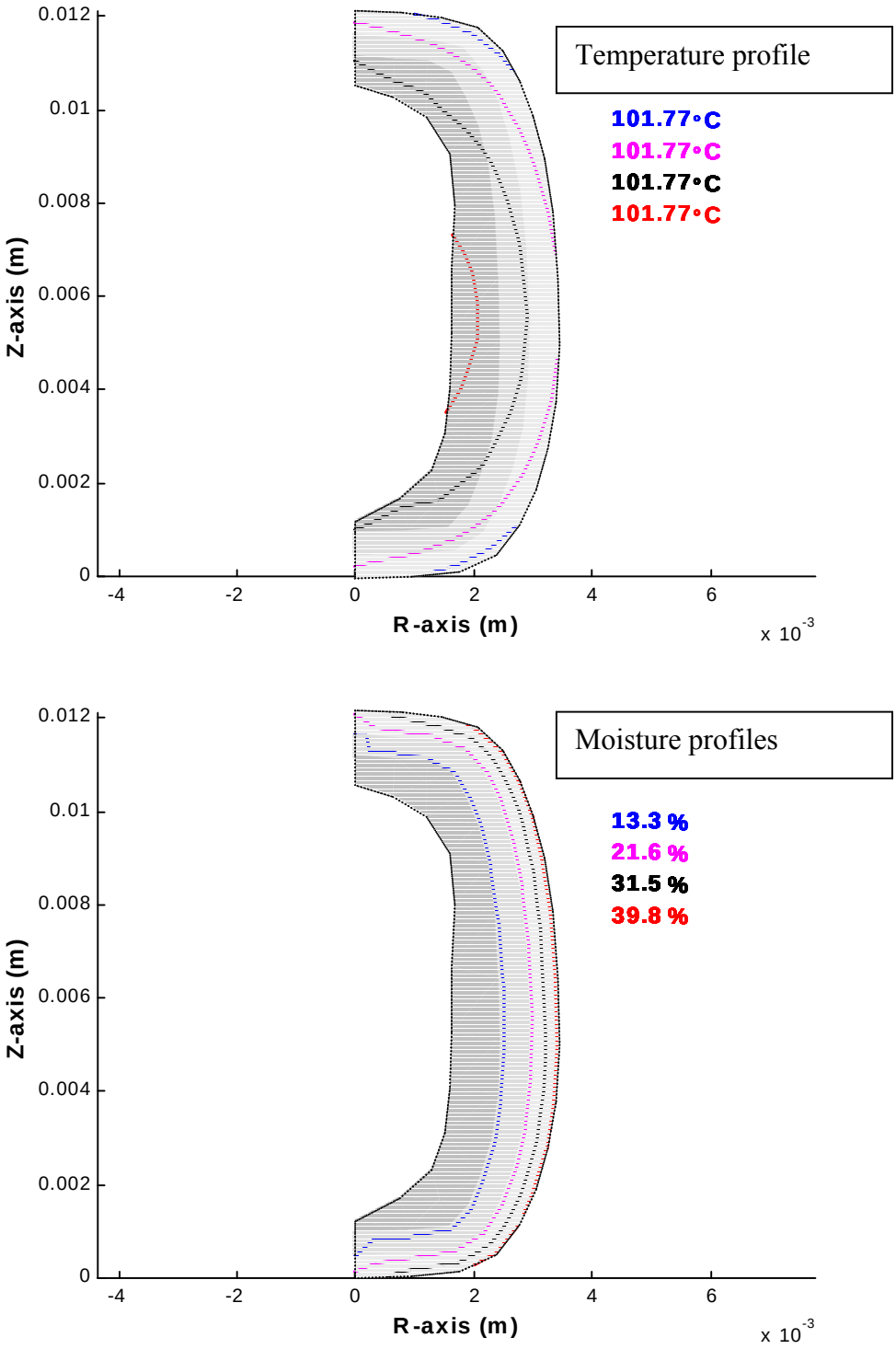

Fig. 3.12. Simulated temperature and moisture profiles (d.b.), by Newton-GMRES method, in a cowpea seed after 300s of steaming.

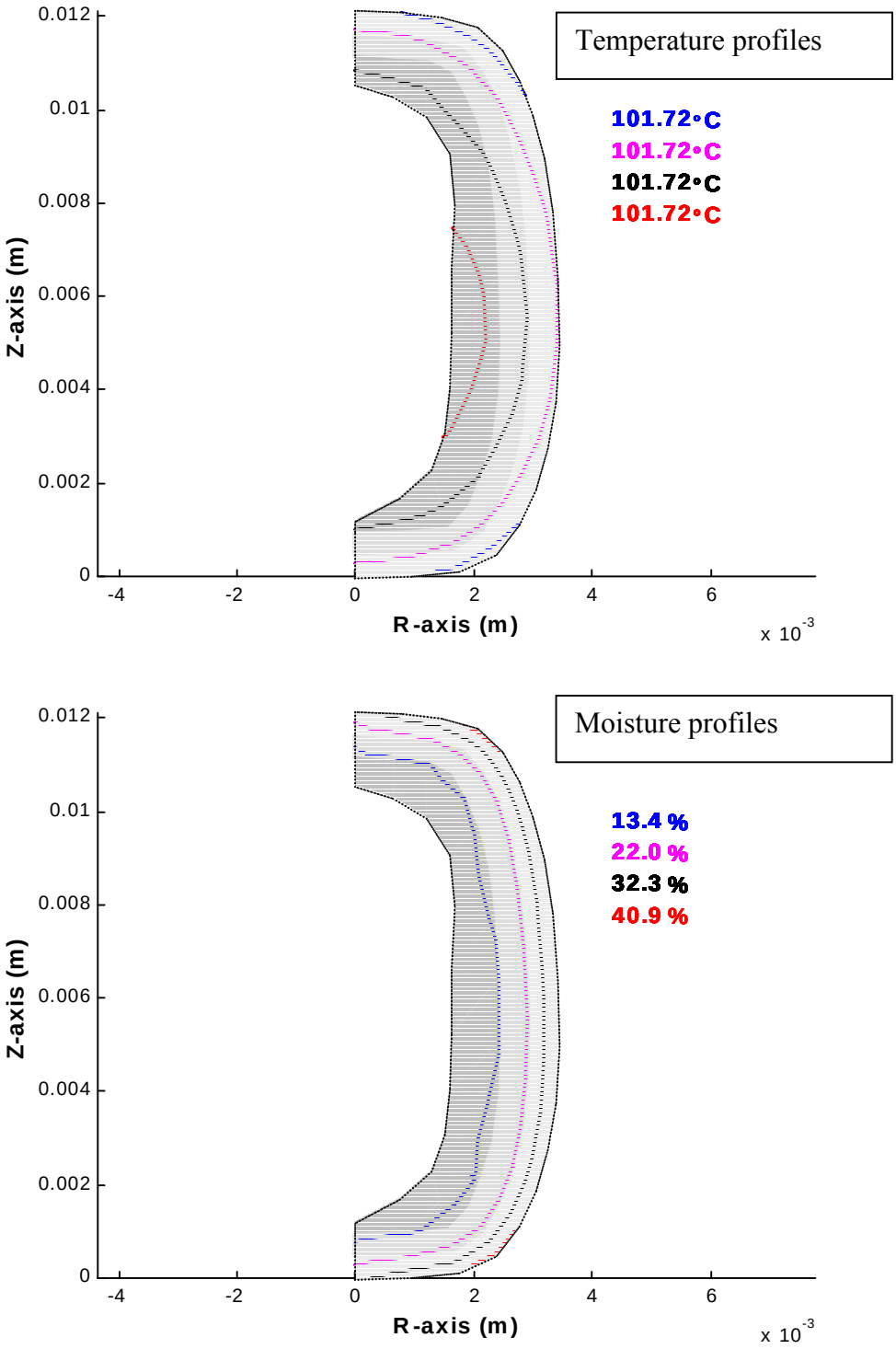

Fig. 3.13. Simulated temperature and moisture profiles (d.b.), by Newton-GMRES method, in a cowpea seed after 600s of steaming.

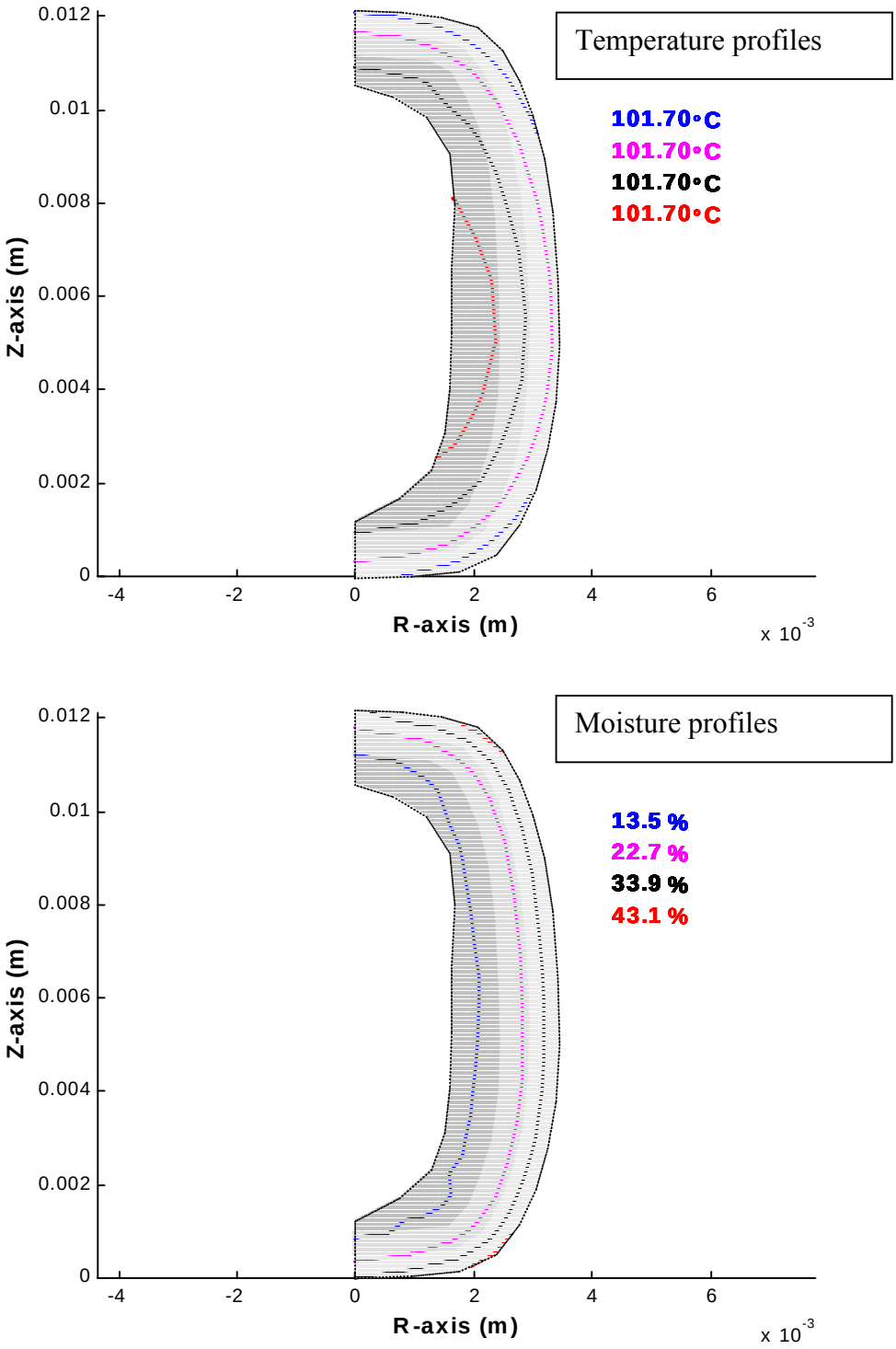

Fig. 3.14. Simulated temperature and moisture profiles (d.b.), by Newton-GMRES method, in a cowpea seed after 900s of steaming.

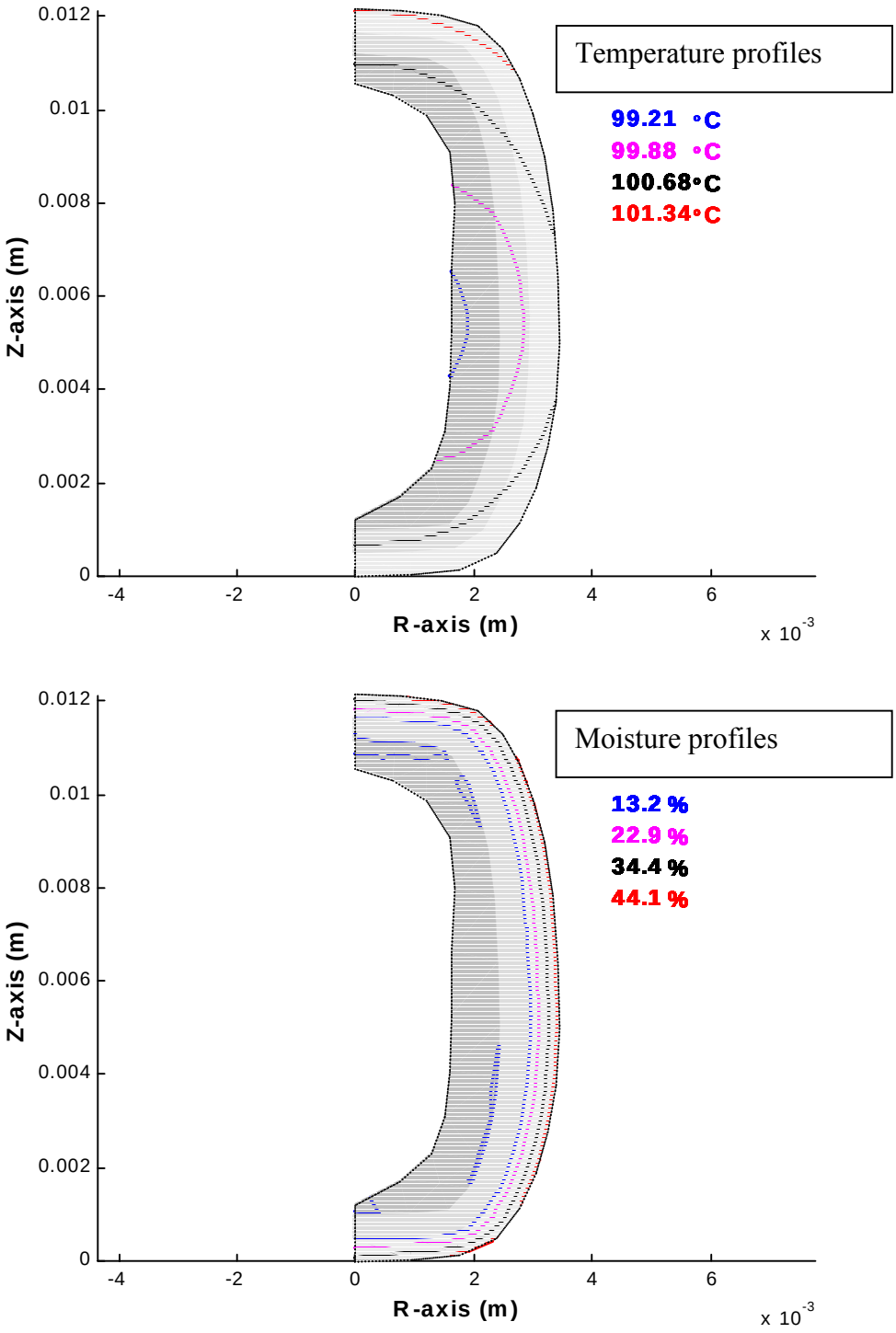

Fig. 3.15. Simulated temperature and moisture profiles, by Gaussian method, in a cowpea seed after 50s of steaming

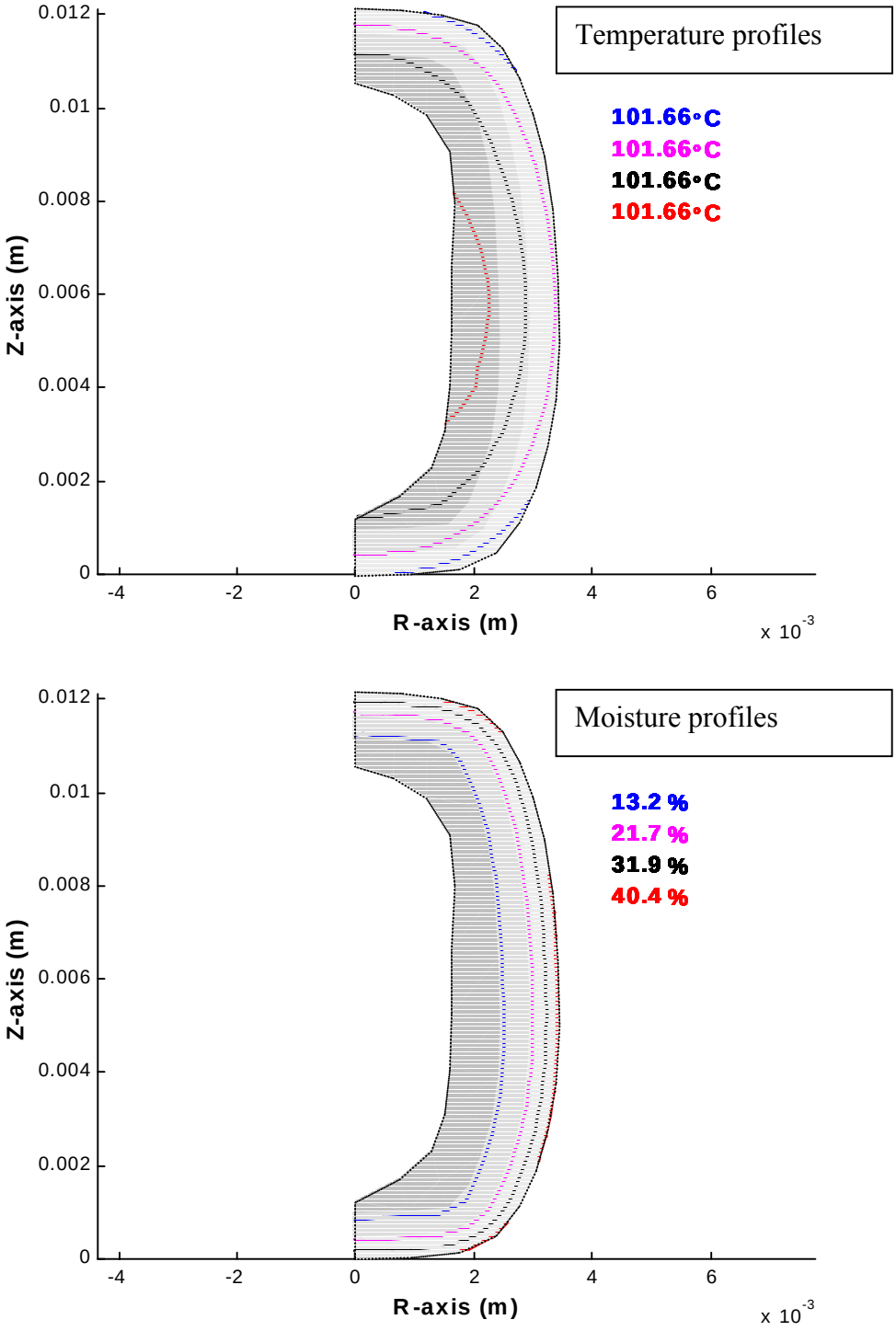

Fig. 3.16. Simulated temperature and moisture profiles, by Gaussian method, in a cowpea seed after 300s of steaming

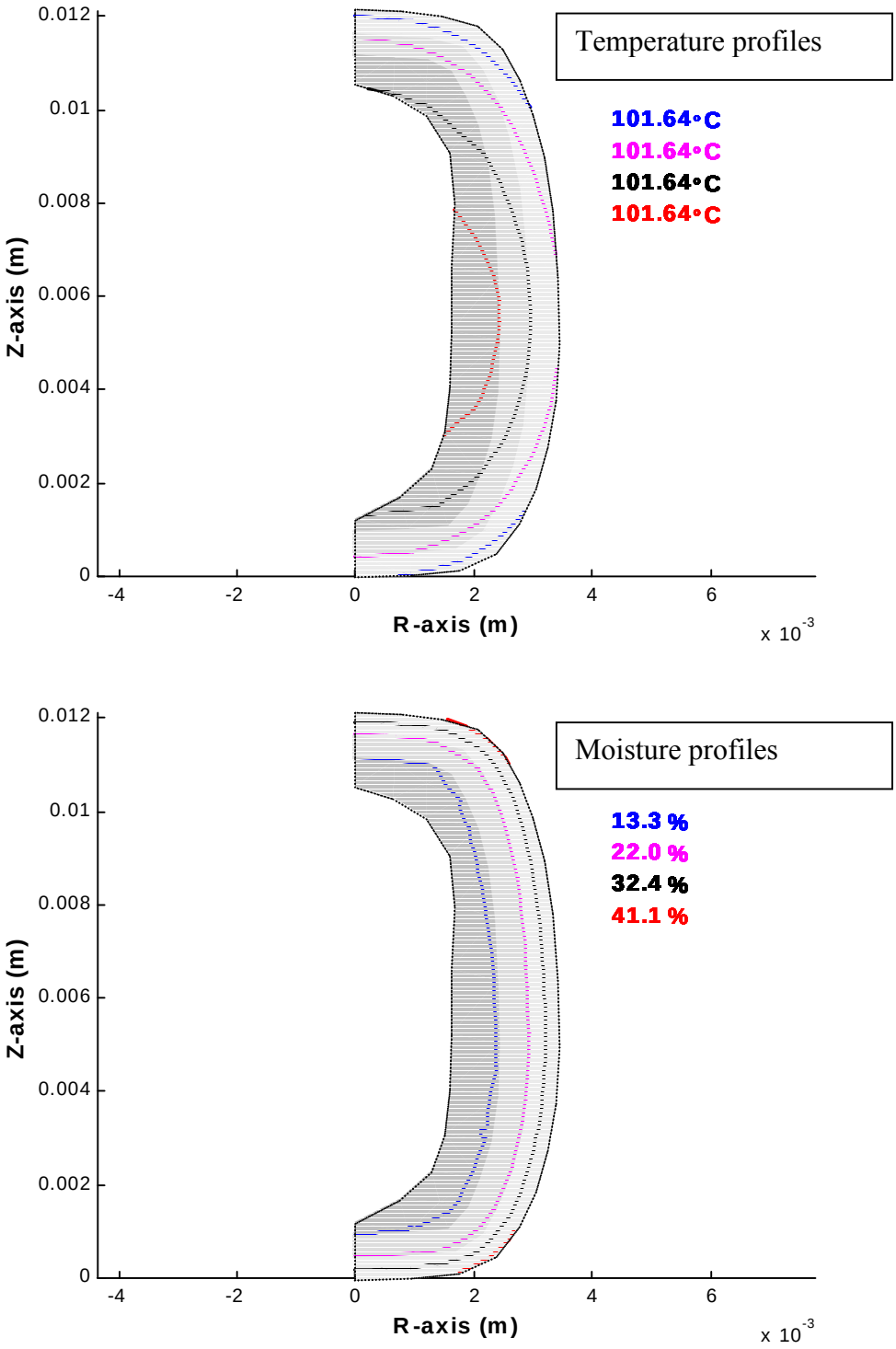

Fig. 3.17. Simulated temperature and moisture profiles, by Gaussian method, in a cowpea seed after 600s of steaming

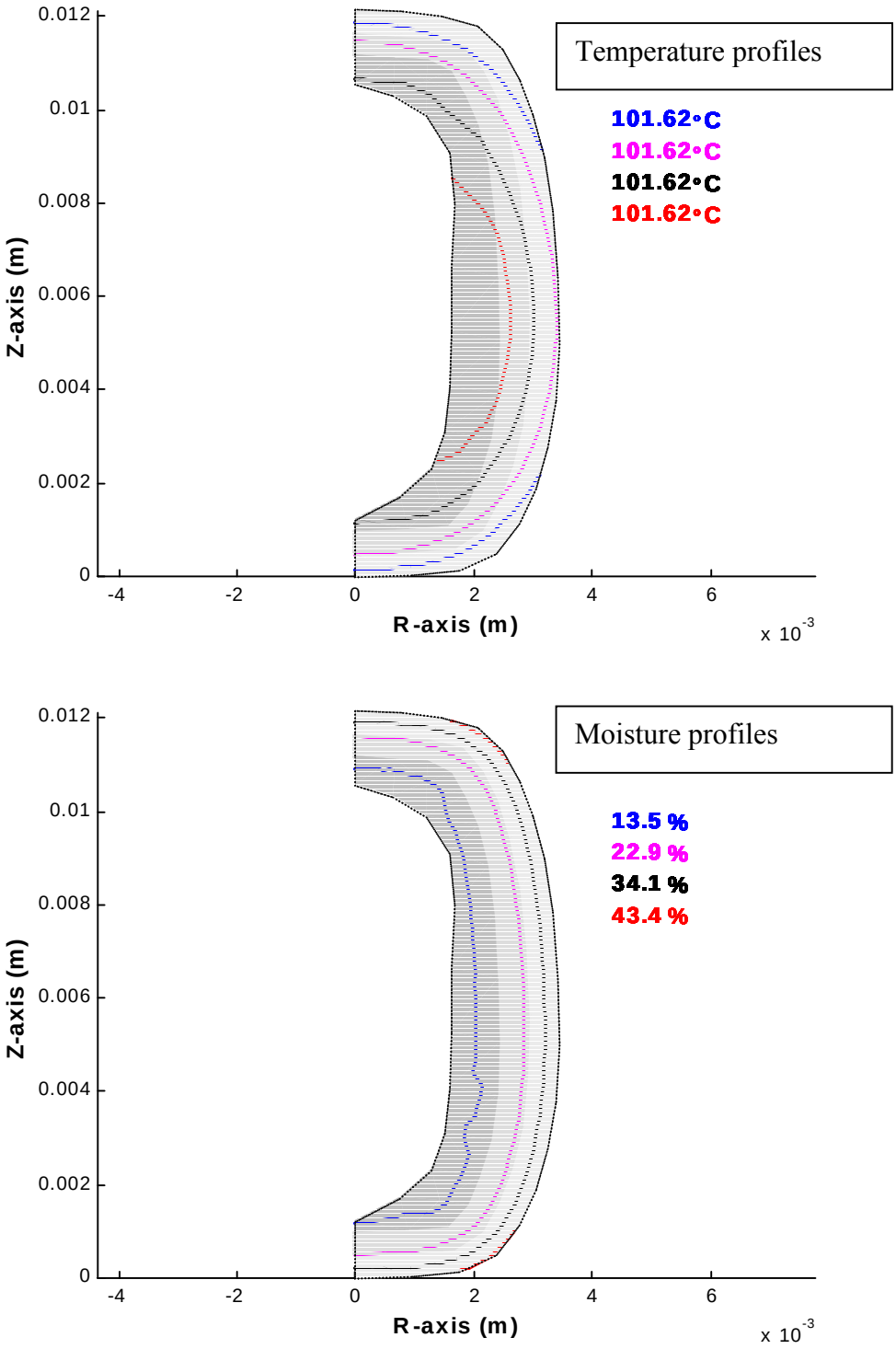

Fig. 3.18. Simulated temperature and moisture profiles, by Gaussian method, in a cowpea seed after 900s of steaming

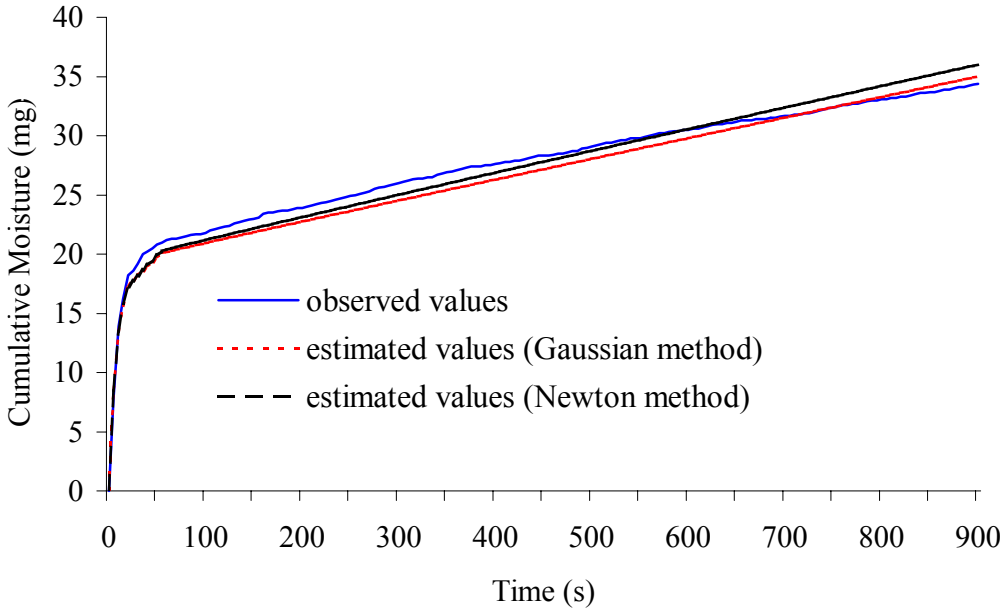

Fig. 3.19. Comparison of observed and estimated cumulative moisture uptake histories during steaming of cowpea seed

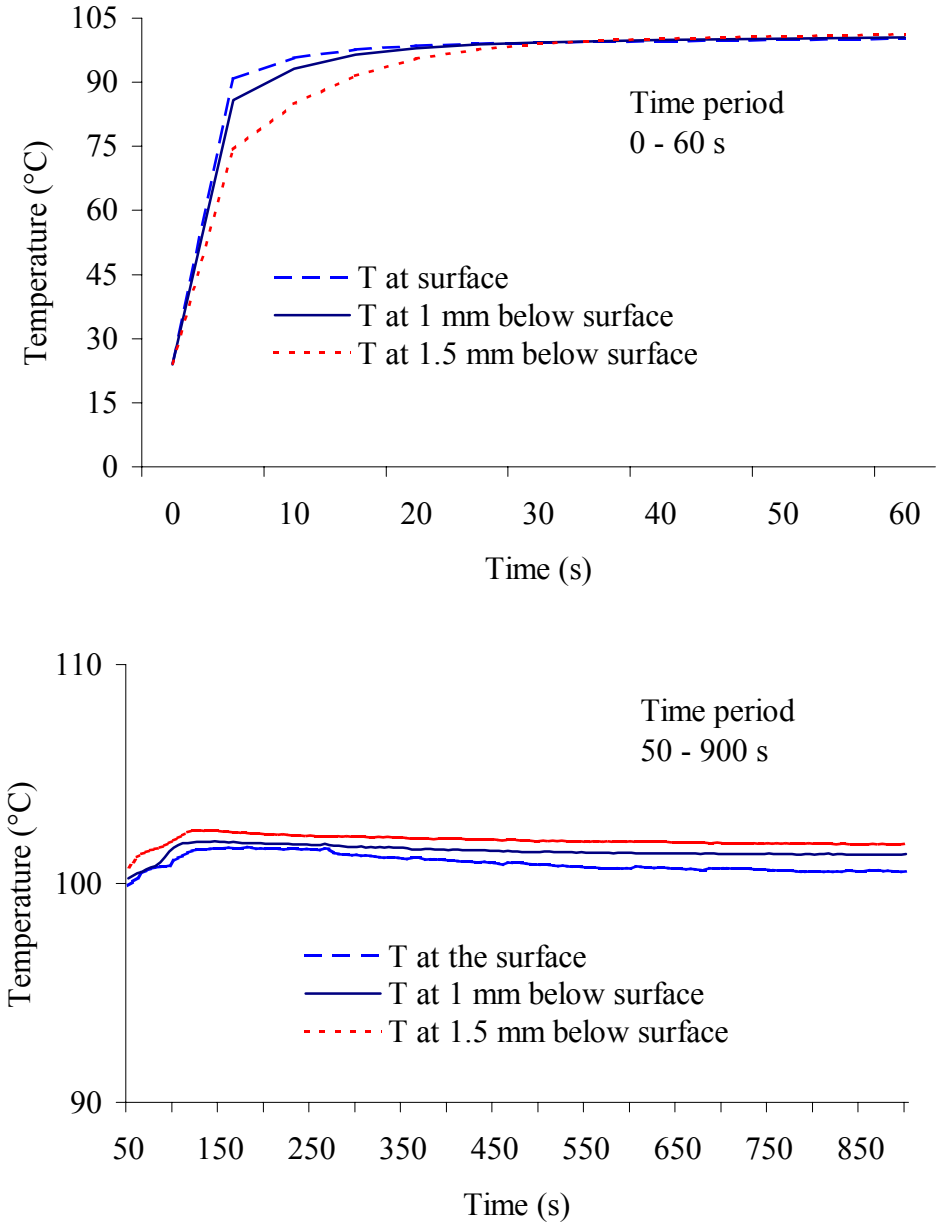

Fig. 3.20. Comparison of observed temperature histories in different locations of cowpea during 15 min of steaming

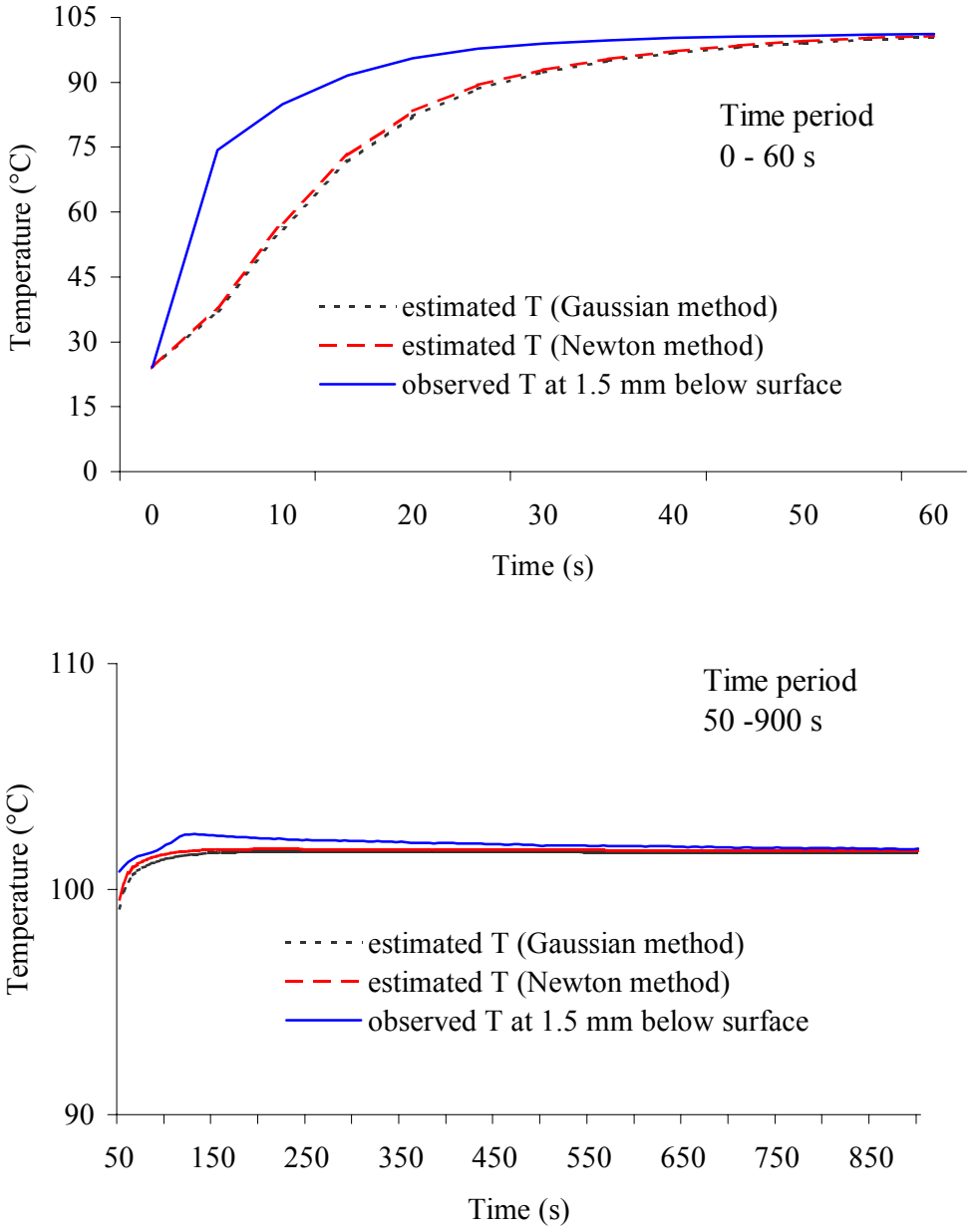

Fig. 3.21. Comparison of observed and estimated temperature histories at 1.5 mm below surface of cowpea during 15 min of steaming

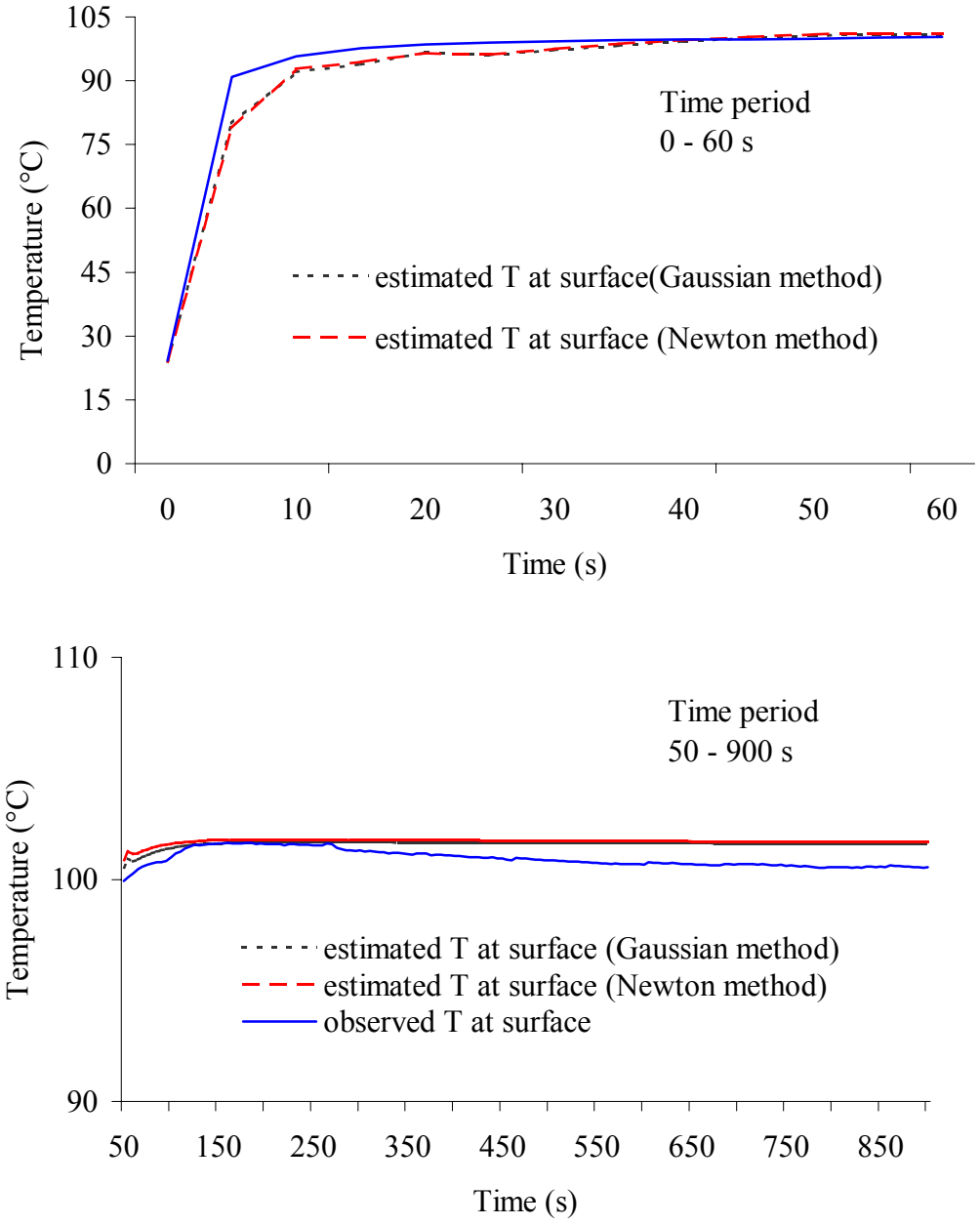

Fig. 3.22. Comparison of observed and estimated temperature histories at surface of cowpea during 15 min of steaming

APPENDIX - NUMERICAL FORMULATION

Matrices and vectors in Eq. (13), page 18

$$\begin{bmatrix} C_T & 0 \\ 0 & C_M \end{bmatrix} \begin{Bmatrix} \dot{T} \\ \dot{M} \end{Bmatrix} + \begin{bmatrix} K_T & 0 \\ 0 & K_M \end{bmatrix} \begin{Bmatrix} T \\ M \end{Bmatrix} = \begin{Bmatrix} F_T \\ 0 \end{Bmatrix} \tag{13}$$

were assembled from the following element matrices (matrix size of 3×3) and element vectors (size 3×1):

$$\begin{bmatrix} \rho C_p N_{ii} & 0 & \rho C_p N_{ij} & 0 & \rho C_p N_{im} & 0 \\ 0 & \rho N_{ii} & 0 & \rho N_{ij} & 0 & \rho N_{im} \\ \rho C_p N_{ji} & 0 & \rho C_p N_{jj} & 0 & \rho C_p N_{jm} & 0 \\ 0 & \rho N_{ji} & 0 & \rho N_{jj} & 0 & \rho N_{jm} \\ \rho C_p N_{mi} & 0 & \rho C_p N_{mj} & 0 & \rho C_p N_{mm} & 0 \\ 0 & \rho N_{mi} & 0 & \rho N_{mj} & 0 & \rho N_{mm} \end{bmatrix} \begin{Bmatrix} \frac{\partial T_i}{\partial t} \\ \frac{\partial M_i}{\partial t} \\ \frac{\partial T_j}{\partial t} \\ \frac{\partial M_j}{\partial t} \\ \frac{\partial T_m}{\partial t} \\ \frac{\partial M_m}{\partial t} \end{Bmatrix} + \begin{bmatrix} \Phi_T k_{ii} & 0 & \Phi_T k_{ij} & 0 & \Phi_T k_{im} & 0 \\ 0 & \Phi_M k_{ii} & 0 & \Phi_M k_{ij} & 0 & \Phi_M k_{im} \\ \Phi_T k_{ji} & 0 & \Phi_T k_{jj} & 0 & \Phi_T k_{jm} & 0 \\ 0 & \Phi_M k_{ji} & 0 & \Phi_M k_{jj} & 0 & \Phi_M k_{jm} \\ \Phi_T k_{mi} & 0 & \Phi_T k_{mj} & 0 & \Phi_T k_{mm} & 0 \\ 0 & \Phi_M k_{mi} & 0 & \Phi_M k_{mj} & 0 & \Phi_M k_{mm} \end{bmatrix} \begin{Bmatrix} T_i \\ M_i \\ T_j \\ M_j \\ T_m \\ M_m \end{Bmatrix} - \begin{Bmatrix} P_{iT} \\ 0 \\ P_{jT} \\ 0 \\ P_{mT} \\ 0 \end{Bmatrix}$$

where,

$$b_i = r_j - r_m,\ b_j = r_m - r_i,\ b_m = r_i - r_j\ ,$$

$$c_i = x_m - x_j,\ c_j = x_i - x_m,\ c_m = x_j - x_i\ ,$$

$$p_{iT} = \frac{A}{12} q_v (R + r_i),\ p_{jT} = \frac{A}{12} q_v (R + r_j),\ p_{mT} = \frac{A}{12} q_v (R + r_m)$$

$$k_{ii} = (b_i^2 + c_i^2),\ k_{jj} = (b_j^2 + c_j^2),\ k_{mm} = (b_m^2 + c_m^2),$$

$$k_{ij} = k_{ji} = (b_i b_j + c_i c_j),\ k_{jm} = k_{mj} = (b_j b_m + c_j c_m),$$

$$k_{mii} = k_{im} = (b_i b_m + c_i c_m),\ \Phi_T = K\frac{R}{12A}, \Phi_M = \rho D \frac{R}{12A}\ ,$$

$$N_{ii} = \frac{A}{30}(R + 2r_i),\ N_{jj} = \frac{A}{30}(R + 2r_j),\ N_{ii} = \frac{A}{30}(R + 2r_m)\ ,$$

$$N_{ij} = N_{ji} = \frac{A}{60}(R + r_i + r_j),\ N_{jm} = N_{mj} = \frac{A}{60}(R + r_j + r_m)\ ,$$

$$N_{mi} = N_{im} = \frac{A}{60}(R + r_i + r_m),$$

Matrices and vectors in Eq. (19), page 19

$$\begin{bmatrix} C_T & 0 \\ 0 & C_M \end{bmatrix}\begin{Bmatrix} \dot{T} \\ \dot{M} \end{Bmatrix}+\begin{bmatrix} K_T & 0 \\ 0 & K_M \end{bmatrix}\begin{Bmatrix} T \\ M \end{Bmatrix}=\begin{Bmatrix} F_T \\ F_M \end{Bmatrix} \tag{19}$$

were assembled from the following element matrices (matrix size of 3×3) and element vectors (size 3×1):

$$\begin{bmatrix} \rho C_p N_{ii} & 0 & \rho C_p N_{ij} & 0 & \rho C_p N_{im} & 0 \\ 0 & \rho N_{ii} & 0 & \rho N_{ij} & 0 & \rho N_{im} \\ \rho C_p N_{ji} & 0 & \rho C_p N_{jj} & 0 & \rho C_p N_{jm} & 0 \\ 0 & \rho N_{ji} & 0 & \rho N_{jj} & 0 & \rho N_{jm} \\ \rho C_p N_{mi} & 0 & \rho C_p N_{mj} & 0 & \rho C_p N_{mm} & 0 \\ 0 & \rho N_{mi} & 0 & \rho N_{mj} & 0 & \rho N_{mm} \end{bmatrix}\begin{Bmatrix} \frac{\partial T_i}{\partial t} \\ \frac{\partial M_i}{\partial t} \\ \frac{\partial T_j}{\partial t} \\ \frac{\partial M_j}{\partial t} \\ \frac{\partial T_m}{\partial t} \\ \frac{\partial M_m}{\partial t} \end{Bmatrix}+\begin{bmatrix} \Phi_T k_{ii} & 0 & \Phi_T k_{ij} & 0 & \Phi_T k_{im} & 0 \\ 0 & \Phi_M k_{ii} & 0 & \Phi_M k_{ij} & 0 & \Phi_M k_{im} \\ \Phi_T k_{ji} & 0 & k_{jjT} & 0 & k_{jmT} & 0 \\ 0 & \Phi_M k_{ji} & 0 & \Phi_M k_{jj} & 0 & \Phi_M k_{jm} \\ \Phi_T k_{mi} & 0 & k_{mjT} & 0 & k_{mmT} & 0 \\ 0 & \Phi_M k_{mi} & 0 & \Phi_M k_{mj} & 0 & \Phi_M k_{mm} \end{bmatrix}\begin{Bmatrix} T_i \\ M_i \\ T_j \\ M_j \\ T_m \\ M_m \end{Bmatrix}-\begin{Bmatrix} P_{iT} \\ P_{iM} \\ P_{jT} \\ P_{jM} \\ P_{mT} \\ P_{mM} \end{Bmatrix}$$

where,

$$C_1 = h_t - \rho\frac{V}{S_a}C_v\frac{\partial M}{\partial t},\quad C_2 = -\rho\frac{V}{S_a}h_{fg}\frac{\partial M}{\partial t}$$

$$K_{jjT} = \Phi_T(b_j^2 + c_j^2) + \frac{C_1 s_i}{4}(r_j + \frac{r_m}{3}),\ K_{mmT} = \Phi_T(b_m^2 + c_m^2) + \frac{C_1 s_i}{4}(r_m + \frac{r_j}{3})$$

$$K_{jmT} = K_{mjT} = \Phi_T(b_j b_m + c_j c_m) + \frac{C_1 s_i}{12}(r_j + r_m),$$

$$p_{jT} = \frac{A}{12}q_v(R + r_j) + \frac{C_1 s_i T_a}{3}(r_j + \frac{r_m}{2}) - C_2 s_i(\frac{1}{3}r_j + \frac{1}{6}r_m)$$

$$p_{mT} = \frac{A}{12}q_v(R + r_m) + \frac{C_1 s_i T_a}{3}(r_m + \frac{r_j}{2}) - C_2 s_i(\frac{1}{3}r_m + \frac{1}{6}r_j)$$

CHAPTER 4

STARCH GELATINIZATION KINETICS OF COWPEA FLOUR DURING HEAT-MOISTURE TREATMENT[1]

[1]Fang, C. and Chinnan, M. S. 2000. To be submitted to Journal of Food Engineering

INTRODUCTION

Starch gelatinization

Starch occurs naturally as discrete granules. The granules are relatively dense and insoluble and hydrate only slightly in cold water. Most starch granules are composed of a mixture of two polymers: an essentially linear polysaccharide, amylose and a highly branched polysaccharide, amylopectin (Fennnema, 1996).

Amylopectin is a major constituent of starch, constituting about 75% in most common starches. It is a large and highly branched molecule: α-(1-4)-glucosidic chain that is linked to side chains by α-(1-6)-glucosidic bonds (Fig. 4.1). The branching occurs every 24-30 glucose residues. The branches of amylopectin molecules are clustered and occur as double helices. Molecular weights of from 10^7 to 5×10^8 make amylopectin molecules among the largest, if not the largest, molecules found in nature (Fennnema, 1996).

Amylose, the other constituent of starch is basically a linear molecule composed of α-(1-4)-glucosidic linkages but contains a few α-(1-6) branches (Fig. 4.1). The number of glucose units in amylose varies, even within the same sample, but in general, there are over 1000 glucose units per amylose molecule.

Undamaged starch granules are insoluble in cold water, but can imbibe water reversibly (Fennnema, 1996). When heated in water, starch granules undergo a process called gelatinization. The most acceptable definition of starch gelatinization is: the collapse (disruption) of molecular orders within starch granules manifesting in irreversible changes in properties such as granular swelling, native crystallite melting, loss of birefringence, and starch solubilization. The point of initial gelatinization and the range over which it occurs is governed by the starch concentration, method of observation, granule type, and heterogeneities within granule population under observation (Atwell et al., 1988).

Evaluation method of starch gelatinization

Most of the studies of starch gelatinization have been based on the application of differential scanning calorimetry (DSC). DSC is a thermoanalytical technique for monitoring changes in the physical and/or chemical properties of materials as a function of temperature by detecting the heat changes associated with such processes (Biliaderis, 1983). Besides studying starch gelatinization, DSC has been used to study protein denaturation, protein interactions, and physical properties of lipids by monitoring the associated changes in enthalpy (Biliaderis, 1983). Hence, it is inappropriate to determine the degree of starch gelatinization in complex foods by DSC, because they may also contain other components such as protein and lipid.

Other methods for determining the degree of gelatinization of starch include observation of the birefringence end point, measurement of increased viscosity, x-ray diffraction, amylose/iodine blue value determination and thermal analysis, enzymatic hydrolysis, nuclear magnetic resonance, light extinction, solubilization or sedimentation of swollen granules and absorption of Congo red dye. These methods are complicated by the differences in starch/water ratio and temperature range over which the gelatinization process can be studied (Reddy, 1991).

Among the methods proposed, enzymatic evaluation method is acceptable to complex foods or foodstuffs without obstruction (Haruhito et al., 1990). The most sensitive methods of measurement of starch gelatinization are based on the loss of birefringence by gelatinized starch or on its increased susceptibility to enzyme attack (Shetty et al., 1974). Birefringence is difficult to apply because starch granules are not only difficult to count in heterogeneous mixtures but also difficult to separate from other components in cooked materials.

The physicochemical change in starch granule is very sensitive to its digestion by enzyme. Starch susceptibility to amylolytic enzyme depends on the conformational state of starch molecule and on the type of enzyme used, where the molecule is in raw (prime),

gelatinized and retrograded state. Thus, the conformational state of starch molecule can be distinguished by using an appropriate enzyme, such as amylase and pullulanase (Haruhito et al., 1990).

Pullulanase (α-(1-6)-debranching enzyme) can hydrolyze α-(1-6) linkage, converting the amylopectins to linear dextrins. Amylase randomly cleaves interior α-(1-4) bonds, thereby producing glucose, maltose and α-dextrins. α-amylase is more efficient than β-amylase. β-amylase binds to and attacks starch granules, but generally, α-amylase and β-amylase do not have a good effect on raw starch granules because raw granules are very resistant to amylolytic digestion (Hyun & Zekius, 1985).

Heat-moisture treatment

Heat-moisture treatment (HMT) refers to the exposure of starch to higher temperatures, commonly above the gelatinization temperature, at very restricted moisture content (18-27% w.b.) (Lilia & Harold, 1999). The heat-moisture treatment of starches has been known to produce remarkable changes in the crystallinity of starch molecules in the granules due to rearrangement or higher degree of association of the starch chains. The treated starch increases the gelatinization temperature and decreases the gelatinization enthalpy, the viscosity peak in its Brabender diagram and the endothermic peak in its DSC curve (Maruta et al., 1998). The HMT experiments can be easily designed to be various combinations of temperatures, moisture contents and starch contents to investigate different conditions for starch gelatinization. Studies on HMT have been conducted on wheat, potato, pea, lentil, and bean starches (Donovan et al., 1983; Hoover & Manuel, 1996; Lilia & Harold, 1999; Kulp & Lorenz, 1981). Few reports have been found on study starch gelatinization in cowpea flour of HMT.

Kinetics of starch gelatinization

Numerous researchers have reported that a kinetic model of starch gelatinization followed pseudo-first order reaction for water/starch systems, in which water was in excess and the reaction rate constant, k depended on temperature, according to the

Arrhenius equation (Lund, 1984; Verlinden et al., 1994; Zanoni et al., 1993). Most kinetic studies on chemical reactions were performed under isothermal conditions, since temperature can then be considered an independent variable and the time dependence can be determined (Lund, 1984). The rate of disappearance of ungelatinized starch can be described by the following first order equation:

$$\frac{dS}{dt} = -kS \tag{1}$$

The fraction of ungelatinized starch, S as a function of time can be computed by solving the Eq. (1) by using an explicit Euler finite difference scheme (Verlinden et al., 1994):

$$S(t_{k+1}) = S(t_k) - k_g(T_k) \cdot S(t_k) \cdot \Delta t \tag{2}$$

The temperature dependence of the gelatinization rate constant, k can be expressed by the Arrhenius law as:

$$k = k_{ref} \exp\left[-\frac{E_{ag}}{R}\left(\frac{1}{T} - \frac{1}{T_{ref}} \right) \right] \tag{3}$$

Qu and Wang (1994) studied the kinetics of the formation of gelatinized starch (high moisture content range) and melted starch (low moisture content range 15-40%). Conversions caused by gelatinization and melting were separately analyzed by using information from DSC isothermal studies. The rate of formation of gelatinized fraction followed first order kinetics and that of melted fraction followed zeroth order. The overall reaction rate followed zeroth order because melting was the dominant mechanism of the two under limited water contents of extrusion cooking conditions. Donovan (1979) pointed out that phase transitions in starch were believed to follow two mechanisms; namely, gelatinization and melting. At higher water content, swelling of the amorphous region in a starch granule promoted the transformation of crystalline regions by pulling the crystallites apart in the process of gelatinization. At lower water content, crystallites melt at significantly higher temperatures.

In summary, under heat-moisture treatment, starch gelatinization depends on the migration of available water and may follow more than one reaction mechanism.

OBJECTIVE

The aim of this study was to construct kinetics of starch gelatinization during HMT, in which various combinations of moisture content and heating time were designed to obtain gelatinization rate constants, k, at a constant temperature of 100°C. The heat-moisture treated cowpea starch gelatinized over a moisture content range occurring in steaming of cowpea seeds. This starch gelatinization model, together with the model already constructed for heat and moisture transfer (Chapter 3), will be applied to investigate the process of starch gelatinization in cowpea seeds during steaming.

MATERIALS AND METHODS

Cowpea flour was used to model kinetics of starch gelatinization. Starch content of cowpea flour is essential to the kinetics of gelatinization. Before construction of the kinetics, it is necessary to know the starch content in cowpea flour.

Preparation of cowpea flour

Cowpea seeds (*Vigna unguiculata,*cv. B5) were purchased (C&F Food Inc., City of Industry, CA) and ground to flour in a coffee mill (Model k7450, Regal Ware Inc., Kewaskum, WI). The milled flour was sieved (USA Standard Testing Sieve, Fisher Scientific Co.) by passing through a 106 μm sieve and stored at 3°C for later testing.

Preparation of cowpea flour for heat-moisture treatment

Moisture content was determined using a vacuum oven method (Approved Method 44-40, AACC 1995) (Isotemp vacuum oven, Model 282A, Fisher Scientific). Cowpea flour samples of known moisture content were individually mixed with deionized water to give total moisture contents of 25, 30, 35, 40, 45 and 50% (w.b.), respectively. Samples weighing 80±1 mg were hermetically sealed into 5.0cm × 2.5cm

high-density polyethylene pouches, which can withstand high internal-pressure (Koch Supplies Inc., Kansas City, MO) to prevent evaporation of water. All packaged pouches were stored in refrigerator (3°C) for 1 day to allow the moisture to distribute uniformly inside the samples.

Enzyme

Pullulanase (Lot 98H4050, EC 3.2.1.41 from *Klebsiella pneumoniae*) and β-amylase (Lot 59H7020, EC 3.2.1.2, Type II-BL crude, from barley) were obtained from Sigma Chemical Co. St. Louis, MO.

Regents for measuring of reducing sugar

Solution A: Sodium carbonate (anhydrous) (25 g) and Rochelle salt (25 g) were completely dissolved in 800 ml deionized water. Deionized water was added to make the solution volume to 1000 ml. Sodium bicarbonate (anhydrous) (20 g) and sodium sulfate (anhydrous) (200g) were then dissolved in the above solution.

Solution B: Cupric sulfate (5-hydrate) (30 g) was dissolved in 200 ml deionized water and 4 drops of H_2SO_4 (96.4%) was slowly added.

Solution C: Ammonium molybdate (25 g) was dissolved in 450 ml deionized water and then 21 ml of H_2SO_4 (96.4%) was slowly added. Sodium arsenate heptahydrate (3 g) was added in 25 ml deionized water. The two solutions were mixed and then deionized water was added to make 500 ml volume. The solution was stored overnight at 37-40°C in an amber color bottle.

Solution D: Solution A (25 ml) and solution B (1 ml) were blended using a vortex mixer to make solution D. This solution was prepared just before it was needed for the experiment.

Measurement of starch content in cowpea seeds

The starch content of cowpea seeds was determined by the method adopted by Nakamura and Suzuki (1977).

1. Preparation of glucose solution for standard curve

Perchloric acid (3.38%, 1 ml) was poured in 50 μg of glucose (G3285, Sigma Chemical co., St. Louis, MO) and then diluted to give concentrations of 10, 20, 30, 40 and 50 μg/ml glucose solutions in 25-ml-volumetric test tubes, respectively. Anthrone reagent (0.2%, 1 ml) was added to each diluted solution, boiled for 7.5 min, and then cooled. The absorbance of the solution was read at 630 nm with a spectrophotometer (Spectronic GenesysTM 5, Spectronic Instruments, Inc., NY). A standard curve of glucose solution was obtained (Fig. 4.2).

2. Starch extraction from cowpea flour

Cowpea flour (0.2-0.5 g) was weighed into 50-ml centrifuge tubes. Ethyl alcohol (80%) was added 10-20 ml, and stirred for 10 min and then centrifuged for 10 min at 3000g; Supernatant (80% ethyl alcohol + alcohol soluble solids) was discarded. This step was repeated. The precipitate was mixed with 5 ml of deionized water, vortex-stirred well before immersing into ice water. Following which perchloric acid (52%, 6.5 ml) was added and vortex-stirred (starch from sample was extracted into 52% perchloric acid). To this mixture, 20 ml deionized water was added and centrifuged for 10 min at 3000g. The supernatant (perchloric acid + starch) was transferred to a 100ml cylinder. This step was repeated. Deionized water was added to the cylinder to make up the final volume of starch extract solution to100 ml.

3. Determination of starch content in cowpea seeds

The extracted starch solution was diluted with deionized water to various concentrations: original solution, 2×, 3×, 5× …(the optimum starch concentration, 5-20 μg starch/1ml). Each diluted starch extract solution (5 ml) was poured into a 25 ml tube and then immersed into ice water. Ten milliliter of anthrone reagent (0.2%) (95% H_2SO_4 200 ml + 0.4 g anthrone) was poured into the test tube, immersed in boiling water for 7.5 min and then immediately placed into ice water (starch decomposed to glucose by H_2SO_4 and dyed to blue-green color by anthrone). The absorbance of the colored solution was

measured at 630nm against deionized water with Spectronic GenesysTM spectrophotometer. Amount of starch was determined by using glucose as standard (Fig. 4.2), amount of starch = 0.9× amount of glucose.

Measurement of degree of starch gelatinization

The degree of starch gelatinization was measured by the method that was followed by Lee et al. (1993).

1. Preparation of standard solution and curve

Maltose (Lot 59H1128, M5885, Sigma Chemical Co., St. Louis, MO) was dried overnight at 95-100°C, to remove all moisture in maltose, and then stored in desiccators. Dried maltose was dissolved in deionized water (1:1 ratio, w/v) to form standard maltose solution. This solution was appropriately diluted to obtain nine concentrations in the range of 0.1 and 0.9 mg/ml. The standard curve of maltose solution was obtained by measuring absorbance at 520nm with the Spectronic GenesysTM 5 spectrophotometer (Fig. 4.3).

2. Heat-moisture treatment

The pouches containing cowpea flour were first immersed in an oil bath (Circulators, VWR Scientific Products, Niles, IL) set at 100°C for 3, 9 and 15min interval. After heating, the treated samples were plunged into 0°C water/ice instantly. The samples were finally freeze-dried in Genesis freeze-dryer (Virtis 25ES, Gardiner, NY).

3. Hydrolysis of starch of HMT sample

In determining degree of gelatinization, digestibility of HMT sample was carried out by a mixed enzyme system: pullulanase and β-amylase. One unit of β-amylase will liberate 1.0mg of maltose from starch in 3 min at pH 4.8 at 20°C. One unit of pullulanase will liberate 1.0μmole of maltotriose from pullulan per min at pH 5.0 at 25°C.

The gelatinized samples (80mg) were homogenized by using a tissue grinder (Wheaton Potter-Elvehjem Tissue Grinders, Fisher Scientific). The pestle's (6mm

diameter) stainless-steel rod was connected to a chuck of a 735W drive motor (Model S 100, Serial 178, Tri-R Instruments, Jamaica, NY). The motor speed can be set from 0 to 5000 RPM. The pestle bottom made of PTFE (polytetrafluoroethylene) conformed to glass tube bottom with a clearance of approximately 0.10 to 0.15mm. The glass tube (working capacity: 15 ml) was hand held and moved up and down 10-20 times along the rotating pestle for a few times approx. 10 min to ensure complete homogenization of samples. The detailed procedure for hydrolysis of starch granules is shown in Fig. 4.4

4. Determination of reducing sugar (Somogyi-Nelson method)

Solution D (1 ml) was poured into the 50 ml test tube containing 1 ml of enzyme-treated sample (Fig. 4.4), capped with aluminum foil and placed in a water-bath set at 95°C-100°C for 20 min. Solution C (1 ml) was added and mixed. The sample mixture was cooled under running tap water for 20 min and then held at room temperature for 20 min. Deionized water was added to the tube to make up the total volume to 25 ml. Absorbance of the solution was read at 520 nm by the Spectronic GenesysTM spectrophotometer. Reducing sugar content in the sample was estimated using the standard curve for maltose solution (Fig. 4.3).

5. Experimental plan for heat-moisture treatment

In order to investigate starch gelatinization in cowpea seeds during steaming, the heat-moisture treatments were designed to cover a wide range of moisture content that was typically encountered in steaming seeds. The kinetics of starch gelatinization was constructed by using cowpea flour that had been treated using heat-moisture method.

The observed temperature at the center of cowpea seed rose rapidly above 90°C after 10s of steaming and exceeded 100°C after 55s of steaming (Chapter 3). The temperature of steaming seeds remained between 100 and 102°C for the most part of the steaming process. Rate of starch gelatinization in the seeds depended primarily on the amount of water available. Hence, the rate of gelatinization of cowpea starch at a

constant temperature of 100°C was considered a function of moisture content of cowpea flour.

The profiles of moisture content in cowpea seeds during steaming showed (Figs. 3.11-3.14) that the moisture content ranged from 11.4 to 40% (w.b.). Since the cowpea flour contains 34 to 52% starch (Kerr et al., 2000), the selected range of moisture content of 25 to 50% (w.b.) was carried out for 3, 9 and 15 min intervals at 100°C (Table 4.1). The HMT experiments were conducted in triplicate for each combination of test parameters.

A standard for completely gelatinized sample was prepared as: 5% cowpea flour solution in 95% deionized water was autoclaved for 1 hr and then freeze-dried. The reducing sugar in the autoclaved sample was measured and its value was assumed to correspond to 100% degree of starch gelatinization.

Raw starch was used as a standard for 0% DG. The reducing sugar in the raw starch sample was measured and its value was taken as 0% degree of starch gelatinization.

6. Calculation for degree of gelatinization

Absorbance value, A, was obtained from sample hydrolyzed by enzyme (Fig. 4.4). Absorbance value, A', was for the same sample treated first by alkali and then by enzyme. Absorbance 'a' was obtained from the blank test. Before conversion of absorbance values to reducing sugar contents, the values A and A' were corrected by deducting the value, 'a' of blank test. The values (A-a) and (A'-a) were converted to reducing sugar contents, B and B' on the basis of the standard curve (Fig. 4.3).

The degree of gelatinization (DG) was calculated based on the ratio of the amount of reducing sugar produced from test samples treated with and without alkali. The degree of gelatinization for a partially gelatinized sample was calculated as:

$$DG(\%) = \left(\frac{B}{B'} - \frac{B_o}{B'_o} \right) \Big/ \frac{B_a}{B'_a} \times 100 \qquad (4)$$

RESULTS AND DISCUSSION

Starch content of cowpea flour

Starch is a major component of cowpeas. The average starch content (dry basis) in the cowpea seed (*Vigna unguiculata,* cv. B5) was 48.8(±1.50)%.

Most studies on starch gelatinization have been based on the physicochemical changes of pure starch granules, which were isolated from raw materials. Wootton & Bamunuarachehi (1979) reported on the gelatinization of three types of maze and wheat starches and listed the minimum levels of moisture for gelatinization as: 31% (w/w, w.b.) for wheat starch, 31% for maize starch, 32% for waxy maize starch and 34% for amylomaize starch. Heat treatment of starches at restricted moisture levels (18-30% w.b.) and high temperature (100°C) for 16h has shown to alter the structure and physicochemical properties of normal maize, waxy maize, high amylose maize, wheat, oat, barley, potato, yam, pigeon pea and laird lentil starches (Hoover & Manuel, 1996). Hoover and Manuel (1996) pointed out that the magnitude of these changes were found to be dependent upon the moisture content during heat treatment and the starch source.

Water binding capacity is very much dependent on the chemical and physical properties of materials. Since starch content in cowpea flour is 48.8% and the water binding capacity of cowpea protein (and other components in cowpea flour) is different from that of starch during its gelatinization, the amount of protein in cowpea flour may affect moisture available for starch gelatinization compared with gelatinization of pure cowpea starch under the same sample size and moisture level.

Effect of particle size of flour on starch content and gelatinization

Berby et al. (1975) using microscopic observation method, studied wheat starch gelatinization in limited water systems. This results showed that there was little swelling of starch which was embedded in the protein matrix of soft wheat flour, since wheat flour protein minimized contact and reaction between starch and water. This indicates that the

particle size of cowpea flour can affect the measurement of starch content as well as the contact and reaction (moisture diffusion) between starch granules and water.

Differences in milling and separation procedures resulted in significant variations in cowpea starch content. Kerr et al. (2000) reported that the greatest difference in compositional values were for cowpea starch level, that ranged from 34.49 to 51.99%. The method of Galvez and Resurreccion (1993) was used in which cowpea flour were hydrolyzed in base and α-amylase, and then subjected to amyloglucosidase before reading glucose content. Starch levels increased in the order of 35.58, 40.66, and 51.99% for unsieved flours milled through 2.0-, 1.0-, and 0.5-mm screens, respectively. Both mill screen and particle size significantly affected starch levels ($P<0.01$). Kerr suggested that one possible reason might be that greater degradation of starch occurred at smaller mill screen sizes due to higher shear conditions.

In our study, the cowpea flour of particle size < 106μm was used in all HMT samples to obtain reproducible results.

Effect of HMT on the susceptibility of samples to enzymatic hydrolysis

Hoover and Manuel (1996) studied the effect of HMT (30% w.b., 100°C) on the physicochemical properties of legume starch: green arrow pea, eston lentil, othello pinto bean, black bean and express filed pea starches. They observed that heat-moisture treatment increased the susceptibility of all legume starches towards hydrolysis by α-amylase.

DG of samples with moisture levels (25-50% w.b.) heated at 100°C for different time intervals is presented in Table 4.2. The values of DG increased with increase in the levels of moisture content of cowpea flour. The result showed that the susceptibility of all flour samples towards β-amylase-pullulanase hydrolysis increased after HMT. Furthermore, this confirmed that some damage to the granules did occur during HMT and the physicochemical characteristics of the starch granules were altered during all the heat-moisture treatments.

The cowpea flour at 25% moisture level (w.b.) gelatinized slightly at 100°C for 3 min. Enzyme susceptibilities of treated flour attained maximum (DG = 37.3%) at moisture content, 50% (w.b.) for 15 min of HMT. Want et al. (1991) concluded, from experimental analysis and computer simulation, that regardless of the source of starch, when starch was cooked with moisture contents higher than 61% (w/w, w.b.), starch could be gelatinized completely and there was only one peak observed on DSC thermograms. However, starch samples with initial moisture contents between 15-40% showed two adjacent transition peaks on DSC thermograms. This suggests that the starch of cowpea flour requires higher moisture content (>61%) to gelatinize completely.

Construction of starch gelatinization kinetics

Research results correlating starch gelatinization, as a function of time and moisture contents have not been well documented. Wang et al. (1989) reported a correlation between rate constant of starch conversion and a nondimensional parameter $T/T_{p.}$ The reaction rate, k was as a function of the parameter, T/T_P, where T was the operating temperature for the reaction and T_p was dependent on the moisture content of sample. In this study, kinetics of cowpea starch was investigated in isothermal treatments, wherein cowpea flour samples with limited moisture content (25-50% w.b.) were heated at 100°C. Hence, the effect of moisture levels and time intervals on gelatinization was taken into account for the kinetics.

Using these experimental values of DG at different levels of moisture content and different time intervals (Table 4.2), starch reaction rate, k was determined by assuming a first order expression, Eq. (5) (Table. 4.3).

$$\frac{dS}{dt} = -kS + C \qquad (5)$$

The intercepts 0.003 and 0.008 were used to fit the experimental data at lower (<40% w.b. or 67% d.b.) and higher (≥40% w.b or 67% d.b.) moisture levels respectively, resulting in a better fit (the values of R^2 were larger). The values of R^2

showed that cowpea starch gelatinization did not follow very well first order reaction at 25 and 30% (w.b.) of moisture content (Table 4.3). However, the experimental data fitted it well at higher moisture content of cowpea flour. Values of C and k estimated for each moisture level which resulted in the greatest R^2 values (using MS Excel, linear fitting) is given in Table 4.3.

The gelatinization rate constants, k were plotted as a function of moisture content in Fig. 4.5.

$$k = 0.0019M + 0.0027 \quad (6)$$

(for moisture content, M (d.b.) <67%, M(w.b) < 40%)

$$k = 0.0079M + 0.0049 \quad (7)$$

(for moisture content, M (d.b.) ≥ 67%, M(w.b) ≥ 40%)

Reaction rate, k increased slowly when moisture content was lesser than 67% (d.b.), corresponding to the slow gelatinization of starch at lower level of moisture content. The reaction constant, k was greater when the moisture content (≥67% d.b.) of the HMT sample was higher (Fig. 4.5). Regression results seem to suggest that starch gelatinization of HTM did not follow a simple reaction mechanism but followed a multi-step reaction under different levels of moisture content of flour.

CONCLUSIONS

The enzymatic method is able to analyze the physicochemical changes of starch in cowpea flour following HMT. Heat-moisture treatment increased the susceptibility of all samples towards hydrolysis by β-amylase-pullulanase. Starch gelatinization can be expressed as a two-step reaction under different ranges of moisture contents. The kinetics relationships are useful for simulation studies of cowpea starch gelatinization at limited water content. More combinations of HMT would further improve the kinetics of gelatinization. For simplicity, the first order reaction kinetics in HMT of cowpea flour

will provide kinetics of gelatinization to investigate the physicochemical changes in cowpea steaming (Chapter 5).

NOTATION

B	Amount of RD produced from sample (mg/ml)
B'	Amount of RD produced from sample treated with alkali (mg/ml)
B_o	Amount of reducing sugar (RD) produced from raw sample (mg/ml)
B'_o	Amount of RD produced from raw sample treated with alkali (mg/ml)
B_a	Amount of RD produced from completely gelatinized sample (mg/ml)
B'_a	Amount of RD produced from completely gelatinized sample treated with alkali (mg/ml)
C	Intercept constant
d.b.	Dry basis
D.G	Degree of starch gelatinization
E_{ag}	Activation energy for the gelatinization process (J/mole)
k	Gelatinization rate constant (1/s)
k_{ref}	Gelatinization rate constant at the reference temperature (1/s)
M	Moisture content
R	Universal gas constant (J/mole K)
S	Degree of ungelatinized starch
t	Time (s)
T	Temperature (K)
T_{ref}	Reference temperature (K)
w.b.	Web basis

REFERENCES

American Association of Cereal Chemists. (1995). Approved Methods of the AACC, 9th Ed. The Association: St. Paul, MN.

Atwell, W. A., Hood, L. F., Lineback, D. R., Varriano-Marston, E. & Zobel, H. F. (1988). The terminology and methodology associated with basic starch phenomena. Cereal Foods World. 33: 306-311.

Bhattacharya, M. & Hanna, M. A. (1987). Kinetics of starch gelatinization of cooked rice. Starch/Starke. 52: 764-766.

Biliaderis, C. G. (1983). Differential scanning calorimetry in food research - a review. Food Chemistry. 10: 239:265.

Derby, R. I., Miller, B. S., Miller, B. F. & Trimbo, H. B. (1975). Visual observation of wheat-starch gelatinization in limited water systems. Journal of Cereal Science. 52: 702:713.

Donovan, J. W. (1979). Phase transition of the starch-water system. Biopolymers. 18: 263-270.

Donovan, J. W., Lorenz, K. & Kulp, K. (1983). Differential scanning calorimetry of heat-moisture treated wheat and potato starches. Cereal Chemistry. 60 (5): 381-387.

Fennema, O. R. (1996). Food Chemistry. Third edition. 191-195. Marcel Dekker, Inc. New York.

Galvez, F. C. F., & Resurreccion, A. V. A. (1993). The effects of decortication and method of extraction on the physical and chemical properties of starch from mungbean (*Vigna radiata (L.) Wilczec*). Journal of Food Processing Preservation. 17: 93-107.

Haruhito, T., Mayumi H., Hiroaki, I., Satoshi, W. & Gisho, G. (1990). Enzymatic evaluation for the degree of starch retrogradation in foods and foodstuffs. Starch/Starke. 42 (6): 213-216.

Hoover, R. & Manuel, H. (1996). Effect of heat-moisture treatment on the structure and physicochemical properties of legume starches. Food Research International. 29 (8): 731-750.

Hyun, H. H. & Zekius, J. G. (1985). Biochemical characterization of thermostable extracellular β-amylases from *Clostridium thermosulfurogenes*. Appl. Environ. Microbiol. 49: 1162-1167.

Kerr, W. L., Ward, C. D. W., McWatters, K. H. & Resurreccion, A. V. A. (2000). Effect of milling and particle size on functionality and physicochemical properties of cowpea flour. Cereal Chemistry. 77 (2): 213-219.

Kim, Y. & Wang, S. S. (1999). Starch cooking with limited water as affected by zein and guar gum. Journal of Food Science. 64 (1): 133-135.

Kulp, K. & Lorenz, K. (1981). Heat-moisture treatment of starches. I. Physicochemical properties. Cereal Chemistry. 58 (1): 46-48.

Lee, B. Y., Mok, C. & Lee, C. (1993). Comparison of differential scanning calorimetry with enzymatic method for the determination of gelatinization degree of cornstarch. Korean Journal of Food Science & Technology. 25 (4): 400-403.

Lilia, S.C. & Harold, C. (1999). Heat-moisture treatment effects on sweet potato starches differing in amylose content. Food Chemistry. 65: 339-346.

Lund, D. (1984). Influence of time, temperature, moisture, ingredients, and processing conditions on starch gelatinization. CRC Critical Reviews in Food Science and Nutrition. 20 (4): 249-273.

Maruta, I., Kurahashi, Y., Takano, R., Hayashi, K., Kudo, K. & Hara, S. (1998). Enzymatic digestibility of reduced-pressurized, heat-moisture treated starch. Food Chemistry. 61 (1/2): 163-166.

Nakamura, M. & Suzuki, S. (1977). Handbook of Starch Science. 165-170. Asakura Shoten Press. Tokyo.

Nakamura Y. (1996). Some properties of starch debranching enzymes and their possible role in amylopectin biosynthesis. Plant Science. 121: 1-18.

Qu, D. & Wang, S. S. (1994). Kinetics of the formations of gelatinized and melted starch at extrusion cooking conditions. Starch/Starke. 46 (6): 225-229.

Reddy, P. R. (1991). Rheological properties and phase transitions of starch-water systems during gelatinization at atmospheric and elevated pressures. Ph.D. Dissertation. University of Minnesota.

Sarikaya, E., Higasa, T., Adachi, M. & Mikami, B. (2000) Comparison of degradation abilities of α- and β-amylases on raw starch granules. Process Biochem. 35: 711-715.

Shetty, R. M., Lineback, D.R. & Seib, P. A. (1974). Determining the degree of starch gelatinization. Cereal Chemistry. 51: 364-375.

Verlinden, B. E., Nicolai, B. M. & Baerdemaeker, J. D. (1994). The starch gelatinization in potatoes during cooking in relation to the modeling of texture kinetics. Journal of Food Engineering. 24: 165-179.

Wootton, M. and Bamunuarachchi, A. (1979). Application of differential scanning calorimetry of starch gelatinization. II. Effect of heating rate and moisture level. Starch/Starke. 31 (8): 262-270.

Wang, S. S., Chiang, W., Yeh, A., Zhao, B. & Kim, I. (1989). Kinetics of phase transition of waxy corn starch at extrusion temperatures and moisture contents. Journal of Food Science. 54 (5): 1298-1301.

Wang, S. S., Chiang, W. C., Zhao, B., Zheng, X. G. & Kim, I. K. (1991). Experimental analysis and computer simulation of starch-water interactions during phase transition. Journal of Food Science. 56: 121-126.

Zanoni, B., Schiraldi, A. & Simonetta, R. (1995). A naïve model of starch gelatinization kinetics. Journal of Food Engineering. 24: 25-33.

LIST OF TABLES

Table 4.1 The experimental plan for heat-moisture treatment at 100°C

Test	Time (min)	Moisture Content (% w.b.)
1		25
2		30
3	3	35
4		40
5		45
6		50
7		25
8		30
9	9	35
10		40
11		40
12		45
13		25
14		30
15		35
16	15	35
17		40
18		45

Table 4.2 The DG of samples with different moisture content, M treated at different time intervals at 100°C

Time (min)	M (% d.b.)	M (% w.b.)	DG (%)
3	33.3	25.0	2.4
	42.9	30.0	4.0
	53.8	35.0	6.4
	66.7	40.0	11.0
	81.8	45.0	22.7
	100.0	50.0	25.9
9	33.3	25.0	5.6
	42.9	30.0	8.1
	53.8	35.0	12.1
	66.7	40.0	17.8
	81.8	45.0	30.0
	100.0	50.0	33.2
15	33.3	25.0	6.4
	42.9	30.0	10.5
	53.8	35.0	14.5
	66.7	40.0	21.0
	81.8	45.0	34.0
	100.0	50.0	37.3

Table 4.3 Estimates of gelatinization rate constants, k
for cowpea flour at different levels of moisture content, M

M % (w.b.)	M % (d.b.)	Constant C	Rate constant (k)	R^2
25.0	33.3	0.003	0.0032	0.6594
30.0	42.9	0.003	0.0034	0.8282
35.0	53.8	0.003	0.0036	0.9998
40.0	66.7	0.003	0.0040	0.9159
45.0	81.8	0.008	0.0120	0.9032
50.0	100.0	0.008	0.0126	0.9124

LIST OF FIGURES

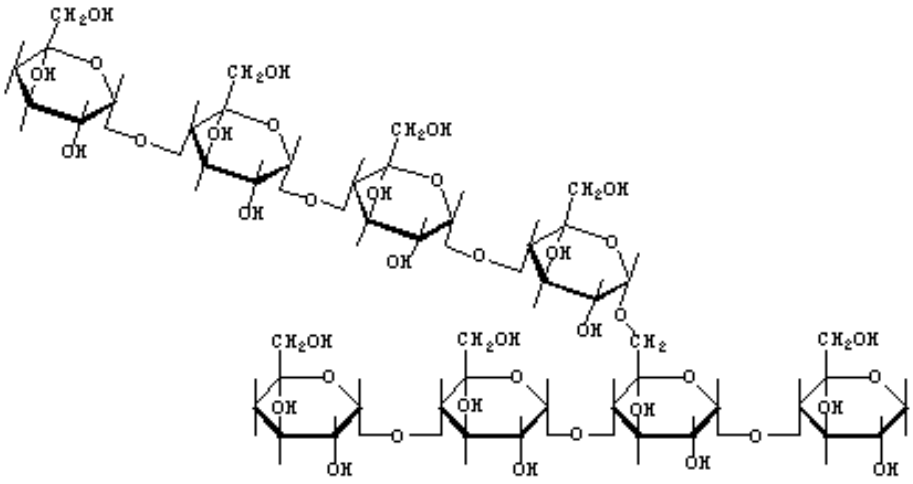

Amylopectin

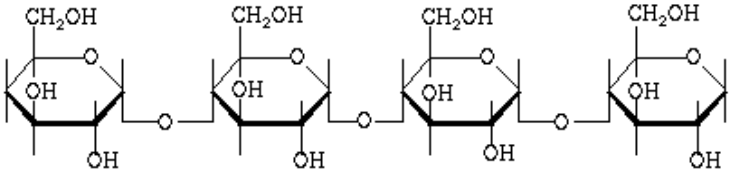

Amylose

Fig. 4.1. Chemical structure of amylopectin and amylose

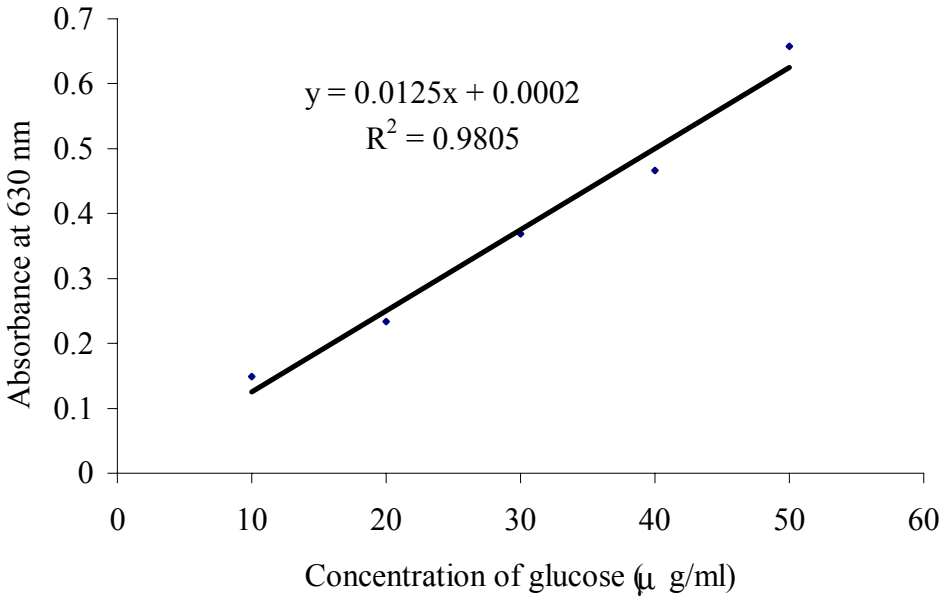

Fig. 4.2. Standard curve of glucose solutions

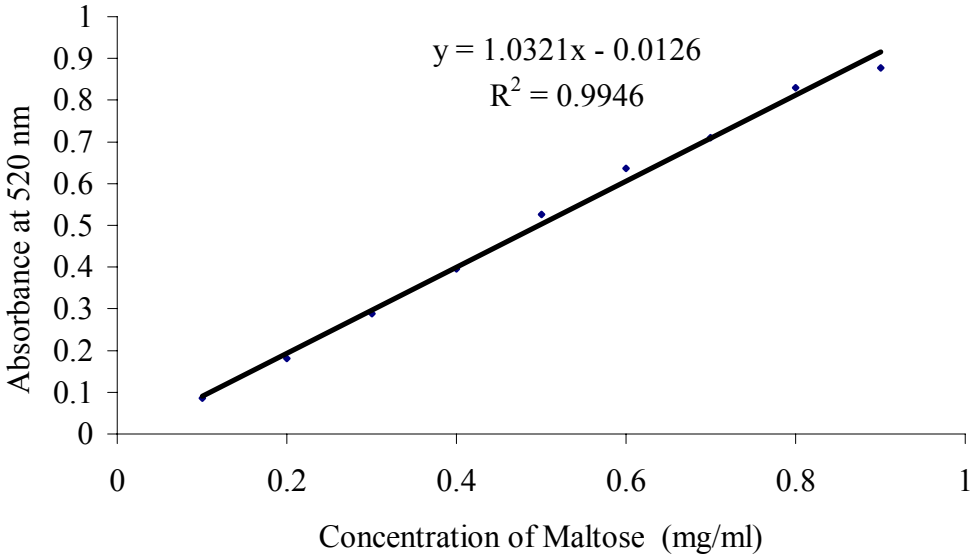

Fig. 4.3. Standard curve of maltose solution

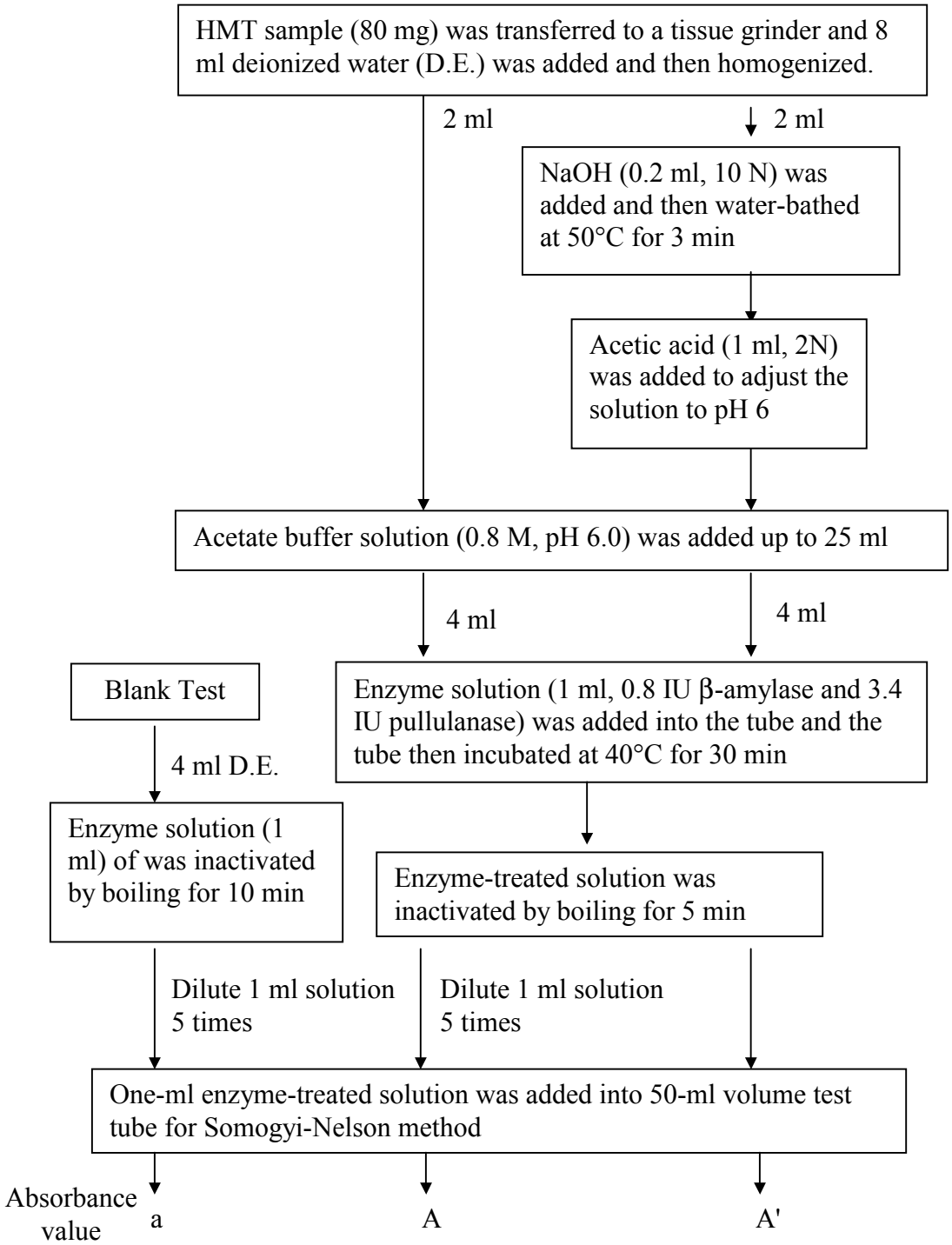

Fig. 4.4. Flow chart showing procedure of hydrolysis of starch

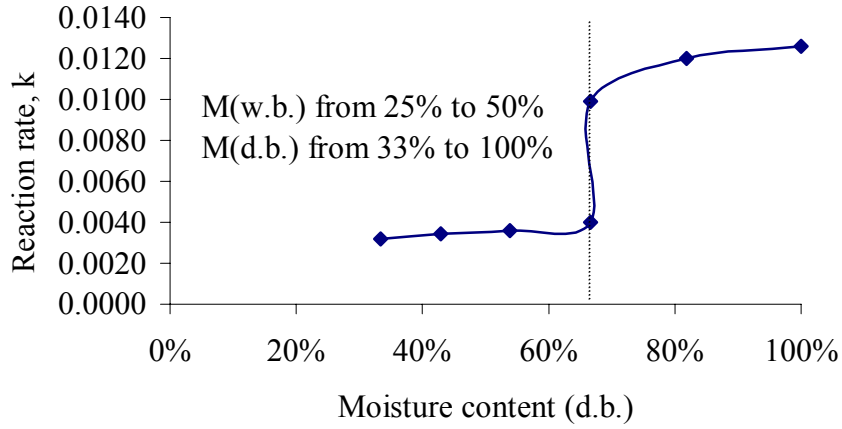

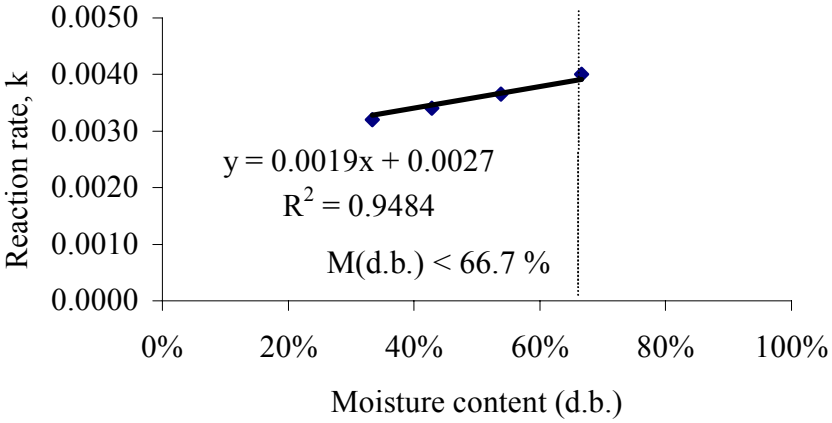

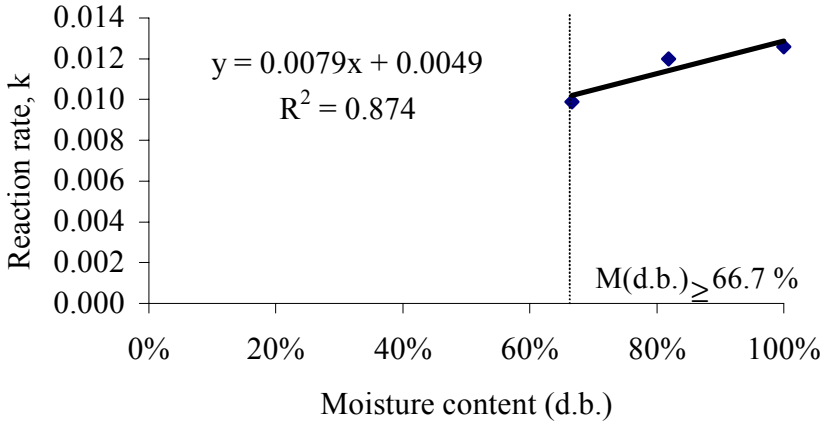

Fig. 4.5. Reaction rate constant, k of starch gelatinization versus moisture content of cowpea flour

CHAPTER 5

MODELING OF STARCH GELATINIZATION IN COWPEA SEEDS DURING STEAMING AND VERIFICATION[1]

[1]Fang, C. and Chinnan, M. S. 2000. To be submitted to Journal of Food Engineering

INTRODUCTION

Very little work has been done on studies of starch gelatinization within intact starchy seeds during steaming. Starch gelatinization in intact seeds during steaming is based on simultaneous heat and mass transfer and the interaction rate between water and seed starch. Localized temperature and moisture contents vary inside seeds during steaming. Hence, rate of gelatinization is a function of spatial temperatures and moisture contents, which vary with positions and time within seeds. This requires an understanding of water diffusion into seeds and kinetics of starch gelatinization during heating.

In recent years, nuclear magnetic resonance (NMR) imaging has been used to nondestructively and noninvasively visualize temperature and moisture distribution in small intact seeds and particles during cooking. Hulbert et al. (1997) studied temperature mapping in cooking of carrot using 2D magnetic resonance imaging (MRI). Water diffusion has been studied in rice grain during boiling (Takeuchi et al., 1997; Horigane et al., 1999) and in wheat grain during boiling and steaming (Stapley et al., 1997b; Stapley et al., 1998). Stapley et al. (1998) reported on finding a much more uniform moisture profile across wheat grains during steaming wherein the moisture levels rose slowly with time; the overall moisture uptake was much slower than that encountered in boiling. Studies have demonstrated that NMR images could depict clear water distribution in intact grains during cooking. The degree of progress in cooking a grain could be measured by the extent of rise in moisture content, which was in fact controlled by gelatinization associated with moisture diffusion that supplied the starch in the grain with the water required for gelatinization (Takeuchi et al., 1997).

Stapley et al. (1997a) studied starch conversion within wheat grain by using DSC to scan intact cereal grains. The information on steaming grains was compiled by comparing DSC scans of steamed and un-steamed wheat grains. It was postulated that the inner core of grains contained unconverted starch, and that the starch conversion was

confined to the outer regions. Stapley et al. (1997a) concluded that in steaming, the rate of starch conversion in whole-wheat grains was controlled by the time taken to achieve a critical moisture content.

Bakshi and Singh (1980) proposed a one-dimensional mathematical model describing simultaneous water diffusion and gelatinization of starch during rice parboiling. They considered gelatinization as an irreversible first-order reaction, which bound water molecules. However, the NMR imaging showed that water did not become immobilized upon gelatinization of starch (Stapley et al., 1998). Verlinden et al. (1994) studied simulation of starch gelatinization in potatoes during cooking. The simulation was carried out to use a gelatinization kinetics, combining with a heat transfer model, to predict profiles of ungelatinized starch fraction. The starch gelatinization in potato was considered as a function of spatial temperature and heating time. Due to high moisture content inside potato, the water diffusion was not considered in the starch gelatinization.

Since an experimental tool for direct quantitative measurement of starch gelatinization in intact seed during steaming is yet to be designed, it is necessary to use mathematical modeling. A finite element model with Newton-GMRES method was developed to describe the behavior of heat and mass transfer successfully (Chapter 3). The prediction from the model agreed well with the experimental data. The model was able to describe well the different transport mechanisms, which varied and interacted with each other during the steaming process. A kinetics of gelatinization of cowpea starch during HMT was constructed (Chapter 4), in which various combinations of moisture content and heating time was designed to obtain gelatinization rate constants, k, at a constant temperature of 100°C. The heat-moisture treated cowpea starch gelatinized over a moisture content range occurring in steaming of cowpea seeds. The starch gelatinization kinetics, together with the model already constructed for heat and moisture transfer can be used to investigate the process of starch gelatinization in cowpea seeds during steaming.

Because most of the starch gelatinization was achieved in the outer regions of seeds during steaming, it is important and possible to validate the extent of the starch gelatinization in the outer regions by designing an appropriate experimental method.

OBJECTIVE

The objective of this study is to investigate starch gelatinization in cowpea seeds during steaming.

1) Predict spatial degree of starch gelatinization in cowpeas during steaming.
2) Validate the predicted values of starch gelatinization in the outer region of the seeds.

MATERIALS AND METHODS

Sample preparation

Cowpea seeds (*Vigna unguiculata*,cv. B5) were obtained from C&F Food Inc. (City of Industry, CA). The sample seeds were selected as described in Chapter 3. In order to collect 80 mg of cowpea flour from different layers of seeds, six seeds (each seed mass: 357±5mg) were selected for each treatment. Cowpea seeds were steamed for 1, 5, 15, 30 and 60 min intervals. The outermost layer and the layer below the outermost layer, each layer 0.5-mm thick, were removed by a grinding blade. The device used in removing these layers is illustrated in Fig. 5.1. The grinding blade (a carborundum disk), powered by a high-speed drill (Dremel, Model 275, Type 5, Racine, WI), was set to rotate at 28,000 RPM. To remove a given layer of material, the seed was manually moved across the rotating blade where the rotating blade was protruding only 0.5 mm above the platform. Material abraded away from the seed was collected as cowpea flour in the collection chamber. Slight negative pressure was maintained in the collection chamber to ensure collection of all flour generated during abrasion (Fig. 5.2). After collection, the ground flour was quickly frozen at -80°C. The frozen sample was freeze-

dried in Genesis Freeze Dryer (Virtis 25ES, Gardiner, NY), and then stored in desiccators for later determination of degree of gelatinization (DG).

Determination of starch gelatinization

The degree of gelatinization of steamed sample was measured by the method proposed in Chapter 4.

Simulation of starch gelatinization

Simulation of gelatinization was carried out by combining the kinetics of cowpea starch gelatinization during HMT (Chapter 4) with the model already constructed for heat and moisture transfer (Chapter 3). The kinetics equation describing starch gelatinization taken from Chapter 4 are represented below:

$$\frac{dS}{dt} = -kS + C \tag{1}$$

where,

for moisture content, M (d.b.) <67%:

$$C = 0.003 \tag{2}$$

$$k = 0.0019M + 0.0027 \tag{3}$$

for moisture content, M (d.b.) ≥ 67%:

$$C = 0.008 \tag{4}$$

$$k = 0.0079M + 0.0049 \tag{5}$$

The fraction of ungelatinized starch, S as a function of time and moisture content at each node can be computed by solving explicit Euler finite difference schemes presented in the equations below

$$S(t_{t+1}) = S(t_t) - k(M_t) \cdot S(t_t) \cdot \Delta t + C \cdot \Delta t \tag{6}$$

Representation of nodes in a finite element model is described in detail in Fig. 3.1.

Average degree of ungelatinized starch, S_{ave} of each layer was obtained by using Eq. (7), volume-averaging the degree of ungelatinized starch of all nodes in each layer at each time step.

$$S_{ave} = \frac{\sum_{e=1}^{n} \frac{\pi A^{(e)}}{6}[(R + r_i)S_i + (R + r_j)S_j + (R + r_m)S_m]}{\sum_{e=1}^{n} \frac{2\pi}{3} A^{(e)} R} \qquad (7)$$

Flow chart of algorithm for modeling of starch gelatinization is shown in detail in Fig. 5.3.

RESULTS AND DISCUSSION

Three Layers and different sections of the cowpea seed are presented in Fig. 5.4. The profiles of ungelatinized starch as a function of steaming time and moisture content in cowpea seed were predicted and plotted (Fig. 5.5-5.7). On comparing the profiles of moisture content (Figs 3.11-3.14), the profiles of gelatinization are found to be extremely moisture content dependent. The simulated starch profiles with the highest DG (the lowest S) at the mid-surface showed the same trend as the profiles of moisture. Ungelatinized starch decreased as moisture diffused into the seed. The lowest contour value of S was 86.0% at 900s of steaming (Fig. 5.7). The starch profiles showed that the lower degree of ungelatinized starch was at the layer closer to surface (Fig. 5.7). Fraction of ungelatinized starch in the innermost layer and layer 2 remained above 98% during 15 min of steaming (Fig. 5.8). Ungelatinized starch disappeared faster in layer 1 than that in layer 2, due to more moisture uptake from steam in layer 1.

The simulation of gelatinization was carried out for only 15 min of steaming, because the kinetics of gelatinization was constructed on the basis of 15 min of HMT experiment. The experimental and predicted values of DG in different layers are presented in Table 5.1. The predicted values in layer 1 agreed well with the experimental

values at 5 and 15 min of steaming. The 79 % of starch in the outermost layer remained ungelatinized after 60 min of steaming. The seeds that were steamed for 60 minutes had 22.7% (w.b.) moisture content (Table 5.2). This indicates that it may take a much longer exposure time to steam vapor for complete gelatinization to occur.

The predicted DG in layer 2 was higher than the experiment data. The observed and simulated fraction of ungelatinized starch in layer 2 remained above 98% at 15 min of steaming. The DG of layer 2 was negative (Table 5.1) at the treatments of 5 min steaming. After the layer 1 of unsteamed seeds was taken off, the seeds were rather fragile due to low moisture content. It was difficult to continue to remove the layer 2. The standard values for DG=0% and DG=100%, which were obtained from the layer 1, were used to calculate the DG of layer 2. This may result into the negative value of DG of the layer 2, since the starch content of the layer 2 is different from that of the layer 1.

The deviation between observed and predicted values may be due to non-uniform distribution of starch contents within the seeds, discrepancy in physicochemical properties between the starch of flour and that of the intact seeds, different grinding gadgets which resulted in variations in the extent of damaged granules, different behaviors of heat and mass transfer between cowpea flour and the seeds.

Effect of starch content on the evaluation of degree of gelatinization

The DG was calculated based on the ratio of the amount of reducing sugar produced from samples treated with and without alkali. The degree of gelatinization for a partially gelatinized sample was calculated by:

$$DG(\%) = \left(\frac{B}{B'} - \frac{B_o}{B'_o} \right) \Big/ \frac{B_a}{B'_a} \times 100 \qquad (8)$$

Cowpea flour (80mg) was removed from the layer 1 of seeds that had been steamed for 15min. The amount of reducing sugar, B =0.0311 (mg/ml), was released from the sample treated with enzyme. The amount, B'= 0.1517 (mg/ml), from the sample treated with alkali + enzyme. The ratio of reducing sugar, B/B' was 0.2050 (Table 5.3).

The ratio of reducing sugar, B_o/B'_o from unsteamed sample was 0.1805 and its value was assumed to correspond to 0% degree of starch gelatinization. The value, B_a/B'_a from autoclaved sample was 0.2346, which was assumed to correspond to 100% degree of starch gelatinization. According to Eq. (8), the DG of the sample was calculated as 10.35% (Table 5.1).

Starch content varied greatly within the same sample size of cowpea flour. Differences in milling and separation procedures resulted in significant variations in cowpea starch content. Kerr et al. (2000) reported that the greatest difference in compositional values were for cowpea starch level, that ranged from 34.49 to 51.99%. Starch levels increased in the order of 35.58, 40.66, and 51.99% for unsieved flours milled through 2.0-, 1.0-, and 0.5-mm screens, respectively. Both mill screen and particle size significantly affected starch levels ($P<0.01$). Kerr suggested that one possible reason might be that greater degradation of starch occurred at smaller mill screen sizes due to higher shear conditions.

Shetty et al. (1974) reported that various amounts (25 to 100 mg) of prime wheat starch with 500 I.U. glucoamylase for 0.5 hr at 37°C were measured for the amount of D-glucose released; the data showed a linear correlation between the D-glucose released during digestion and the quantity of granular starch available to glucoamylase. The plots of glucoamylase digestibility (D-glucose released) versus time for the three kinds of starches (corn, wheat and potato) were linear to 2 hr of digestion.

Cowpea flour removed from steamed seeds was not uniform in particle size, which resulted in variations in starch content even within the same sample size. The variation of values of B' confirmed that starch contents were different within the same sample size (80±1 mg) (Table 5.3). Hence, the evaluation of DG must be based on the total starch content of sample due to linear correlation between the release of reducing sugar and total starch available to enzyme. This holds true especially for non-uniform sample because of its variation in the starch content within the same sample size.

Effect of starch content in different layers on degree of gelatinization

The average amount of reducing sugar, B' = 0.1572 (mg/ml) released from layer 1 was lower than that produced from layer 2, B' = 0.1824 (mg/ml) (Table 5.3). This suggested that the starch content in layer 2 was higher than that of layer 1. The model assumed that the fraction of ungelatinized starch was uniform within unsteamed cowpea seeds. Hence, this model did not account for the actual variation of starch content from layer to layer.

If starch content were uniformly distributed within seeds, starch gelatinization would depend directly on moisture diffusion seeds during steaming. Due to the variations in starch content in different layers, gelatinization was presumed to be affected by the ratio of water to starch. If cowpea flour samples with identical mass and moisture level differ in their starch content, then the level of starch content would affect significantly the DG in the same any given HMT. The flour with lower starch content would gelatinize to a different degree compared with the flour with higher starch content. For example, Sample A (5 g, 50% starch content, 50% protein) is mixed with 1 g water; Sample B (5g, 30% starch content, 70% protein) is mixed with 1 g water. The amount of water available for starch gelatinization in sample B is different from that in sample A, since water binding capacity of protein (or other components in cowpea flour) is different from that of the starch. Hence, DG of sample B is supposed to be different from that of sample A. This modeling ignored the effect of starch content in different layers on DG, which perhaps contributed to the inconsistencies in the data.

Effect of different grinding methods on the evaluation of DG

A kinetics of starch gelatinization was constructed by using cowpea flour ground in a coffee mill (Model k7450, Regal Ware Inc., Kewaskum, WI) (Chapter 4). The kinetics was then included in the heat and mass transfer model (Chapter 3) to simulate starch gelatinization in steaming of cowpea seeds. The predicted DG was validated by using cowpea flour, which was milled using a high-speed grinding blade (Fig. 5.1). The

digestibility of raw cowpea flour ground using the two devices was compared. The ratio (B_o/B'_o) of reducing sugar (0.06) of raw flour ground in a coffee mill was lower than that (0.18) obtained using a grinding blade. This suggests that the cowpea flour milled using the grinding blade was more susceptible to enzyme attack than that milled in the coffee mill and the extent of granule damage strongly depended on the grinding methods adopted.

Starch granules could partially or completely, lose crystallinity, depending on the extent of damage caused by forces of compression, impact, shear, or attrition (Karkalas et al., 1992). When mechanically deformed or damaged granules were hydrated, they swelled and gelatinized at ambient temperature and were rapidly hydrolyzed by amylases, in contrast to the native granules, which were relatively resistant to enzymatic attack.

It can be suggested that the high-speed circular blade (rotation at 28,000 RPM) generated localized high temperatures leading to cowpea starch degradation. Another reason might be the high shear, which affected the physical properties of starch granules and its enzyme digestibility. Karkalas et al. (1992) studied the differences between mechanically damaged and gelatinized starch, and pointed out that in general, thermally gelatinized starch granules released amylose into solution, while mechanically damaged granules predominantly gave rise to amylopectin fragments. However, gelatinized and damaged starch appeared to be equally susceptible to α-amylase. Hence, the extent of damage produced by using two different grinding procedures on starch granules of cowpea seeds could raise the enzymatic hydrolysis of cowpea starch. In determining the degree of gelatinization, the different correction standards (B_o/B'_o) of untreated samples derived from with different grinding methods might have contributed to the errors, as it is difficult to distinguish whether the susceptibility of cowpea starch to enzymatic attack resulted from mechanical or thermal effect. Measurement of starch gelatinization due to thermal effect should maintain the structural integrity of granules without any other

obstruction such as mechanical damage of granules or has the same correction standard for mechanical damage of granules.

Effect of moisture diffusivity on DG profiles

A power law relationship with moisture for effective moisture diffusivity, $D=9.5e\text{-}8*(M_{wb.})^{3.5}$ and 1.41e-10, which were reported for wheat grains during boiling (Stapley et al., 1998), were used in the numerical simulations during the initial phase and the main steaming phase, respectively . Moisture diffusion and the DG profiles strongly depended on moisture diffusivity. The predicted DG, volume-averaging DG at each nodes of the same layer, was validated through comparing the average predicted DG with experimental DG of the same layer. However, the DG at every node could not be verified in this study. In order to improve the simulation of starch gelatinization and verify the profile of DG in steaming cowpeas, more precise information regarding moisture diffusivity is required. Water diffusivity in seeds can be measured by PGSE NMR nondestructively and non-invasively. The NMR techniques can directly visualize moisture diffusion and provide clear data on moisture distributions in an intact seed during steaming (Stapley et al., 1997b). Through interpretation of NMR imaging, combined with finite element modeling, water diffusivity could be obtained and the profile of moisture and spatial degree of starch gelatinization could be then validated.

CONCLUSIONS

The simulated and observed values of DG (Table. 5.1) showed that gelatinization of starch was dependent on the location in the seed; starch in the outermost layer of seed gelatinized to a greater degree than that of in the inner layer. The main factors that determine the extent of starch gelatinization are the diffusion of water and time during steaming of cowpea seed. The predicted DG in the outmost layer was found to be in good agreement with the experimental data. The combined model was able to describe well the complex phenomenon of gelatinization during steaming of cowpea seeds.

NOTATION

A	Element area (m^2)
B_o	Amount of reducing sugar (RD) produced from sample (mg/ml)
B'_o	Amount of RD produced from raw sample treated with alkali (mg/ml)
B	Amount of RD produced from sample (mg/ml)
B'	Amount of RD produced from sample treated with alkali (mg/ml)
B_a	Amount of RD produced from autoclaved sample (mg/ml)
C	Constant
d.b.	Dry basis
D.G.	Degree of starch gelatinization
k	Gelatinization rate constant (1/s)
M	Moisture content (d.b.)
n	Total number of nodes per layer
r, z	Cylindrical coordinates (m)
R	$R=r_i+r_j+r_m$ (m)
S	Degree of ungelatinized starch
t	Time (s)
Δt	Time step (s)
T	Temperature (K)
w.b.	Wet basis

Subscripts

0	Initial
ave	Average
e	Element
i, j, m	Number order of nodes per element

Superscripts

e	Element

REFERENCES

Bakshi, A. S. & Singh, R. P. (1980). Kinetics of water diffusion and starch gelatinization during rice parboiling. Journal of Food Science. 45:1387-1392.

Burros, B. C., Young, L. A., & Carroad, P. A. (1987). Kinetics of corn meal gelatinization at high temperature and low moisture. Journal of Food Science. 52 (5): 1372:1376.

Hulbert, G. J., Litchfield, J. B. & Schmidt, S. J. (1997). Determination of convective heat transfer coefficients using 2D MRI temperature mapping and finite element modeling. Journal of Food Engineering. 34:193-201.

Karkalas, J., Tester, R. F. & Morrison, W. R. (1992). Properties of damaged starch granules. I. Comparison of a micromethod for the enzymatic determination of damaged starch with the standard AACC and Farrand methods. Journal of Cereal Science. 16: 237-251.

Kerr, W. L., Ward, C. D. W., McWatters, K. H. & Resurrection, A. V. A. (2000). Effect of milling and particle size on functionality and physicochemical properties of cowpea flour. Cereal Chemistry. 77 (2): 213-219.

Kimura, A. & Robyt, J. F. (1995). Reaction of enzymes with starch granules: kinetics and products of the reaction with glucoamylase. Carbohydrate Research. 277: 87-107.

Shetty, R. M., Lineback, D.R., & Seib, P. A. (1974). Determining the degree of starch gelatinization. Cereal Chemistry. 51: 364-375.

Stapley, AGF. & Fryer, P. J. (1998). Diffusion and reaction in whole wheat grains during boiling. AIChE Journal. 44 (8): 1777-1789.

Stapley, AGF., Gladden L. F. & Fryer, P. J. (1997a). A differential scanning calorimetry study of wheat grain cooking. International Journal of Food Science and Technology. 32: 473-486.

Stapley, AGF., Hyde, T. M. Gladden, L. F. & Fryer, P. J. (1997b). NMR imaging of the wheat grain cooking process. International Journal of Food Science and Technology. 32: 355-275.

Takeuchi, S., Maeda, M., Gomi, Y., Fukuoka, M. & Watanabe, H. (1997). The change of moisture distribution in a rice grain during boiling as observed by NMR imaging. Journal of Food Engineering. 33: 281-297.

Verlinden, B. E. Nicolai, B. M. & Baerdemaeker, J. D. (1994). The starch gelatinization in potatoes during cooking in relation to the modeling of texture kinetics. Journal of Food Engineering. 24: 165-179.

LIST OF TABLES

Table 5.1 Degree of gelatinization (DG) in different layers from different treatments

Steaming Time (min)	Obs. T (°C)	Layer 1*				Layer 2*			
		Pred. M.C. (d.b.%)	DG (%)			Pred. M.C. (d.b. %)	DG (%)		
			Obs.	Pred.	Error**		Obs.	Pred.	Error
0	24	12.9	0	0		12.9	0	0	
5	102.1	29.5	7.95	6.33	1.62 (20.3)	15.1	-1.72	0.40	2.12 (123.2)
15	101.8	33.7	10.35	9.50	0.85 (8.2)	20.7	1.60	1.80	0.2 (12.5)
30			13.68				2.17		
60			20.49				5.05		

* Layer 1 =outermost layer, Layer 2 =layer below outermost layer

** Error is absolute difference between observed (Obs.) and predicted (Pred.) values in parentheses refer to relative error

Table 5.2 Overall moisture content of cowpea seeds after various steaming intervals

Time (min)	0	1	5	10	15	20	30	60
M.C. (w.b.) %	11.4	16.4	17.4	18.4	19.2	19.7	20.6	22.7

Table 5.3 The reducing sugar (B and B') released from samples as a result of different treatments

Seed layers*	Time (min)	B(mg/ml)	B'(mg/ml)	B/B'
	0	0.0387	0.2144	0.1805
	5	0.0316	0.1585	0.1993
Layer 1	15	0.0311	0.1517	0.2050
	30	0.0342	0.1611	0.2128
	autoclaved 1h	0.0519	0.2021	0.2346
	5	0.0326	0.1843	0.1766
Layer 2	15	0.0338	0.1840	0.1844
	30	0.0361	0.1944	0.1858

*Layer 1 =outermost layer, Layer 2 =layer below outermost layer

LIST OF FIGURES

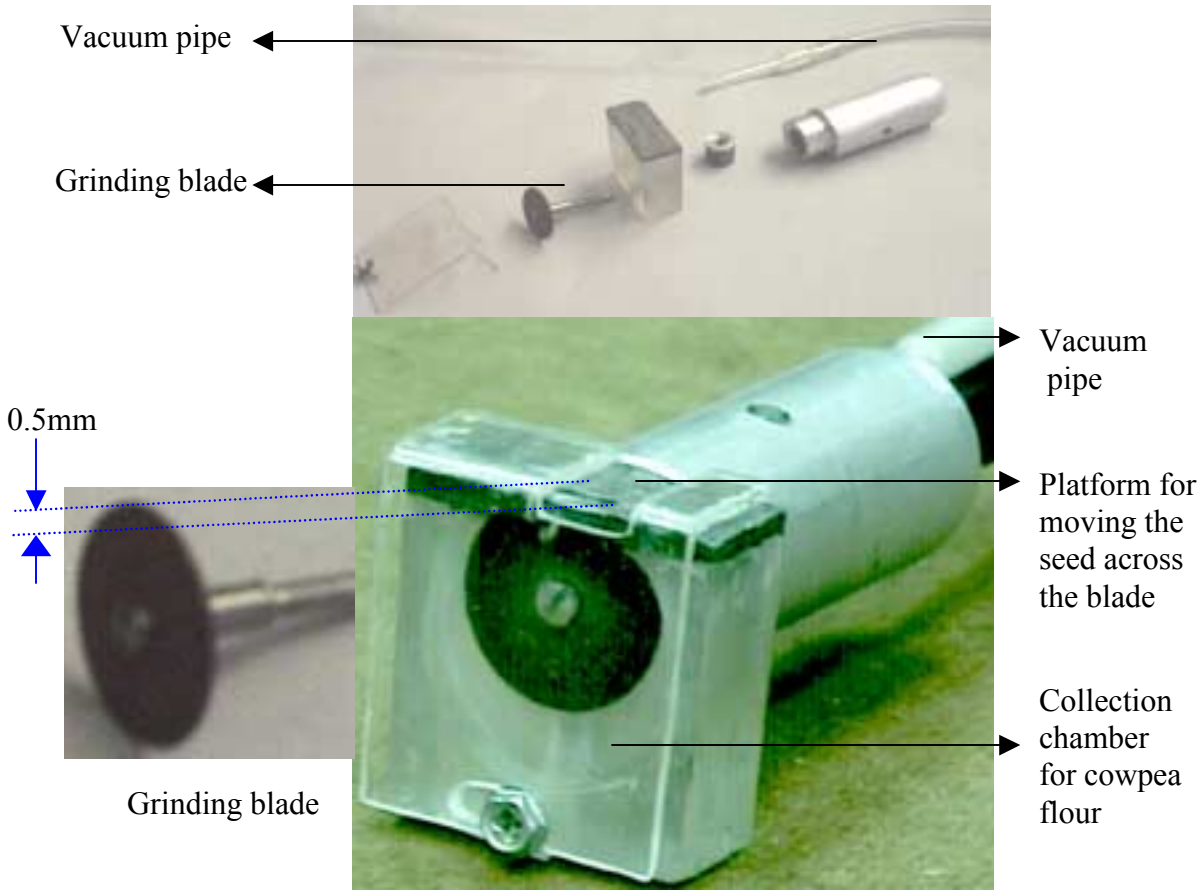

Fig. 5.1. Grinding apparatus to remove 0.5-mm outer layer of cowpea seeds

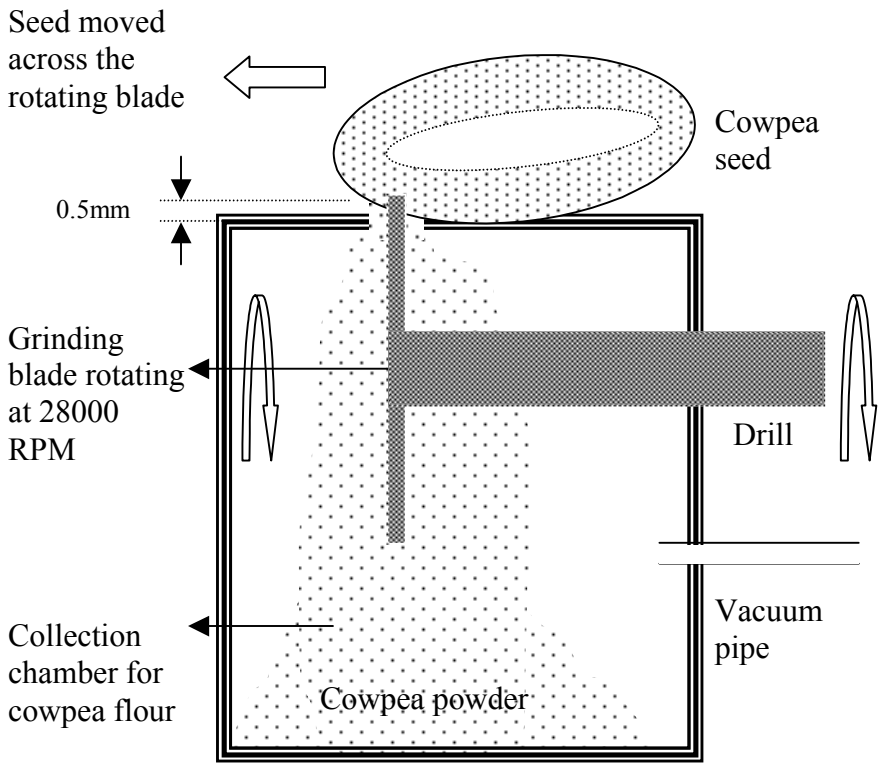

Fig. 5.2. Schematic diagram of removing 0.5-mm outer layer of a cowpea seed

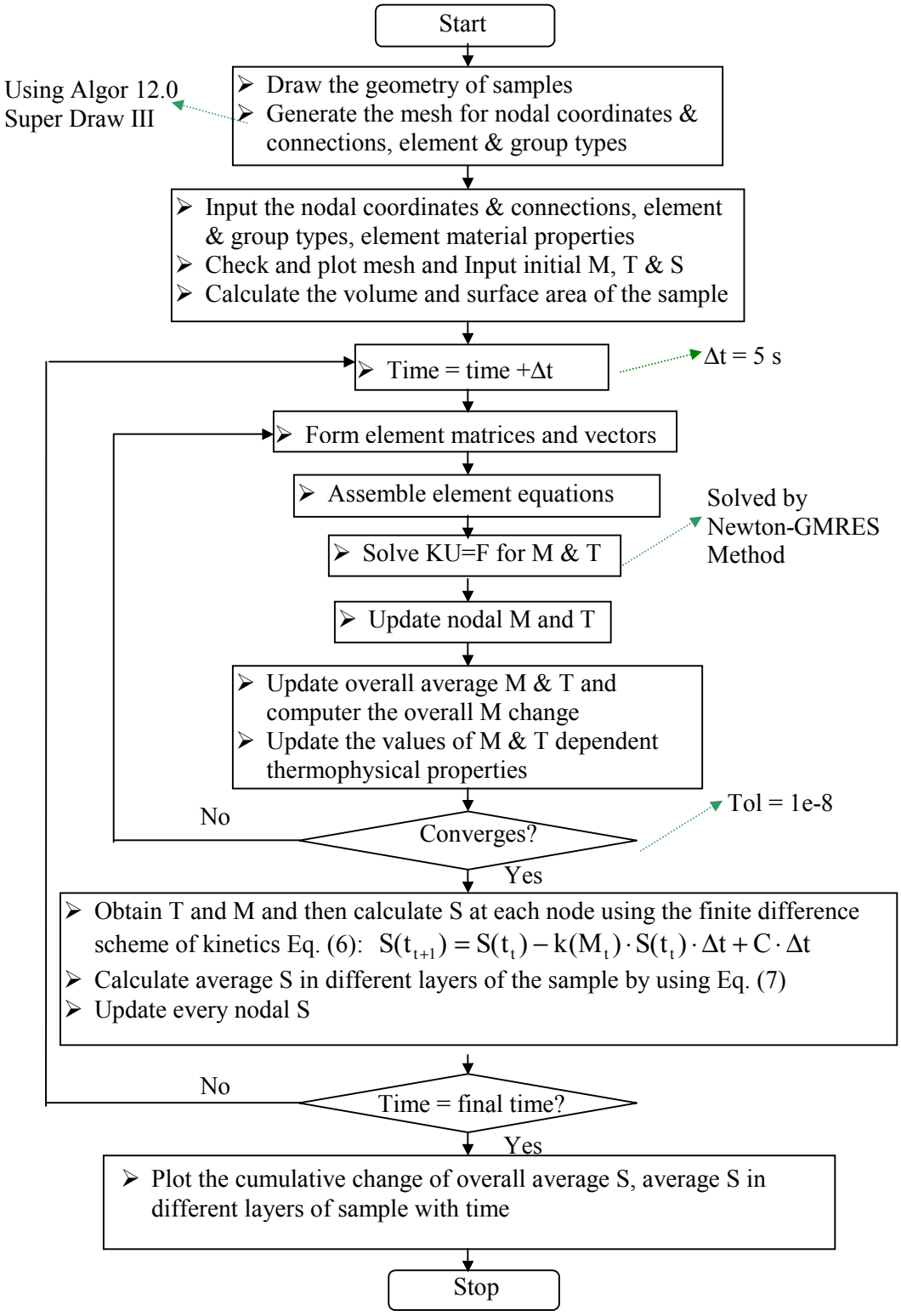

Fig. 5.3. Flow chart showing algorithm for modeling of starch gelatinization

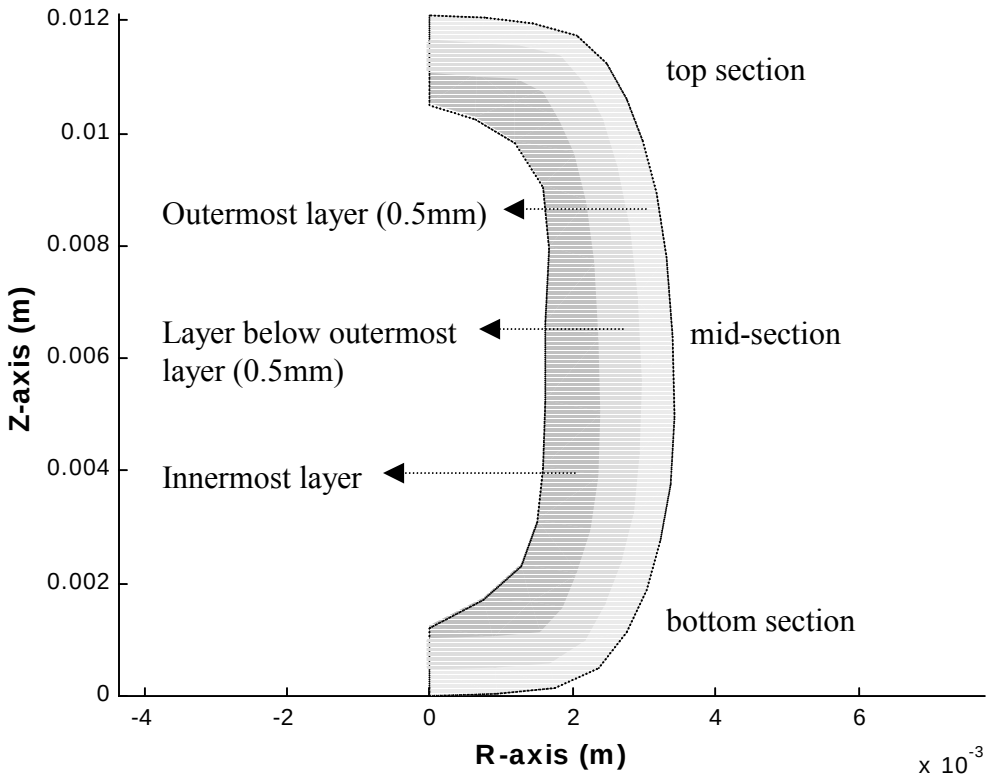

Fig. 5.4. Three layers in a half of cross-section of the cowpea seed

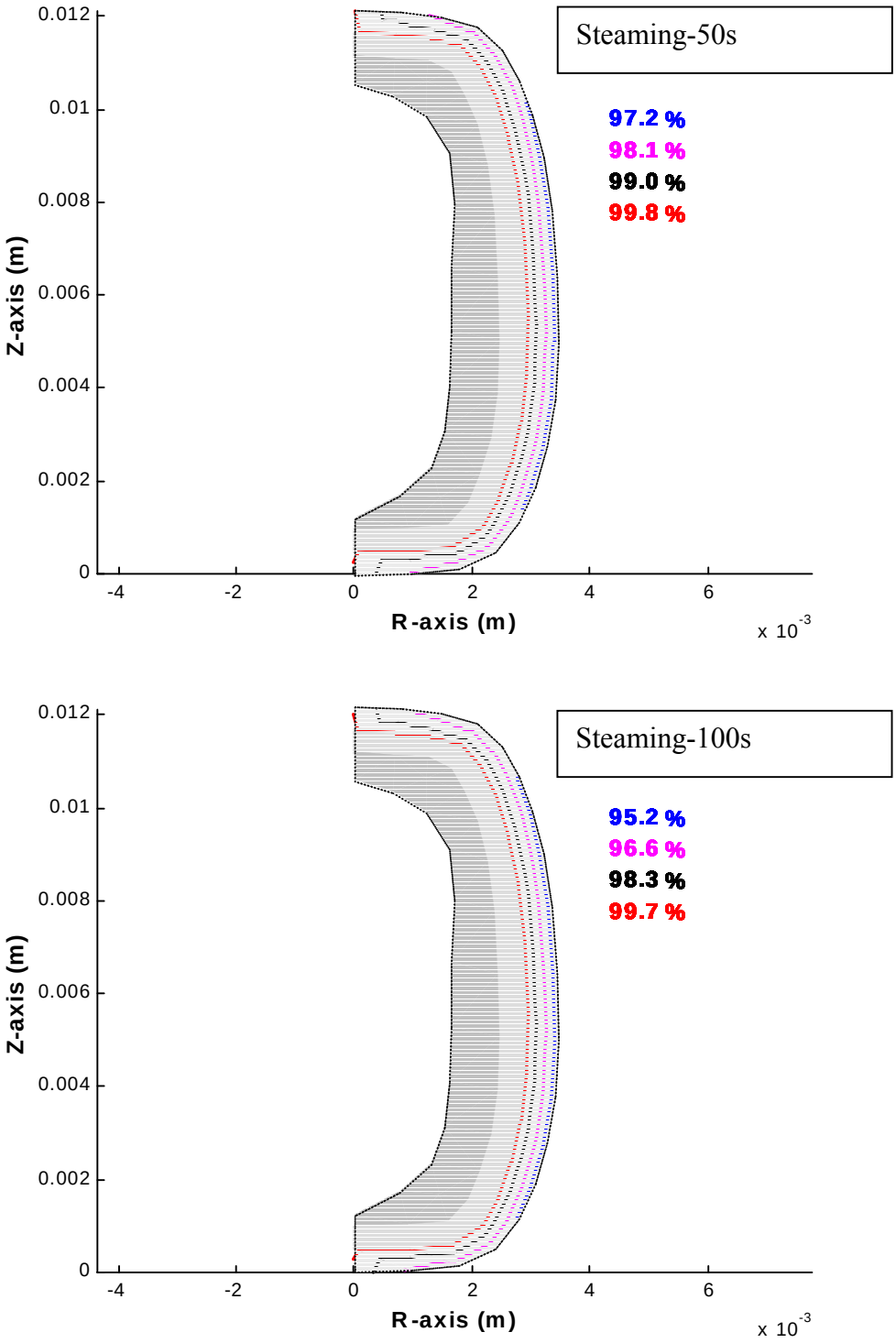

Fig. 5.5. Simulated profiles of fraction of ungelatinized starch, by Newton-GMRES method, in a cowpea seed.

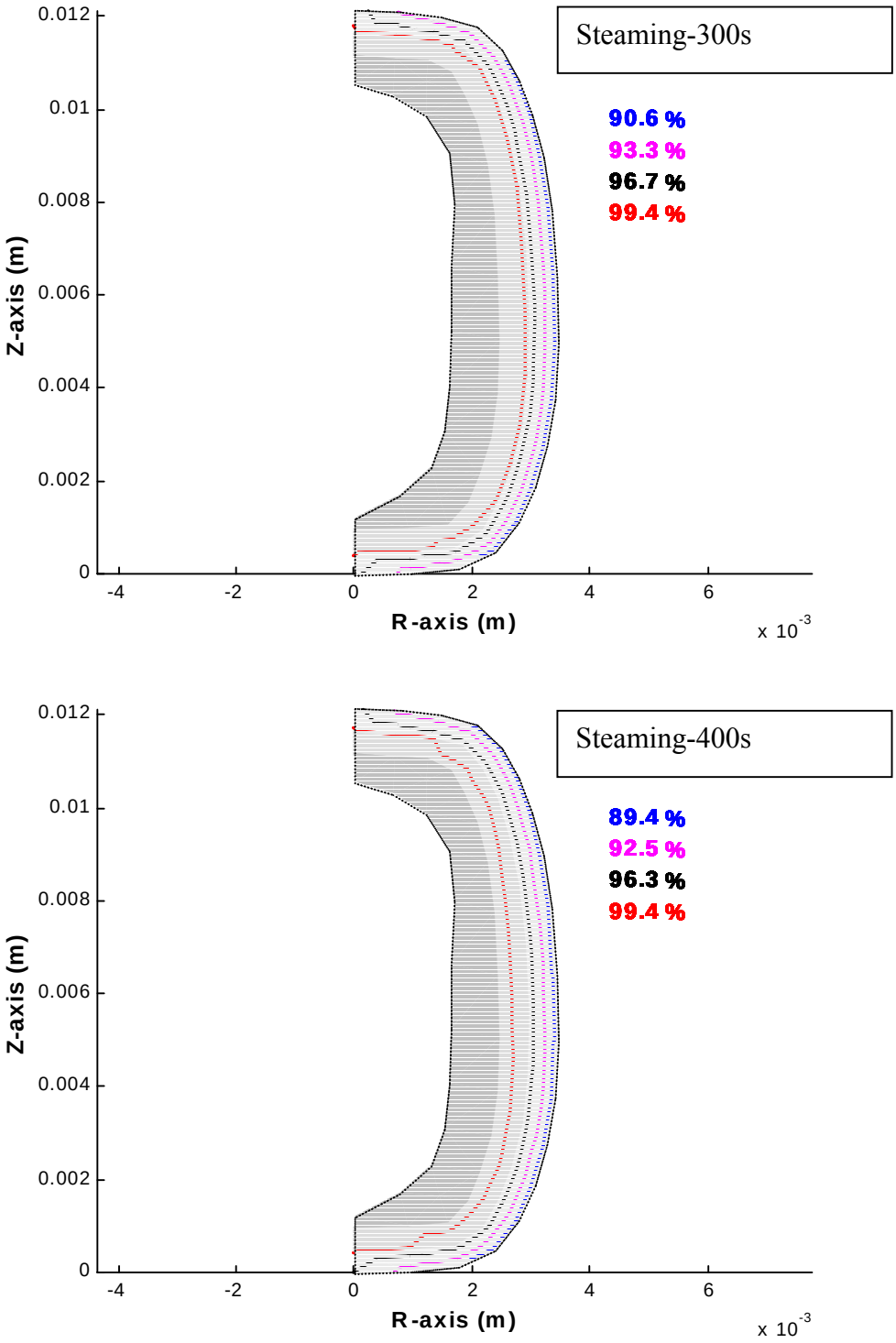

Fig. 5.6. Simulated profiles of fraction of ungelatinized starch, by Newton-GMRES method, in a cowpea seed.

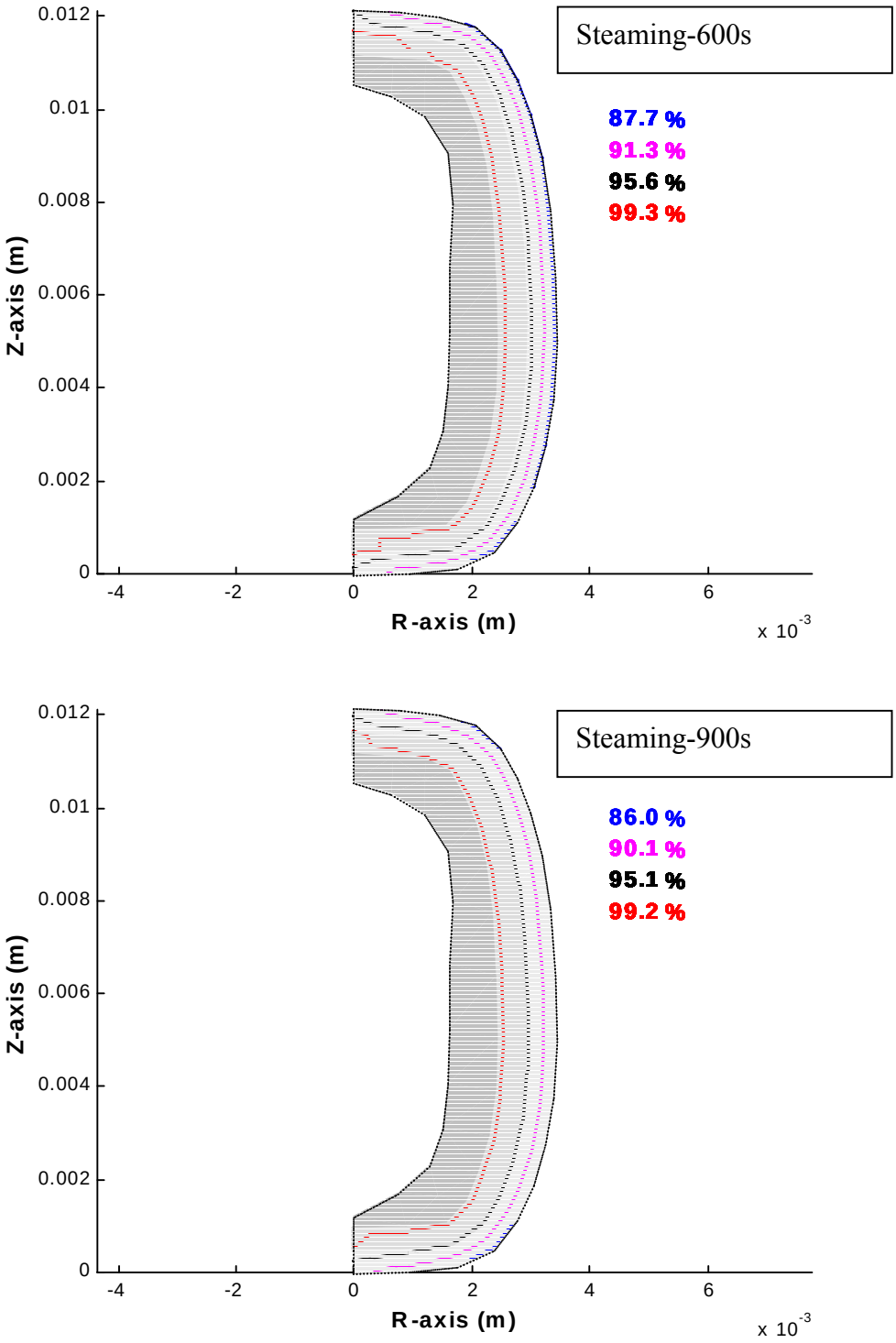

Fig. 5.7. Simulated profiles of fraction of ungelatinized starch, by Newton-GMRES method, in a cowpea seed.

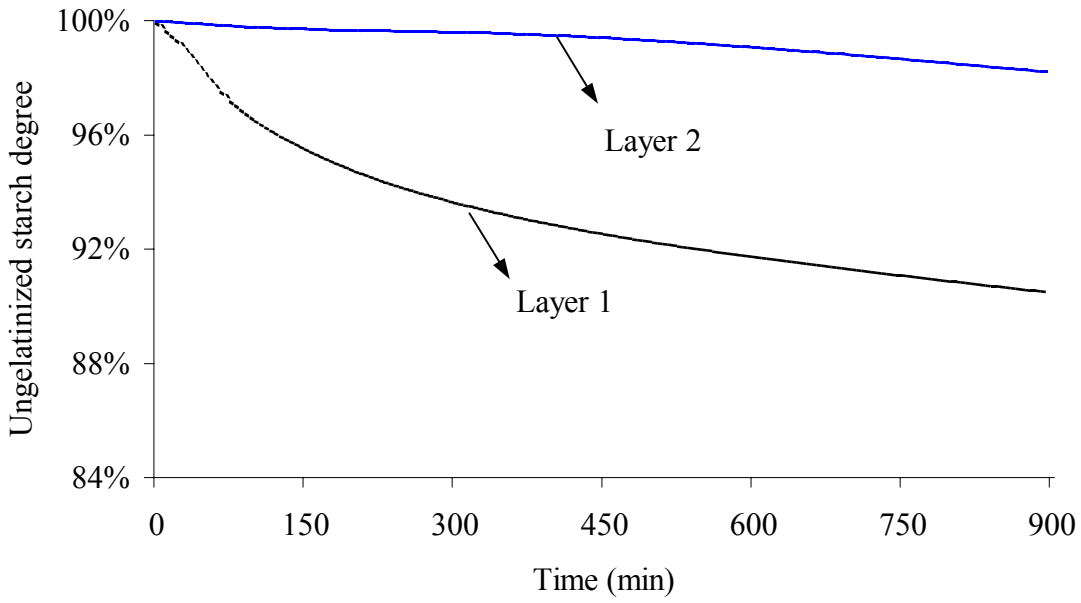

Fig. 5.8. Comparison of the predicted ungelatinized starch histories in different layers in the steaming of a seed (Newton-GMRES method)

CHAPTER 6

SUMMARY AND CONCLUSIONS

There were different transport behaviors occurring during the steaming process. The simulation and experiments showed how the different transport mechanisms varied and interacted with each other. The mass transfer was due to water condensing on the cold seed surface that was dominant initially followed by gelatinization of starch at the outermost layer of seeds during the main steaming phase. During the main steaming period, the decrease in the rate of mass transfer gradually reduced the rate of heat transfer and temperature difference. The drop in temperature difference indicated a decline in the rate of starch gelatinization in the cowpea seed. The prediction from the model agreed well with the experimental data even though the model slightly underestimated the temperature during the initial steaming phase. The model was able to describe well the different transport mechanisms.

The heat and mass transfer within the cowpea seed occurred very rapidly during the initial steaming process, which basically set the pattern of moisture profiles and gelatinized starch distribution. It is very difficult to determine the transient behavior merely from experimental methods. Hence, computer modeling, together with experimental method helped to quantitatively investigate transient heat and mass transfer behaviors and physicochemical changes encountered in steaming of cowpea seeds. A clear knowledge of the mechanism of heat and mass transfer and starch gelatinization behavior will further enable us to design efficient protective methods to provide the cowpea measures to combat weevil infestation.

The temperature and moisture distributions in cowpea seeds during steaming were described by two-way coupled nonlinear heat and mass transfer equations. Two solution

methods: Newton-GMRES method and Gaussian method were used to solve the two-way coupled nonlinear system. The coupling effect of heat and mass transfer was completely carried out through iterations until convergence during calculation with Newton-GMRES. The results showed the solution method of Newton-GMRES obtained a better agreement compared to the experimental data.

The predicted degree of gelatinization in outermost layer of seeds was found to be in good agreement with experimental data. The combined model was able to describe the process of gelatinization in steaming of cowpea seeds. The deviation between observed and simulated DG may be due to non-uniform distribution of starch within seeds, different behaviors of heat and moisture transfer between cowpea flour and cowpea seeds and various grinding gadgets employed resulting in variation in the extent of granule damage. It is necessary to further modify the grinding method to reduce the mechanical damage of starch granule as much as possible.

Even though gravimetric method and thermocouple measurements were sufficient to analyze and validate the steaming process, there is still a need to validate spatial moisture data and spatial DG. The results showed that the rate of gelatinization in cowpea seed was extremely dependent on water diffusion during the steaming process. The amount of moisture diffusivity strongly affected spatial moisture content and the DG profiles. NMR techniques can visualize moisture diffusion nondestructively and non-invasively and provide clear data on moisture diffusion in intact seeds during steaming. Through interpretation of NMR imaging, combined with finite element modeling, water diffusivity could be obtained. The prediction accuracy would be further improved.

The digestibility of cowpea seed after steaming and solar drying treatment needs to be further investigated by appropriate enzymes and methods. To find satisfactory answers to all the questions about the treatment and its effect on weevil infestation, further investigation is needed.